THE UNIVERSITY
of EDINBURGH

This thesis has been submitted in fulfilment of the requirements for a postgraduate degree (e.g. PhD, MPhil, DClinPsychol) at the University of Edinburgh. Please note the following terms and conditions of use:

This work is protected by copyright and other intellectual property rights, which are retained by the thesis author, unless otherwise stated.
A copy can be downloaded for personal non-commercial research or study, without prior permission or charge.
This thesis cannot be reproduced or quoted extensively from without first obtaining permission in writing from the author.
The content must not be changed in any way or sold commercially in any format or medium without the formal permission of the author.
When referring to this work, full bibliographic details including the author, title, awarding institution and date of the thesis must be given.

Probing large-order perturbative expansions in lattice gauge theories with fermions

Gianluca Filaci

Doctor of Philosophy
The University of Edinburgh
June 2019

Abstract

Many perturbative expansions in quantum field theories are believed to be plagued by factorial divergences. This can be seen as a reflection of the fact that an all-order perturbative computation cannot give a complete description of the theory, as it misses all the nonperturbative features. In some cases the divergence is related to the existence of condensates, and being able to keep the asymptotic behaviour of the series under control is necessary to provide a sound definition of the condensates themselves.

The goal of this work is to investigate the large-order behaviour of perturbative expansions in gauge theories. In order to achieve that, we employ Numerical Stochastic Perturbation Theory (NSPT), a numerical technique that allows for perturbative computations in quantum field theory. We present an implementation of NSPT that is able to yield results for high orders in the perturbative expansion of lattice gauge theories coupled to fermions. Performing calculations with fermions requires to overcome some challenges, due for example to the lack of chiral symmetry, or to the presence of doublers. Moreover, twisted boundary conditions (TBC), used to remove the gauge zero-momentum mode that spoils the convergence of the stochastic process, cannot accommodate easily fermions in all representations. In particular, we are forced to introduce a smell degree of freedom in order to include fermions in the fundamental representation with TBC.

As a first application, we compute with NSPT the critical mass of two flavours of Wilson fermions up to order $O(\beta^{-7})$ in a SU(3) gauge theory. We also implement, for the first time, staggered fermions in NSPT. The residual chiral symmetry of staggered fermions protects the theory from an additive mass renormalisation. We compute the perturbative expansion of the plaquette with two flavours of massless staggered fermions up to order $O(\beta^{-35})$ in a SU(3) gauge theory, and investigate the renormalon behaviour of such series. We are able to subtract the

power divergence in the Operator Product Expansion (OPE) for the plaquette and estimate the gluon condensate in massless QCD. Our results confirm that NSPT provides a viable way to probe systematically the asymptotic behaviour of perturbative series in QCD and, eventually, gauge theories with fermions in higher representations.

Lay summary

The Standard Model of particle physics is able to describe three of the four known fundamental interactions in the universe. Quantum chromodynamics (QCD), the theory that deals with the strong force, is one of the pillars of the Standard Model: for example, QCD describes how quarks, elementary particles among the fundamental constituents of matter, are kept together and form protons and neutrons; it is also responsible for binding protons and neutrons in atomic nuclei.

This theory provides a challenging field for theoretical investigations, as many of its properties still elude our current understanding. The main reason for this is that the strong coupling constant, which regulates the strength of the interaction, is not constant after all. The coupling changes with the energy scale: it is large at low energy, and decreases at the energies probed by particle accelerators. This feature causes perturbation theory, the main tool used to compute analytical predictions in particle physics, to break down at the scale we live in. In perturbation theory, the interaction between particles is modelled by an exchange of force carriers, called gluons in QCD; such exchange happens with a probability proportional to the strength of the interaction. If the coupling is small, the involvement of many mediators would happen with such a small probability that can be safely neglected. Considering only the contribution from a small number of mediator exchanges, which correspond to a small number of perturbative orders, provides therefore a good approximation of a physical process. This approach works very well for computing QCD predictions in high-energy collisions, but it cannot be used to describe large-coupling interactions like QCD at low energies: so far, no one has been even able to explain from first principles how quarks are confined into protons. In this respect, many results have been achieved thanks to numerical simulations.

QCD must be defined on a discrete spacetime, called lattice, in order to be simulated on a computer. The goal of this work is to exploit this lattice

formulation and develop tools that perform numerically perturbative calculations at high orders in QCD (and a large class of similar theories). In particular, we will focus on Numerical Stochastic Perturbation Theory (NSPT), a numerical technique that allows handling perturbation theory in an automated way. Since we know that in QCD perturbation theory is not the full story, probing many perturbative orders is particularly interesting: it turns out that the magnitude of the perturbative predictions grows extremely fast with the order. From the study of this behaviour, it is possible to learn characteristics of the nonperturbative nature of QCD.

Declaration

I declare that this thesis was composed by myself, that the work contained herein is my own except where explicitly stated otherwise in the text, and that this work has not been submitted for any other degree or professional qualification except as specified.

Parts of this work have been published in Refs. [1–3].

(*Gianluca Filaci, June 2019*)

Acknowledgements

First of all, I would like to thank my supervisor, Luigi Del Debbio, for his guidance throughout my PhD. His way of thinking about physics, approaching research, tackling problems without giving up on difficulties, has really inspired me. If I managed to get even just a little part of it, it is only his merit.

I wish to express my sincere gratitude to Francesco Di Renzo, who taught me everything about NSPT. His advice, both scientific and personal, has been indispensable for me, and it has been a pleasure to visit Parma several times.

I am also indebted to Guido Cossu and his endless patience in explaining to me the inner workings of Grid.

I would like to thank all the PPT group; special thanks go to Christian and Joël, for making these years in Edinburgh so much fun.

I am also lucky I can always count on Andrea, Gianluca, Matteo, and all my friends in Rome: every time I come back, it always feels like we are not living that far from each other.

Thanks to my family and in particular to my parents, who constantly stood by my side and gave me their unconditional support.

I am sure this thesis would have never seen the light without Veronica. Thank you for these amazing years, and for your smile each time I needed it the most.

Contents

List of Figures

List of Tables

Chapter 1

Introduction

Quantum Chromodynamics (QCD) is the theory that describes the strong interaction. A perturbative approach fails to describe the observed spectrum of hadrons due to asymptotic freedom: as the coupling constant increases at low energies, the dynamics becomes nonperturbative. This is the reason that makes so hard to understand from first principles how confinement arises in such a theory. At the same time, field correlators at short distances are reliably approximated by perturbative expansions in the running coupling at a large momentum scale. However, remnants of nonperturbative effects are still present: perturbative expansions in QCD are expected to be divergent for all values of the coupling, and the asymptotic behaviour can be related to the nonperturbative structure. Thanks to Numerical Stochastic Perturbation Theory (NSPT), a numerical technique that allows for perturbative computations in quantum field theory, it is possible to probe by means of computer simulations the large-order perturbative behaviour of gauge theories regularised on a lattice. This will be the subject of this work.

In this first chapter we introduce gauge theories in the continuum and on the lattice, mainly to fix our notation. In Chapter 2 we present a survey of the standard arguments supporting the divergence of perturbative series, and examine the relationship between renormalons and condensates. Numerical Stochastic Perturbation theory is introduced in Chapter 3 and Chapter 4, together with the techniques required to include fermions in perturbative simulations. Our results for the critical mass of Wilson fermions and the plaquette in massless QCD are presented respectively in Chapter 5 and Chapter 6. We draw our conclusions in

1.1 Gauge theories

Gauge theories are the building blocks of the Standard Model: we now describe how these theories are defined, and set our conventions. We remark that we will always deal with Euclidean theories, obtained from a *Wick rotation* of the corresponding theories in Minkowski space. The time x^0_M in Minkowski space is rotated in the complex plane to a new $x^0_E = ix^0_M$, turning in this way the Minkowski metric into the Euclidean metric. We refer to Appendix A for group theory notation, and use $\mu, \nu = 1, \ldots, 4$ for Lorentz indices.

The Euclidean action for a SU(N_c) gauge theory coupled with fermions in the representation R is

$$S[A, \psi, \bar{\psi}] = S_G[A] + S_F[A, \psi, \bar{\psi}]\,, \tag{1.1}$$

where

$$S_G[A] = \frac{1}{4g^2} \int d^4x \sum_{a,\mu,\nu} F^a_{\mu\nu}(x) F^a_{\mu\nu}(x) \tag{1.2a}$$

$$S_F[A, \psi, \bar{\psi}] = \sum_{f=0}^{N_f} \int d^4x\, \bar{\psi}_f(x) \left(\sum_\mu \gamma_\mu (D_R)_\mu - m_f \right) \psi_f(x)\,. \tag{1.2b}$$

The integer N_c stands for the number of *colours* of the theory. The gauge field $A^a_\mu(x)$ is a vector boson field transforming in the adjoint representation of the gauge group; the field-strength tensor is

$$F^a_{\mu\nu} = \partial_\mu A^a_\nu - \partial_\nu A^a_\mu - \sum_{b,c} f^{abc} A^b_\mu A^c_\nu\,. \tag{1.3}$$

The factor g is the coupling, and determines the strength of the interaction; the combination

$$\alpha = \frac{g^2}{4\pi} \tag{1.4}$$

is a quantity analogous to the fine-structure constant in Quantum Electrodynamics (QED). The fermion fields $\psi(x)$, $\bar{\psi}(x)$ are Grassmann-valued Dirac spinors transforming in the representation R of SU(N_c). We are assuming to have N_f flavours, each with mass m_f. The Euclidean gamma matrices γ_μ are Hermitian

matrices satisfying

$$\{\gamma_\mu, \gamma_\nu\} = 2\delta_{\mu\nu}\mathbb{1}\,, \qquad \gamma_5 = \gamma_1\gamma_2\gamma_3\gamma_4\,, \tag{1.5}$$

and the covariant derivative acts as

$$(D_R)_\mu = \partial_\mu + i(A_R)_\mu\,, \qquad \text{with} \qquad (A_R)_\mu = \sum_a T_R^a A_\mu^a\,. \tag{1.6}$$

The action built in this way is symmetric under the following local gauge transformation $\Omega(x) \in \mathrm{SU}(N_c)$, i.e. a colour rotation different for each spacetime point,

$$A_\mu \to A_\mu^\Omega = \Omega A_\mu \Omega^\dagger + i(\partial_\mu\Omega)\Omega^\dagger \tag{1.7a}$$

$$\psi \to \Omega_R\psi \qquad \bar\psi \to \bar\psi(\Omega_R)^\dagger\,, \tag{1.7b}$$

where Ω_R is the matrix Ω in the representation R. If fermions are degenerate, we are free to perform rotations in flavour space that result in an additional global *vector symmetry* $\mathrm{U}(N_f)$. Another significant symmetry, called *chiral* (or *axial*) *symmetry*, arises when all fermions are massless: in this case, the action is invariant under transformations like

$$\psi \to e^{i\epsilon\gamma_5}\,\psi\,, \qquad \bar\psi \to \bar\psi\, e^{i\epsilon\gamma_5}\,, \tag{1.8}$$

and the global flavour symmetry group is enlarged to $\mathrm{U}(N_f) \times U(N_f)$.

Any physical observable can be extracted from correlators: the expectation value of an operator $O[A, \psi, \bar\psi]$ is defined (for simplicity, in the case of N_f degenerate fermions of mass $m_f = m$) via the path integral

$$\begin{aligned}\left\langle O[A,\psi,\bar\psi]\right\rangle &= \frac{\int \mathcal{D}[A,\psi,\bar\psi]\, e^{-S[A,\psi,\bar\psi]}\, O[A,\psi,\bar\psi]}{\int \mathcal{D}[A,\psi,\bar\psi]\, e^{-S[A,\psi,\bar\psi]}} = \\ &= \frac{\int \mathcal{D}[A]\, e^{-S_G[A]}\, \left[\det\left(\sum_\mu \gamma_\mu (D_R)_\mu - m\right)\right]^{N_f}\, O_{\text{Wick}}[A]}{\int \mathcal{D}[A]\, e^{-S_G[A]}\, \left[\det\left(\sum_\mu \gamma_\mu (D_R)_\mu - m\right)\right]^{N_f}}\,.\end{aligned} \tag{1.9}$$

In the second line, the integral over the fermion field resulted in the determinant of the Dirac operator, and O_{Wick} is the operator O after Wick contractions have been performed[1]. For physical gauge-invariant observables, the invariance

[1] In the space generated by the complex Grassmann variables $\{\theta_i, \bar\theta_i\}_{i=1}^N$, the following

of the integrand and the measure under gauge transformations poses clearly a convergence issue. This is resolved by the Faddeev-Popov procedure, which amounts to replacing

$$e^{-S_G[A]} \quad \to \quad e^{-S_G[A]-\frac{1}{2\alpha}\int d^4x\, G(A)^2} \det\left(\nabla_\Omega G(A^\Omega)\right) \tag{1.10}$$

in Eq. (1.9). $G(A)$ defines a gauge-fixing hypersurface, α is an arbitrary gauge-fixing parameter, and the determinant can be written in terms of ghost fields. The Lie derivative $\nabla_\Omega G(A^\Omega)$ of G is defined in Eq. (A.14). The function G should be ideally such that a unique Ω is fixed from $G(A^\Omega) = 0$: when this is not the case, *Gribov copies* are present. These multiple solutions add additional complexity in the nonperturbative definition of the path integral.

Nevertheless, the technique of gauge fixing provides a solid framework for perturbation theory. To perform a perturbative expansion in gauge theories, we need to rescale the gauge field $A = gA'$ first: this gives $F_{\mu\nu} = g\, G_{\mu\nu}$ with

$$G^a_{\mu\nu} = \partial_\mu (A')^a_\nu - \partial_\nu (A')^a_\mu - g \sum_{b,c} f^{abc} (A')^b_\mu (A')^c_\nu \,, \tag{1.11}$$

and allows getting rid of the nonlinear term in the field-strength of the free theory. The integrand is then expanded in g, and correlators are expressed as power series in the coupling whose coefficients can be computed essentially by solving Gaussian integrals. The exchange of summation and integration in this procedure could be done only under some regularity conditions, that usually are not satisfied. Some implications of this matter will be described in Chapter 2.

The presence of many infinities in quantum field theory requires the theory to be first regularised, and then renormalised: the couplings and normalisations of the fields are rescaled in order to fix the values of some correlators at an energy scale μ; if the theory is renormalisable, at the end of the procedure the regularisation can be removed. Renormalised parameters depend on the renormalisation scale

---

Gaussian integral holds

$$\int \left(\prod_{k=1}^N d\theta_k d\bar\theta_k\right) \exp\left(\sum_{l,m=1}^N \bar\theta_l M_{lm} \theta_m\right) \bar\theta_{i_1}\theta_{j_1} \dots \bar\theta_{i_n}\theta_{j_n} = \\ = \det M \sum_P \mathrm{sign}(P) (M^{-1})_{j_{P(1)} i_1} \dots (M^{-1})_{j_{P(n)} i_n} \,,$$

where M is an arbitrary $N \times N$ matrix and the sum runs over all the permutations P of $1, \dots, n$. We call $\sum_P \mathrm{sign}(P) (M^{-1})_{j_{P(1)} i_1} \dots (M^{-1})_{j_{P(n)} i_n}$ the Wick contraction of $\bar\theta_{i_1}\theta_{j_1} \dots \bar\theta_{i_n}\theta_{j_n}$.

μ: from the renormalised coupling $g_R(\mu)$, one can define the β-function as

$$\beta(g_R) = \frac{dg_R}{d\log\mu} = -\left[\beta_0 \frac{g_R^3}{16\pi^2} + \beta_1 \frac{g_R^5}{(16\pi^2)^2} + \dots\right] = \\ = -(b_0 g_R^3 + b_1 g_R^5 + \dots) \tag{1.12}$$

or

$$\beta(\alpha_R) = \frac{d\alpha_R}{d\log\mu} = -2\alpha_R\left[\beta_0 \frac{\alpha_R}{4\pi} + \beta_1 \left(\frac{\alpha_R}{4\pi}\right)^2 + \dots\right], \tag{1.13}$$

with the first two scheme-independent perturbative coefficients

$$\beta_0 = \frac{11}{3}C_2(G) - \frac{4}{3}T(R)N_f \tag{1.14a}$$

$$\beta_1 = \frac{34}{3}C_2(G)^2 - \left[\frac{20}{3}C_2(G) + 4C_2(R)\right]T(R)N_f \tag{1.14b}$$

$$b_n = \frac{\beta_n}{(16\pi^2)^{n+1}}, \tag{1.14c}$$

and G is the gauge bosons representation (the adjoint representation). For fermions in the fundamental representation these coefficients are

$$\beta_0 = \frac{11}{3}N_c - \frac{2}{3}N_f \tag{1.15a}$$

$$\beta_1 = \frac{34}{3}N_c^2 - \left(\frac{13}{3}N_c - \frac{1}{N_c}\right)N_f, \tag{1.15b}$$

and asymptotic freedom (i.e. $\beta_0 > 0$) is realised whenever $N_f < 11N_c/2$. We note also that the scale

$$\Lambda = \mu\,[g_R(\mu)]^{-b_1/b_0^2}\, e^{-1/(2b_0 g_R(\mu)^2)}\, \exp\left[-\int_0^{g_R(\mu)} dg\, \left(\frac{1}{\beta(g)} + \frac{1}{b_0 g^3} - \frac{b_1}{b_0^2 g}\right)\right] \tag{1.16}$$

arises naturally as a dimensionful renormalisation group invariant quantity.

The one-loop running coupling can be determined by integrating Eq. (1.12) with all the coefficients of the β-function, except for b_0, set to zero,

$$\alpha_R(k) = \frac{\alpha_R(Q)}{1 + \alpha_R(Q)\,\frac{\beta_0}{2\pi}\log\frac{k}{Q}} = \frac{\alpha_R(Q)}{\log\frac{k}{\Lambda}}. \tag{1.17}$$

The theories we will deal with are *asymptotically free theories*, i.e. they have $\beta_0 > 0$: the running coupling is small at high energies, implying that in this

regime perturbation theory can be trusted. On the other hand, the coupling grows at low energies and, in particular, $\alpha_R(k)$ diverges at the *Landau pole* $k = \Lambda$; of course the divergence in the running is not physical, since perturbation theory ceases to be applicable as soon as the coupling starts to grow.

We will refer to massless QCD as the gauge theory with $N_c = 3$ colours, and $N_f = 2$ massless flavours in the fundamental representation.

1.2 Lattice gauge theories

Lattice gauge theories are gauge theories defined on a discrete spacetime. The lattice spacing is denoted by a; if the size of the lattice is finite, with N^4 points, then the physical volume is $L^4 = a^4 N^4$ (we assume hypercubic symmetry for simplicity). A SU(N_c) matrix $U_\mu(x)$ is associated to each link joining the points x and $x + a\hat{\mu}$: these *link variables* are the fundamental degrees of freedom, and are related to the gauge potential via

$$U_\mu(x) = e^{iagA_\mu(x)} \,. \tag{1.18}$$

The basic ingredient for developing a lattice action is the product of link variables around the 1×1 plaquette $\Box$,

$$U_\Box = U_{\mu\nu}(x) = U_\mu(x) U_\nu(x + a\hat{\mu}) U_\mu(x + a\hat{\nu})^\dagger U_\nu(x)^\dagger \,. \tag{1.19}$$

In the limit of small lattice spacing, the *plaquette operator*

$$P_{\mu\nu}(x) = \frac{1}{N_c} \operatorname{Re} \operatorname{Tr}(1 - U_{\mu\nu}(x)) = \frac{a^4 g^2}{4N_c} \sum_c G^c_{\mu\nu}(x) G^c_{\mu\nu}(x) + O(a^6) \tag{1.20}$$

approximates the field strength: this means that the action $S_G[A]$ can be recovered in the naive limit $a \to 0$ by summing over all the plaquettes of the lattice. In particular, we will make use of the Wilson action [4]

$$S_G\,[U] = -\frac{\beta}{2N_c} \sum_\Box \operatorname{Tr}\left(U_\Box + U_\Box{}^\dagger\right) = -\frac{\beta}{N_c} \sum_\Box \operatorname{Re} \operatorname{Tr} U_\Box \,, \tag{1.21}$$

where the lattice coupling is

$$\beta = \frac{2N_c}{g^2} \,. \tag{1.22}$$

A fundamental property that all lattice actions must preserve is invariance under gauge transformations, with $\Omega(x) \in \mathrm{SU}(N_c)$,

$$U_\mu(x) \to \Omega(x) U_\mu(x) \Omega(x + a\hat{\mu})^\dagger \,, \tag{1.23}$$

which is a transformation analogous to the one in Eq. (1.7a).

Expectation values in a pure gauge theory are computed from

$$\langle O[U] \rangle = \frac{\int \mathcal{D}[U]\, e^{-S_G[U]}\, O[U]}{\int \mathcal{D}[U]\, e^{-S_G[U]}} \,. \tag{1.24}$$

The advantage of this formulation is twofold. First, the lattice spacing a provides a natural ultraviolet cutoff, so that the regularised theory preserves gauge invariance. Second, the path integral measure is the measure on the compact group $\mathrm{SU}(N_c)$, and is not a formal measure as in the continuum case; if the number of lattice points is finite, Eq. (1.24) consists of a finite number of integrals. The lattice serves as a nonperturbative definition of gauge theories. Moreover, in this framework the theory is ready to be simulated numerically, and expectation values can estimated from Monte Carlo simulations.

The outcome of a lattice computation clearly depends on the lattice spacing: after renormalisation, the regulator must be removed to obtain results in the continuum limit. This implies that the bare parameters must be adjusted as the lattice spacing goes to zero to keep physical quantities constant. For example, given the renormalised coupling defined by $g = Z_g(g, a\mu) g_R(\mu)$, if we want to send $a \to 0$ and keep g_R constant we are forced to tune the bare coupling accordingly. The lattice bare β-function,

$$\beta_L(g) = -a \frac{dg}{da}\bigg|_{\substack{\text{physical} \\ \text{quantities}}} \,, \tag{1.25}$$

describes how to adjust the bare coupling in order to reach the continuum limit. The shape of $\beta_L(g)$ determines whether this limit can be reached: in asymptotically free theories, $a \to 0$ corresponds to $g \to 0$.

1.3 Fermions on the lattice

So far we neglected the presence of fermions. A naive lattice version of the fermion action amounts to replacing ordinary derivatives with finite differences,

$$\partial_\mu \psi(x) \quad \to \quad \frac{1}{2}\left(\delta_\mu + \delta_\mu^*\right)\psi(x) = \frac{1}{2a}\left[\psi(x + a\hat{\mu}) - \psi(x - a\hat{\mu})\right] , \tag{1.26}$$

where

$$\delta_\mu \psi(x) = \frac{1}{a}\left[\psi(x + a\hat{\mu}) - \psi(x)\right] \quad \text{and} \quad \delta_\mu^* \psi(x) = \frac{1}{a}\left[\psi(x) - \psi(x - a\hat{\mu})\right] , \tag{1.27}$$

and writing an interaction invariant under the gauge transformation in Eqs. (1.23) and (1.7b),

$$(D_R)_\mu \psi(x) = \frac{1}{2a}\left[(U_R)_\mu(x)\,\psi(x + a\hat{\mu}) - (U_R)_\mu(x - a\hat{\mu})^\dagger\,\psi(x - a\hat{\mu})\right] , \tag{1.28}$$

where $(U_R)_\mu(x)$ is the link $U_\mu(x)$ in the representation R. These particular choices of discretisation are made so that derivative and covariant derivative are antihermitian. Therefore, for one flavour, the *naive fermion action* is

$$S_F[U, \psi, \bar{\psi}] = a^4 \sum_x \bar{\psi}(x) \left(\sum_\mu \gamma_\mu (D_R)_\mu - m \right) \psi(x) . \tag{1.29}$$

Unfortunately, it turns out that this action describes 16 fermions in the continuum limit, as it can be shown by looking at the poles of the free propagator in momentum space: this phenomenon is known as *species doubling*.

In general, the Nielsen-Ninomiya theorem [5, 6] prevents us from building a discretisation of the four-dimensional Dirac operator which at the same time is local, has the correct continuum limit without any doublers, and does not break chiral symmetry in the massless case. All the possible lattice fermion actions must necessarily give up at least one of these conditions. Among the many proposed discretisations, we will focus on those that will be needed in the following: *Wilson fermions* and *staggered* (or *Kogut-Susskind*) *fermions*.

Wilson fermions

Wilson's strategy [7] for removing doublers consists in adding a new term to the naive action so that doublers acquire a mass proportional to $1/a$, and decouple in the continuum limit. Wilson's fermion action reads

$$S_F[U,\psi,\bar{\psi}] = a^4 \sum_x \bar{\psi}(x) \left(\sum_\mu \gamma_\mu (D_R)_\mu - m - \frac{ar}{2}\, \delta^*_\mu \delta_\mu \right) \psi(x)\,, \tag{1.30}$$

where r is an arbitrary parameter, which from now on we will take equal to 1. In momentum space, it is easy to see that the new term does not affect the zero momentum component of ψ, which is indeed related to the physical fermion that remains after removing the lattice spacing. The downside of this approach reveals itself when dealing with the quantum theory: since Wilson's term is not invariant under Eq. (1.8), chiral symmetry gets explicitly broken, causing renormalisation to become more involved. For example, the mass must be additively renormalised, as it will be explained in detail in Chapter 5.

Staggered fermions

A way to preserve chiral symmetry and reduce the number of doublers has been proposed in Refs. [8, 9] with the introduction of staggered fermions. The key idea is noting that thanks to the unitary space-dependent transformation

$$\psi(x) \quad \to \quad \gamma_1^{n_1}\gamma_2^{n_2}\gamma_3^{n_3}\gamma_4^{n_4}\,\psi(x)\,, \tag{1.31}$$

where $n = x/a$ is the site index vector, we can trade the gamma matrices in the Dirac operator for a space-dependent phase,

$$\gamma_\mu \psi(x \pm a\hat{\mu}) \quad \to \quad \alpha_\mu(x)\,\gamma_1^{n_1}\gamma_2^{n_2}\gamma_3^{n_3}\gamma_4^{n_4}\,\psi(x \pm a\hat{\mu})\,, \tag{1.32}$$

with $\alpha_\mu(x) = (-1)^{\sum_{\nu=1}^{\mu-1} n_\nu}$, that is

$$\alpha_1(x) = 1 \tag{1.33a}$$
$$\alpha_2(x) = (-1)^{n_1} \tag{1.33b}$$
$$\alpha_3(x) = (-1)^{n_1+n_2} \tag{1.33c}$$
$$\alpha_4(x) = (-1)^{n_1+n_2+n_3}\,. \tag{1.33d}$$

If $\bar{\psi}(x)$ is then transformed analogously

$$\bar{\psi}(x) \quad \rightarrow \quad \bar{\psi}(x)\,\gamma_4^{n_4}\gamma_3^{n_3}\gamma_2^{n_2}\gamma_1^{n_1}\,, \tag{1.34}$$

the naive fermion action becomes simply

$$S_F[U,\psi,\bar{\psi}] = a^4 \sum_x \bar{\psi}(x)\,(D_R - m)\,\psi(x)\,. \tag{1.35}$$

with

$$D_R\psi(x) = \frac{1}{2a}\sum_\mu \alpha_\mu(x)\left[(U_R)_\mu(x)\,\psi(x+a\hat{\mu}) - (U_R)_\mu(x-a\hat{\mu})^\dagger\,\psi(x-a\hat{\mu})\right]\,. \tag{1.36}$$

The resulting Dirac operator is proportional to the identity in Dirac space, and the four spinor components of ψ will be just copies of each other: keeping just one of these, we can expect that the number of doublers is reduced by a factor of four, leading to $16/4 = 4$ physical fermions in the continuum limit. This is indeed the case, and the four doublers are referred to as *tastes* of the staggered fermion. The staggered action is thus

$$S_F[U,\chi,\bar{\chi}] = a^4 \sum_x \bar{\chi}(x)\,(D_R - m)\,\chi(x)\,, \tag{1.37}$$

where the fields χ, $\bar{\chi}$ have no spinor structure and the Dirac operator is as in Eq. (1.36). It is now worth to have a look at the symmetries of such action. The transformations in Eqs. (1.31) and (1.34) induce

$$\bar{\psi}(x)\gamma_5\psi(x) \quad \rightarrow \quad (-1)^{n_1+n_2+n_3+n_4}\,\bar{\psi}(x)\psi(x)\,, \tag{1.38}$$

and let relate the matrix γ_5 to the phase $\alpha_5(x) = (-1)^{n_1+n_2+n_3+n_4}$. Indeed, in the massless case, the action is invariant under

$$\chi \rightarrow e^{i\epsilon\alpha_5(x)}\,\chi\,, \qquad \bar{\chi} \rightarrow \bar{\chi}\,e^{i\epsilon\alpha_5(x)}\,, \tag{1.39}$$

which corresponds to the global chiral symmetry of the staggered theory; no additive mass renormalisation emerges. We also note that, due to the staggered phase, the action in Eq. (1.37) is only invariant under shifts of two lattice spacings, $x \rightarrow x + 2a\hat{\mu}$.

In Monte Carlo simulations, one often relies on the trick of *rooting* in order to

remove three out of four tastes. The method consists in replacing the fermion determinant in Eq. (1.9) with its fourth root. Whether rooting represents a legitimate procedure at finite lattice spacing is still debated in the literature; the reader is referred to Ref. [10] for a review on this matter. We just point out that, in perturbation theory, as long as the counterterms required for renormalisation are polynomials in N_f, rooted staggered fermions correctly reproduce order by order renormalised correlation functions in the continuum theory with N_f flavours.

Chapter 2

Renormalons and OPE

It is almost always the case in physics that, as soon as real and interesting features of a system are taken into account, it is not possible to find exact solutions: in order to make predictions from a theory, one often relies on some kind of approximation. Perturbation theory is surely one of the most common, and it proves to be useful each time a small parameter can be identified.

The goal of this section is to study perturbative series in quantum field theories. We will argue that these expansions are typically divergent, and that the pattern of divergence might be related to nonperturbative physics: for example, we could learn about the presence of condensates by looking at high orders in perturbation theory. We remark that many results in this section are not supported by mathematically rigorous arguments. They are based on physical intuition, study of toy models, analysis of specific limits of theories (e.g. large N_c, large N_f), numerical simulations. Even if in gauge theories there is general consensus on the divergence of perturbative series, that can be inferred just by looking at the growth of the number of diagrams, analytical evidences are still lacking in the case of some sources of divergence that we will discuss in the following.

2.1 The divergence of perturbative series

Generally, we have the problem of estimating some unknown function of the coupling $R(\alpha)$ as a power series

$$R_{\text{pert}}(\alpha) = \sum_{n=0}^{\infty} r_n \alpha^{n+1} \,. \tag{2.1}$$

We assume, without loss of generality, that $R(0) = 0$, and we also define the remainder

$$R_N(\alpha) = R(\alpha) - \sum_{n=0}^{N} r_n \alpha^{n+1} \,. \tag{2.2}$$

It would be ideal to know how well R_{pert} approximates R when only a finite number of r_n are known, or if there is room for improving our knowledge of R by computing more coefficients of its perturbative series. In this section we wish to discuss what is possible to tell about the relation between R and R_{pert}, and under which circumstances a resummed value for R_{pert} can be defined.

First, it is worthwhile to recall some mathematical properties of power series. Let D be a simply connected compact domain in the complex plane containing the origin. R_{pert} is said to be *uniformly convergent*, from now on just *convergent*, to R in D if, given an arbitrary $\epsilon > 0$, we can always find an N such that $|R_n(\alpha)| < \epsilon$ for all $n > N$ and $\alpha \in D$. This situation is realised if and only if $R(\alpha)$ is analytic in D, in which case R_{pert} is nothing but the Taylor series of R: one usually writes simply that $R = R_{\text{pert}}$.

More often, $R(\alpha)$ is not analytic in any neighbourhood of the origin, and R_{pert}, if it exists, is not equal to R. It is worth summarising the original heuristic argument of Dyson [11] about the analyticity of observables in QED. The energy of a system consisting of a large number N of interacting particles, each one with charge $e \sim \sqrt{\alpha}$, is

$$E \sim NK + \frac{N^2}{2}\alpha V \,, \tag{2.3}$$

where K and V are respectively the mean kinetic and Coulomb energy, and $\binom{N}{2} \sim \frac{N^2}{2}$ is the number of interacting pairs. If $\alpha > 0$, then the energy increases as more particle are considered, and the system is stable and protected against pair production from the vacuum; on the other hand, in a universe where $\alpha < 0$ (i.e. equal/opposite charges attract/repel each other), for large enough N the system decreases its energy every time new particles are created: the Hamiltonian

is unbounded from below, and no ground state exists. As a consequence of this different behaviour reversing the sign of the coupling, physical quantities cannot be analytic functions of α.

The possibilities left are that either R_{pert} diverges or R_{pert} exists but differs from R by some non-analytic function. If we want to discard the situation in which R_{pert} does not provide any form of approximation to R, so that R and R_{pert} would be completely unrelated to each other, we must hope that R_{pert} is an asymptotic approximation of R: R_{pert} is *asymptotic* to R if, given some $N > N_0$ and an arbitrary $\epsilon > 0$, we can always find a neighbourhood A of the origin such that $|R_N(\alpha)| < \epsilon\,|\alpha^{N+1}|$ for all $\alpha \in A$. By this definition, a series may be asymptotic to a function without being convergent. A convergent series has a remainder that, for fixed α, vanishes as $N \to \infty$; an asymptotic series has a remainder that, for fixed N, is much smaller that the last retained term as $\alpha \to 0$. Even though R has a unique asymptotic power expansion around $\alpha = 0$, there are infinitely many functions, differing by subleading non-analytic terms, that share the same asymptotic power expansion.

It is widely believed that power series in quantum field theory are factorially divergent (unless symmetries are invoked). Let us focus again on Dyson's argument. When $\alpha < 0$, the critical number of particles that determines when the energy starts decreasing is $N_c = -K/(\alpha V)$. It is reasonable to expect that the power series R_{pert} converges up to an order $k \sim N_c$, since it is only at order N_c that diagrams allowing the creation of N_c particles from the vacuum come into play. When R_{pert} starts diverging, $r_k \alpha^k \sim r_{k+1}\alpha^{k+1}$ implies $r_{k+1}/r_k \sim 1/\alpha \sim N_c \sim k$, or $r_k \sim k!$. We will present concrete evidences supporting the factorial divergence in the following sections.

Starting from a divergent series R_{pert}, one might think of defining a new object

$$B[R_{\text{pert}}](z) = \sum_{n=0}^{\infty} \frac{r_n}{n!} z^n \,, \tag{2.4}$$

which clearly has higher chances to converge. We call $B[R_{\text{pert}}]$ the *Borel transform* of R_{pert}. If the Borel transform has a non-vanishing radius of convergence, the integral

$$\tilde{R}(\alpha) = \int_0^{\infty} dz\, e^{-z/\alpha}\, B[R_{\text{pert}}](z) \,, \tag{2.5}$$

defines the *Borel sum* of the series for $\alpha > 0$[1]. If $\tilde{R}$ exists, the series is said to be *Borel summable*. The definition of the Borel sum is trivial if $R_{\rm pert}$ converges: indeed, in that case we are entitled to exchange summation and integration, and it is easy to show that $\tilde{R} = R_{\rm pert}$. When a Borel summable $R_{\rm pert}$ diverges, then $\tilde{R}$ serves as a possible definition of the sum of the series. The conditions that guarantee $\tilde{R} = R$ are given by the Watson-Nevanlinna-Sokal theorem [12], and are not satisfied for QCD. This is another signal that perturbation theory is not enough to describe such a theory[2].

Nevertheless, the Borel transform is a useful tool for investigating factorially divergent patterns. The Borel transform computed from $r_n = K a^n \Gamma(n + 1 + \gamma)$ with $\gamma > 0$ is

$$B[R_{\rm pert}](z) = \frac{K\,\Gamma(1+\gamma)}{(1-az)^{1+\gamma}}\,. \tag{2.6}$$

The factorial growth is mapped to the pole (possibly a branch point as well, depending on γ) at $z = 1/a$ in the Borel plane: this pole is called *renormalon* [14]. It is worth mentioning that in the literature the term renormalon is reserved only for the kind of singularities that will be described in Sect. 2.4. Stronger divergences lead to poles closer to the origin: in particular, if $R_{\rm pert}$ is an alternating series ($a < 0$), the singularity lies on the negative z-axis, and the series is Borel summable; if $R_{\rm pert}$ is a fixed-sign series ($a > 0$), the singularity lies on the positive z-axis, and the integral in Eq. (2.5) is ill-defined. In the latter case, one could still give a prescription to move the contour above or below the pole. The finite value for $\tilde{R}$ obtained in this way is then affected by an intrinsic ambiguity related to the prescription used: a measure of this ambiguity is the

[1] For $\alpha < 0$ we could equally define

$$\hat{R}(\alpha) = -\int_{-\infty}^{0} dz\, e^{-z/\alpha}\, B[R_{\rm pert}](z)\,.$$

[2] Because of the shape of the analyticity region in QCD, other types of resummation suffer from the same problem, as explained in Ref. [13].

spurious imaginary part gained by $\tilde{R}$,

$$\begin{aligned}
\operatorname{Im}\tilde{R} &= K\,\Gamma(1+\gamma)\,\frac{\alpha\,e^{-1/(a\alpha)}}{(-a\alpha)^{1+\gamma}}\,\operatorname{Im}\int_{-1/(a\alpha)}^{+\infty} dt\,\frac{e^{-t}}{t^{1+\gamma}} = \\
&= K\,\Gamma(1+\gamma)\,\frac{\alpha\,e^{-1/(a\alpha)}}{(-a\alpha)^{1+\gamma}}\,\left(\mp\frac{2\pi}{2}\operatorname*{Res}_{t=0}\frac{e^{-t}}{t^{1+\gamma}}\right) = \\
&= K\,\Gamma(1+\gamma)\,\frac{\alpha\,e^{-1/(a\alpha)}}{(-a\alpha)^{1+\gamma}}\,\left(\frac{\mp\pi}{(-1)^{\gamma}\Gamma(1+\gamma)}\right) = \\
&= \pm\,\frac{\pi K}{a}\,\frac{e^{-1/(a\alpha)}}{(a\alpha)^{\gamma}}\,. \qquad (2.7)
\end{aligned}$$

It is interesting to note that the ambiguity is non-analytic in the variable α, which later will be identified with the coupling constant.

We will argue that singularities in the Borel plane might arise in field theory from stationary solutions of the action, and from the large- and small-momentum behaviour of loop integrals at high perturbative orders. The position of these singularities, and therefore Borel summability, depends on the theory under study. The interested reader can find a more complete survey about the divergence of perturbative expansions in quantum field theories in Refs. [13, 15, 16].

2.2 The role of instantons

One of the first methods for calculating high-order terms in perturbative series was proposed by Lipatov in Ref. [17]. The underlying idea can be explained by looking at a zero-dimensional version of the ϕ^4 theory: the partition function is

$$Z = \int d\phi\, e^{-\phi^2 - g\phi^4} = \sum_{n=0}^{+\infty} Z_n g^n\,, \qquad (2.8)$$

and Z_n are the coefficients of its perturbative expansion. Even though in this toy model it would be possible to compute the Z_n analytically, we seek only a way to have access to their asymptotic behaviour. Therefore, we express each coefficient with the residue formula,

$$Z_n = \int_C \frac{dg}{2\pi i g^{n+1}}\,Z = \int_C \frac{dg}{2\pi i g}\int d\phi\, e^{-\phi^2 - g\phi^4 - n\log g}\,, \qquad (2.9)$$

where C is a contour in the complex plane that goes around the origin in the anticlockwise direction, and then study the large-n limit of the integral. In the

saddle point approximation, we can look at the stationary points of the exponent: non-trivial saddle points, $\bar{\phi}$, $\bar{g}$, satisfy

$$\bar{\phi}^2 = -\frac{1}{2\bar{g}}, \qquad \bar{g} = -\frac{n}{\bar{\phi}^4} = -\frac{1}{4n}\,, \tag{2.10}$$

and we get readily (neglecting prefactors) the factorial divergence of the series,

$$Z_n \sim e^{-n-n\log\left(-\frac{1}{4n}\right)} \sim (-4)^n n!\,. \tag{2.11}$$

This is a first hint that classical solutions (with finite and non-zero action) of the equations of motion, i.e. *instantons*, are related to factorial divergences. A formal way to understand this connection is provided by 't Hooft [14]: starting from the partition function

$$Z = \int \mathcal{D}\phi\, e^{-S[\phi]} = \int_0^{+\infty} dt\, e^{-t}\, B(t)\,, \tag{2.12}$$

we define the Borel transform

$$B(t) = \int \mathcal{D}\phi\, \delta(t - S[\phi]) = \int_{S[\phi]=t} \frac{\mathcal{D}\sigma}{|\nabla S[\phi]|}\,, \tag{2.13}$$

where in the last equality the simple layer formula[3] was used to turn the functional integral into a surface integral on the hypersurface (embedded in the functional space of all possible field configurations) defined implicitly by the level set $S[\phi] = t$. At the denominator we find the norm of the gradient of the action $|\nabla S[\phi]| = \left\|\frac{\delta S[\phi]}{\delta\phi(x)}\right\|$. It is evident that the Borel transform develops a pole (in general, a branch point) whenever ϕ is a classical solution of the equations of motion. Close to the singularity, the Borel transform can be approximated with

$$B(t) \simeq \int_{t=\bar{t}+\frac{1}{2}v^T H v} \frac{\mathcal{D}\sigma}{\sqrt{v^T H^2 v}}\,, \tag{2.14}$$

where we switched to a handier notation,

$$H_{x,y} = \left.\frac{\delta^2 S[\phi]}{\delta\phi(x)\delta\phi(y)}\right|_{\bar{\phi}}, \qquad v_x = \phi(x) - \bar{\phi}(x)\,, \tag{2.15}$$

and $\bar{\phi}$ is a stationary solution with action $S[\bar{\phi}] = \bar{t}$. If U is the unitary transformation that diagonalises H, then it is easy to see that field configurations

[3] See Theorem 6.1.5 in Ref. [18].

of the form $v_x \propto U_{x,x_0}$ lead to a square root branch point contribution,

$$\frac{\mathrm{Tr}\, H^{-1/2}}{\sqrt{2(t-\bar{t}\,)}}\,. \tag{2.16}$$

As it was shown in Sect. 2.1, a pole in the Borel representation corresponds to a factorial divergence in perturbation theory: if $B(t) \sim (1-t/\bar{t}\,)^{-\alpha}$, then[4]

$$\begin{aligned}\int_0^{+\infty} dt\, e^{-t}\,(1-t/\bar{t}\,)^{-\alpha} &= \int_0^{+\infty} dt\, e^{-t} \sum_{n=0}^{+\infty} \frac{\Gamma(n+\alpha)}{\Gamma(\alpha)} \frac{1}{n!} \left(\frac{t}{\bar{t}}\right)^n = \\ &= \sum_{n=0}^{+\infty} \frac{\Gamma(n+\alpha)}{\Gamma(\alpha)}\,(\bar{t}\,)^{-n}\,. \end{aligned} \tag{2.17}$$

The leading divergence of the perturbative series is associated to the pole closest to the origin. For example, in Yang-Mills theory we expect singularities associated to BPST instantons [19]: since the action of a single instanton is $S = 8\pi^2/g^2$, we expect an infinite series of poles on the positive real axis at $t = 8N\pi^2/g^2$ (N is the instanton winding number). These singularities make the integral in Eq. (2.17) ill-defined, confirming that QCD is not a Borel resummable theory.

A final remark is in order: when the number of degrees of freedom is finite, 't Hooft argument in Eq. (2.13) provides a necessary and sufficient condition for having singularities in the Borel transform of the partition function. This means that there would be no room for the singularities at $t = \beta z_0 = \frac{\sigma}{b_0 g^2}$ that we will study in Sect. 2.4. These latter singularities can arise only in the limit of infinite number of degrees of freedom. Some authors have argued that, even in that case, their existence is controversial [20, 21].

2.3 Nonperturbative corrections to the OPE

The Operator Product Expansion (OPE) is a technique introduced by Wilson [22] to evaluate the product of local operators at short distances in perturbation theory. If $A(x)$ and $B(y)$ are local operators, we can factorise their product at

[4] The saddle points have an action proportional to the inverse of the coupling, thus the expansion must be performed in $\bar{t}^{-1}$.

short distance, $|x-y| \to 0$, as

$$A(x)B(y) = C_{\mathbb{1}}(x-y)\mathbb{1} + \sum_n C_n(x-y)O_n(x,y)\,, \tag{2.18}$$

where the coefficients $C_{\mathbb{1}}$, C_n are called *Wilson coefficients* (singular functions as $x \to y$), and $O_n(x,y)$ are bilocal normal-ordered operators (regular as $x \to y$). By definition, normal-ordered operators have a vanishing vacuum expectation value, implying that

$$\langle 0|A(x)B(y)|0\rangle = C_{\mathbb{1}}(x-y)\,. \tag{2.19}$$

It is useful to order the right-hand side of Eq. (2.18) according to the operator dimensions: then, by dimensional analysis, the Wilson coefficients will be less and less singular as n increases. In this way, the first few terms of the OPE capture the leading behaviour as $x \to y$, while the operators $O_n(x,y)$ can be safely Taylor expanded in terms of local operators. The fundamental characteristic of the OPE is that it holds as an operator identity, i.e. when $A(x)B(x)$ is inserted in any correlator: the Wilson coefficients needs to be computed only once, and they will be the same for all physical processes.

The OPE has been rigorously proved in perturbation theory only [23–25]. Nevertheless, it is interesting to make use of this tool a little bit outside of its original scope, and examine how nonperturbative effects modify the perturbative predictions at short distances. The idea proposed in QCD by Shifman, Vainshtein and Zakharov [26, 27] is to consider the role of the physical vacuum in the OPE. It might be the case that Eq. (2.19) holds only in the perturbative vacuum; in the physical nonperturbative vacuum, composite local operators appearing in the OPE might develop a non-zero expectation value. Indeed, the physical vacuum in QCD exhibits characteristics, like chiral symmetry breaking and confinement, that cannot be inferred from a perturbative analysis. The implications for Eq. (2.19) are more transparent in momentum space, where instead of short distances we deal with high momentum Q: it can be postulated that the Fourier transform of the vacuum expectation value of the product of two operators has the following expansion,

$$i\int d^4x\, e^{iQ\cdot x}\langle A(x)B(0)\rangle = C_{\mathbb{1}}(Q)\langle\mathbb{1}\rangle + \sum_n C_n(Q)\langle O_n\rangle\,. \tag{2.20}$$

Since the O_n are ordered according to their dimension, the coefficients $C_n(Q)$ will appear with increasing powers of $1/Q$: the effect of nonperturbative physics

is encoded in these *power corrections*. The quantities $\langle O_n \rangle$ are the *condensates*: they are fundamental quantities, which are in principle supposed to parametrise power corrections in a universal way. While the explicit form of the functions $C_n(Q)$ depends on the operators A, B, under study, by determining the value of a condensate in one context, one gains insight into different physical processes. We stress again that condensates are chosen to vanish in perturbation theory or, in other words, they are normal ordered in the perturbative vacuum[5]. This definition is somehow natural in dimensional regularisation, where $\int d^D p \, (p^2)^\lambda = 0$ is assumed for all complex D, λ [29].

In asymptotically free theories, perturbation theory can be applied at short distances, where the coupling is small. In this respect, Eq. (2.20) disentangles in a physical process the short-distance contribution, which is computed in perturbation theory, from the long-distance contribution, which is dominated by nonperturbative effects. The separation between these two regimes must be set at some scale μ (with $\Lambda < \mu < Q$). In other words, this factorisation is realised by integrating the high-frequency contributions down to the scale μ: in the new effective description, the operators O_n and the Wilson coefficients encode respectively long- and short-distance physics.

Since the separation of scales in the OPE does not correspond completely to a separation between perturbative and nonperturbative physics, defining the condensate as a purely nonperturbative object might lead to ambiguities (see the interesting discussions in Refs. [30, 31]). This is not always the case: for example, the *fermion condensate* is well defined since, being the order parameter of chiral symmetry breaking, it must vanish in perturbation theory. On the other hand, the *gluon condensate* O_G is not the order parameter of any spontaneously broken symmetry, and the above definition is ambiguous [32]. One could also notice that O_G, in its renormalisation group invariant form, is proportional to the β-function, and could then be related to the breaking of scale invariance due to quantum effects. The fact that scale symmetry breaking appears in perturbation theory tells us that a purely nonperturbative definition of O_G cannot lead to a sound OPE. This ambiguity is reflected in the fixed-sign factorial growth of the perturbative series for $C_{\mathbb{1}}$: the choice of a prescription to sum such divergent series turns out to have an ambiguity that cancels exactly the one associated with O_G. The divergence in the Wilson coefficient goes under the name of *infrared*

[5] It is useful to keep in mind that other definitions of condensates are possible, see e.g. Ref. [28].

renormalon [14, 33–36]. We point out that renormalons would not be present if the OPE were evaluated strictly in Wilson's spirit, embedding in the Wilson coefficients only contributions from momenta $k > \mu$, as it will be shown in detail at the end of Sect. 2.4. Renormalons arise because such rigid cutoff is clearly unpractical in real calculations, with dimensional or lattice regularisations, and arbitrary small momenta are always included in the Wilson coefficients instead.

2.4 Renormalons

Following Refs. [37, 38], the renormalisation group invariant form of the expectation value of a dimension-2σ correlator is

$$W = \int_0^{Q^2} \frac{dk^2}{k^2} \left(\frac{k^2}{Q^2}\right)^\sigma f(k)\,, \tag{2.21}$$

where $f(k) = f\left(\frac{k}{Q}, \alpha_R(Q)\right)$ is some dimensionless renormalisation group invariant function, and Q is a hard scale[6]. Here we do not wish to consider what happens for momenta greater than Q. In that case, new sources of factorial divergence would be present: these are called *ultraviolet renormalons*. In an asymptotically free theory, ultraviolet renormalons do not lead to ambiguities when resumming the divergent series. They can be removed by adding higher-dimensional operators to the Lagrangian, and are completely understood as a renormalisation effect [34].

The function $f(k)$ is given at first order by one-gluon exchange diagrams, so it must be proportional to $\alpha_R(k)$. Therefore, we can take $f(k) = \alpha_R(k)$, as it can be argued that having higher powers of $\alpha_R(k)$ in Eq. (2.21) would lead to the same conclusions we will obtain in the following. Clearly the running coupling in Eq. (1.17) makes W divergent due to the Landau pole in the domain of integration: this signals that the small-momentum behaviour is influenced by nonperturbative physics, i.e. the theory is strongly coupled in the infrared. We will see that the perturbative expansion of $\alpha_R(k)$ will turn the small momentum behaviour into a factorial divergence.

To understand the structure of W, we try to recast Eq. (2.21) in the form of a Borel representation. By integrating exactly the two-loop running coupling in

[6] On the lattice one has naturally $Q \sim 1/a$.

Eq. (1.12), we obtain

$$\log\frac{k}{Q} = -\frac{1}{2b_0 g_R(Q)^2}\left[1-\frac{g_R(Q)^2}{g_R(k)^2}\right] + \\ + \log\left(\frac{g_R(k)}{g_R(Q)}\right)^{b_1/b_0^2} + \log\left(\frac{1+\frac{b_1}{b_0}\,g_R(k)^2}{1+\frac{b_1}{b_0}\,g_R(Q)^2}\right)^{-b_1/(2b_0^2)}, \tag{2.22}$$

or

$$\left(\frac{k^2}{Q^2}\right)^{\sigma} = e^{-z\beta}\left(\frac{\alpha_R(Q)}{\alpha_R(k)}\right)^{-\gamma}\left(\frac{1+\frac{4\pi b_1}{b_0}\,\alpha_R(k)}{1+\frac{4\pi b_1}{b_0}\,\alpha_R(Q)}\right)^{-\gamma} \\ = e^{-z\beta}\left(1-\frac{z}{z_0}\right)^{-\gamma}\left(\frac{1+\frac{b_1}{b_0}\,\frac{2N_c}{\beta}\,\frac{1}{1-\frac{z}{z_0}}}{1+\frac{b_1}{b_0}\,\frac{2N_c}{\beta}}\right)^{-\gamma}, \tag{2.23}$$

where we introduced the new variables

$$z = z_0\left(1-\frac{\alpha_R(Q)}{\alpha_R(k)}\right), \quad z_0 = \frac{\sigma}{2N_c b_0}, \quad \gamma = \frac{\sigma b_1}{b_0^2}, \tag{2.24}$$

and $\beta = 2N_c/g_R(Q)^2$ corresponds to a Wilson action coupling. It is useful now to change the integration variable in Eq. (2.21) from k to the z defined in Eq. (2.24): even though the original domain of integration includes the Landau pole, where $\alpha_R(k)$ diverges, the variable z is formally well defined and monotonic, as shown in Figure 2.1. Using again the two-loop running coupling, we have that

$$\frac{dk^2}{k^2}\alpha_R(k) = -\frac{dz}{z_0}\frac{1}{4\pi b_0}\left(\frac{\alpha_R(Q)}{\alpha_R(k)}\right)^{-1}\frac{1}{1+\frac{4\pi b_1}{b_0}\,\alpha_R(k)} = \\ = -\frac{dz}{z_0}\frac{1}{4\pi b_0}\left(1-\frac{z}{z_0}\right)^{-1}\frac{1}{1+\frac{b_1}{b_0}\,\frac{2N_c}{\beta}\,\frac{1}{1-\frac{z}{z_0}}}. \tag{2.25}$$

Thanks to the change of variable, W has been reshaped in a form resembling a Borel representation,

$$W = \int_0^{+\infty}\frac{dz}{4\pi b_0 z_0}\,\frac{e^{-\beta z}}{\left(1-\frac{z}{z_0}\right)^{1+\gamma}}\,\frac{\left(1+\frac{b_1}{b_0}\,\frac{2N_c}{\beta}\right)^{\gamma}}{\left(1+\frac{b_1}{b_0}\,\frac{2N_c}{\beta}\,\frac{1}{1-\frac{z}{z_0}}\right)^{1+\gamma}} = \\ = \frac{1}{4\pi b_0 z_0}\int_0^{+\infty}\frac{dz}{1+\frac{b_1}{b_0}\,\frac{2N_c}{\beta}}\,\frac{e^{-\beta z}}{\left(1-\frac{1}{1+\frac{b_1}{b_0}\,\frac{2N_c}{\beta}}\,\frac{z}{z_0}\right)^{1+\gamma}}. \tag{2.26}$$

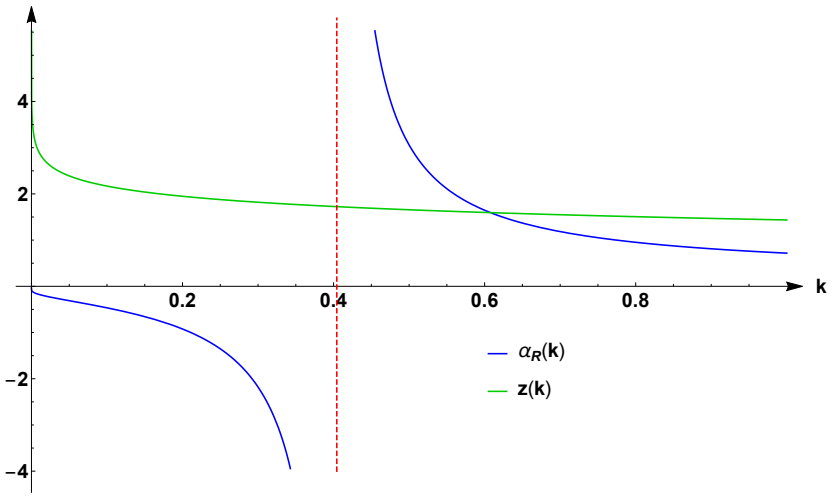

Figure 2.1 *One-loop running coupling $\alpha_R(k)$, compared to the corresponding variable z defined in Eq.* (2.24) *(both axes are in arbitrary units). The vertical asymptote in red is the leading-order evaluation of Λ. Even though the coupling diverges at the Landau pole, the new variable z is well defined at all scales.*

So far, the perturbative expansion in the coupling has not been performed yet, and this expression is exact in the limit of switching off all the coefficients of the β-function higher than b_1.

Setting $b_1 = 0$ as well, i.e. considering the one-loop β-function only, we indeed recover the Borel integral

$$W = \frac{1}{4\pi b_0 z_0} \int_0^{+\infty} dz \, \frac{e^{-\beta z}}{1 - \frac{z}{z_0}} \,. \tag{2.27}$$

The result of the integration is still divergent, because of the pole at $t = \beta z_0$: this is the infrared renormalon. As usual, the renormalon in the Borel transform implies the factorial divergence of the perturbative evaluation of W: expanding the integrand in β and exchanging summation with integration, it is

$$\begin{aligned} W_{\text{ren}} &= \frac{1}{4\pi b_0 z_0 \beta} \sum_{n=0}^{+\infty} \int_0^{+\infty} dt \, e^{-t} \left(\frac{t}{\beta z_0} \right)^n \\ &= \sum_{n=0}^{+\infty} \frac{c_n}{\beta^{n+1}} \,, \quad \text{with} \quad c_n = \frac{\Gamma(n+1)}{4\pi b_0} \frac{1}{z_0^{n+1}} \,. \end{aligned} \tag{2.28}$$

The divergence of the original integral is reflected in the fixed-sign factorial growth of its perturbative expansion.

On the other hand, it is striking that a simple rescaling of z is enough to compute

exactly the Borel transform at two loops [39]: if we define $\tilde{z} = z/(1 + \frac{b_1}{b_0}\frac{2N_c}{\beta})$, then Eq. (2.26) leads to an exact Borel representation in the shifted coupling $\tilde{\beta} = \beta + \frac{2N_c b_1}{b_0}$,

$$W = \frac{1}{4\pi b_0 z_0} \int_0^{+\infty} d\tilde{z}\, \frac{e^{-\tilde{\beta}\tilde{z}}}{\left(1 - \frac{\tilde{z}}{z_0}\right)^{1+\gamma}}\,. \tag{2.29}$$

The position of the pole is not modified, but $b_1 \neq 0$ unveils the branch-point nature of $\tilde{z} = z_0$. An expansion in β leads to

$$W_{\rm ren} = \sum_{n=0}^{+\infty} \frac{\Gamma(n+1+\gamma)}{4\pi b_0 \Gamma(1+\gamma)} \frac{1}{\tilde{\beta}^{n+1}} = \sum_{n=0}^{+\infty} \frac{c'_n}{\beta^{n+1}} \tag{2.30}$$

with

$$c'_n = \frac{\Gamma(n+1+\gamma)}{4\pi b_0 \Gamma(1+\gamma)} \frac{1}{z_0^{n+1}} \sum_{k=0}^{n} \binom{n}{k} \frac{\Gamma(k+1+\gamma)}{\Gamma(n+1+\gamma)} (-\gamma)^{n-k}\,, \tag{2.31}$$

and the relation between $\tilde{\beta}^{-1}$ and β^{-1} is given by the binomial series

$$\frac{1}{\tilde{\beta}^{n+1}} = \frac{1}{\beta^{n+1}} \sum_{k=0}^{+\infty} \binom{n+k}{n} \left(-\frac{b_1}{b_0}\frac{2N_c}{\beta}\right)^k\,. \tag{2.32}$$

Collecting in some constant C all the higher-order corrections that contribute to the same singularity, the contribution due to the leading renormalon reads

$$W_{\rm ren} = \sum_{n=0}^{+\infty} \frac{c_n^{\rm ren}}{\beta^{n+1}} \qquad \text{with} \qquad c_n^{\rm ren} = \frac{C}{z_0^{n+1}}\,\Gamma(n+1+\gamma)\,. \tag{2.33}$$

It is interesting to try and define the integral in Eq. (2.26) by avoiding the pole in the domain of integration. For any prescription, we know from Eq. (2.7) that the integral acquires an imaginary part proportional to the residue at the pole: the imaginary part turns out exactly equal to

$$\pi C\,(z_0\beta)^\gamma\, e^{-\beta z_0} = \pi C\,(2N_c z_0)^\gamma \left(\frac{\Lambda}{Q}\right)^{2\sigma}\,. \tag{2.34}$$

Such ambiguity is nonperturbative in the coupling, and corresponds to a power correction in Λ, as defined from Eq. (1.16). It is a common belief that the ambiguity is going to be cancelled exactly by the corresponding ambiguity in the definition of the condensate: therefore the renormalon is by itself a signal that

power corrections ought to be added in the OPE,

$$W = W_{\rm ren} + O(e^{-\beta z_0})\,. \tag{2.35}$$

We can also adopt another point of view and consider the high-frequency contributions of Eq. (2.21), as in Refs. [38, 40]. In the spirit of the OPE, we might want to adhere to a strict scale separation paradigm, and include in W only momenta above $\mu = r\Lambda$ for some $r > 1$,

$$W_0 = \int_{r^2\Lambda^2}^{Q^2} \frac{dk^2}{k^2} \left(\frac{k^2}{Q^2}\right)^\sigma \alpha_R(k)\,. \tag{2.36}$$

Now the domain of integration avoids the Landau pole, and W_0 is expected to converge. To understand how this can happen, we can retrace the same steps as before to compute the Borel transform of W_0 (with $b_1 = 0$, for simplicity). With the same change of variable from k to z, the new domain of integration becomes

$$0 < z < z_{\rm IR} = z_0 \left(1 - \frac{\alpha_R(Q)}{\alpha_R(r\Lambda)}\right)\,, \tag{2.37}$$

and since $z_{\rm IR} < z_0$, the quantity

$$W_0 = -\frac{e^{-\beta z_{\rm IR}}}{4\pi b_0} \int_{-\beta z_0}^{-\beta(z_0 - z_{\rm IR})} dt\, \frac{e^{-t}}{t} \tag{2.38}$$

is not affected by any singularity. W_0 can be expressed in terms of incomplete Gamma functions[7],

$$W_0 = -\frac{e^{-\beta z_0}}{4\pi b_0} \left[\Gamma\left(0, -\beta z_0\right) - \Gamma\left(0, -\beta(z_0 - z_{\rm IR})\right)\right]\,, \tag{2.40}$$

[7] The incomplete gamma function is defined as

$$\Gamma(s,z) = \int_z^{+\infty} dt\, e^{-t}\, t^{s-1} = z^{s-1}\, e^{-z} \sum_{k=0}^{+\infty} \frac{\Gamma(k+1-s)}{\Gamma(1-s)}\, (-z)^{-k}\,, \tag{2.39}$$

where the last equality holds for $|z| \to +\infty$ and $|\arg z| < 3\pi/2$ (see e.g. http://dlmf.nist.gov/8.11.E2).

and expanded in β^{-1} as

$$W_0 = \frac{1}{4\pi b_0 \beta z_0} \sum_{n=0}^{+\infty} \frac{\Gamma(n+1)}{(\beta z_0)^n} \left[1 - \frac{e^{-\beta z_{\rm IR}}}{\left(1 - \frac{z_{\rm IR}}{z_0}\right)^{n+1}} \right] = \\ = \sum_{n=0}^{+\infty} \frac{c_n}{\beta^{n+1}} \left[1 - \frac{e^{-\beta z_{\rm IR}}}{\left(1 - \frac{z_{\rm IR}}{z_0}\right)^{n+1}} \right] . \tag{2.41}$$

From the one-loop running coupling it is straightforward to compute

$$z_{\rm IR} = -\frac{2\sigma}{\beta} \log \frac{r\Lambda}{Q} , \tag{2.42}$$

and obtain

$$W_0 = \sum_{n=0}^{+\infty} \frac{c_n}{\beta^{n+1}} \left[1 - \frac{\left(\frac{r\Lambda}{Q}\right)^{2\sigma}}{\left(1 + \frac{4N_c b_0}{\beta} \log \frac{r\Lambda}{Q}\right)^{n+1}} \right] \\ = \sum_{n=0}^{+\infty} \frac{c_n}{\beta^{n+1}} \left[1 - \left(\frac{r\Lambda}{Q}\right)^{2\sigma} d_n \right] = \sum_{n=0}^{+\infty} \frac{f_n}{\beta^{n+1}} \tag{2.43}$$

with

$$d_n = \sum_{k=0}^{n} \binom{n}{k} \frac{c_k}{c_n} \left(-4N_c b_0 \log \frac{r\Lambda}{Q} \right)^{n-k} = \sum_{k=0}^{n} \frac{1}{k!} \left(2\sigma \log \frac{Q}{r\Lambda} \right)^k . \tag{2.44}$$

The renormalon growth is explicitly modified by a power correction with the same dimension as W. This power correction is essential for the convergence of W_0: indeed, as $n \to +\infty$, the sum in Eq. (2.44) approximates an exponential series, $d_n \sim \left(\frac{Q}{r\Lambda}\right)^{2\sigma}$, and the factorial growth is exactly cancelled, as shown in Figure 2.2. This mechanism is analogous to the one described in Ref. [41] for the exponentiation of finite-volume effects. It must also be said that higher perturbative orders are more sensitive to higher coefficients of the β-function: an analysis of the behaviour of the series at large (not infinite) values of n should take this fact into account.

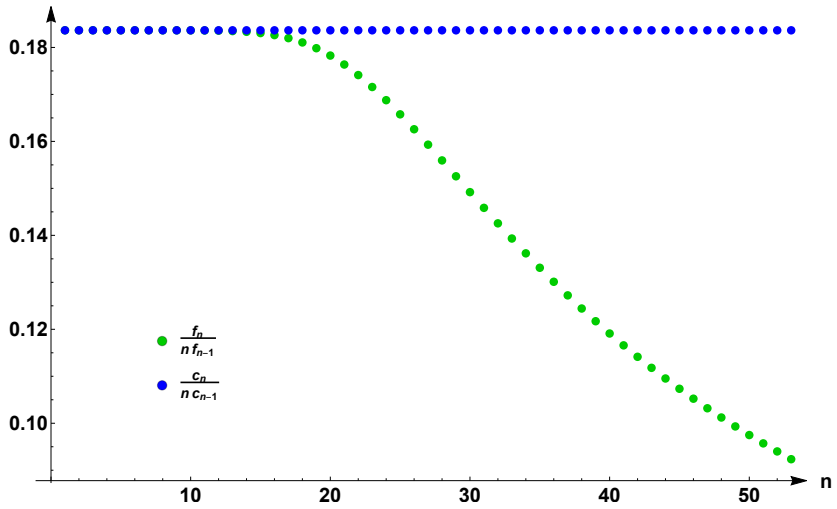

Figure 2.2 *Comparison between the coefficients c_n, defined in Eq.* (2.33)*, and f_n, defined in Eq.* (2.43) *(both axes are in arbitrary units). The series associated to W_0 does not display a factorial growth thanks to the introduction of the infrared cutoff $r\Lambda$.*

2.5 How to determine condensates from lattice simulations

So far, we did not put emphasis on the fact that condensates are composite operators: we will address now the problem of their renormalisation, and of how they can be extracted from lattice simulations [42–45].

Let us consider a theory regularised by a cutoff $1/a$, and let $O(a)$ be a bare composite operator of dimension d. It is possible to define a renormalised operator through

$$O_R(\mu) = Z_O(g, a\mu) \left[O(a) - \sum_{k=0}^{d-1} \frac{\tilde{Z}_{O_k}(g)}{a^{d-k}} O_k(a) \right] . \tag{2.45}$$

$Z_O(g, a\mu)$ represents the multiplicative renormalisation of O, and depends on the bare coupling g and the renormalisation scale μ. In perturbation theory, it can be expressed as a power series in g where the coefficient of the term g^k is a polynomial in $\log a\mu$ of order $k-1$. We are assuming for simplicity that O does not mix with operators of the same dimension (otherwise Z_O would be a matrix). The second term in the square brackets represents mixing with lower-dimensional operators and acts as an additive renormalisation to eliminate power divergences. We can call

$$O_{\text{sub}} = \sum_{k=0}^{d-1} \tilde{Z}_{O_k}(g)\, a^k\, O_k(a) = \sum_{k=0}^{d-1} \tilde{Z}_{O_k}(g)\, O_{L,k} \, . \tag{2.46}$$

The operator $O_k(a) = a^{-k} O_{L,k}$ has dimension k, and the coefficient $\tilde{Z}_{O_k}(g)$ does not depend on the scale (in perturbation theory, it is a power series in g without any logarithm) [46]. In particular, we note that $O_0 = \mathbb{1}$: the contribution emerging from the perturbative evaluation of $\langle O(a) \rangle$ corresponds to the expansion in g of $\tilde{Z}_{\mathbb{1}}(g)$. The renormalisation procedure assures that, in any correlation function, we can take safely the limit $a \to 0$ in the right-hand side to obtain a finite result.

Evaluating the renormalisation factors in perturbation theory defines a scheme to subtract power divergences[8]: $\langle O_R(\mu) \rangle$ vanishes in perturbation theory or, in other words, condensates are normal ordered in the perturbative vacuum. In a common jargon, in order to extract a condensate one must isolate a nonperturbative residue from the perturbative background, i.e. one must subtract a *perturbative tail*.

It is evident that this procedure is not well defined: if the series for $\tilde{Z}_{\mathbb{1}}(g)$ is truncated at some fixed order, then the unsubtracted residue would still scale as a^{-d}, and diverge in the continuum limit. Moreover, it is not possible to sum all the terms of the series for $\tilde{Z}_{\mathbb{1}}(g)$ as, from the discussion in Sect. 2.3, it is a divergent series affected by renormalons. The only chance to save this scheme is to impose a prescription to resum the divergent series: clearly this has a price, and any prescription comes with an intrinsic ambiguity associated to the sum. Thus, a corresponding ambiguity must be assigned to the condensate itself. For example, a possible prescription is to stop the series for $\tilde{Z}_{\mathbb{1}}(g)$ at its minimum term, so that the order of truncation grows as the continuum limit ($g \to 0$) is approached. We will talk in detail about this prescription in Sect. 6.4.

After having defined a scheme to deal with the objects in Eq. (2.45), we can go on and study the renormalisation group properties of $O_R(\mu)$, encoded in the evolution equation

$$\mu \frac{d}{d\mu} O_R(\mu) = \gamma_O(g_R) O_R(\mu) \,, \tag{2.47}$$

with the anomalous dimension

$$\gamma_O(g_R) = \mu \frac{d}{d\mu} \log Z_O(g, a\mu) \,. \tag{2.48}$$

As it is evident from Eq. (2.47), the anomalous dimension and the renormalised operator cannot depend on the cutoff: they must be functions of the running

[8] It is worth mentioning the existence of other schemes in which power divergences are subtracted nonperturbatively, see e.g. Ref. [47].

coupling only, which is defined through $g = g_R(\mu) Z_g(g, a\mu)$. This observation allows expanding the anomalous dimension as

$$\gamma_O(g_R) = \gamma_{O,1}\, g_R(\mu)^2 + \gamma_{O,2}\, g_R(\mu)^4 + \dots\,, \tag{2.49}$$

and to write Eq. (2.47) as

$$\beta(g_R)\frac{d}{dg_R} O_R(\mu) = \gamma_O(g_R) O_R(\mu)\,. \tag{2.50}$$

The renormalisation group equation is solved exactly by

$$\begin{aligned} O_R(\mu) &= O_R(\bar\mu) \exp\left[\int_{g_R(\bar\mu)}^{g_R(\mu)} dg'\, \frac{\gamma_O(g')}{\beta(g')}\right] = \\ &= O_R(\bar\mu) \exp\left[\left(\int_{g_R(\bar\mu)}^{0} + \int_0^{g_R(\mu)}\right) dg'\, \left(\frac{\gamma_O(g')}{\beta(g')} + \frac{\gamma_{O,1}}{b_0 g'}\right)\right] \left(\frac{g_R(\mu)}{g_R(\bar\mu)}\right)^{-\gamma_{O,1}/b_0} = \\ &= \frac{\Gamma_O(\bar\mu)}{\Gamma_O(\mu)}\, O_R(\bar\mu)\,, \end{aligned} \tag{2.51}$$

where we introduced the quantity

$$\Gamma_O(\mu) = g_R(\mu)^{\gamma_{O,1}/b_0} \exp\left[-\int_0^{g_R(\mu)} dg'\, \left(\frac{\gamma_O(g')}{\beta(g')} + \frac{\gamma_{O,1}}{b_0 g'}\right)\right]. \tag{2.52}$$

Subtracting the one-loop anomalous dimension term allowed extending to zero the lower limit of the domain of integration. We realise soon that the combination

$$O_{\rm RGI} = \Gamma_O(\mu)\, O_R(\mu) = \Gamma_O(\bar\mu)\, O_R(\bar\mu) \tag{2.53}$$

is renormalisation group invariant. Having found a renormalisation group invariant combination turns out particularly useful, as the renormalisation of $O_{\rm RGI}$ reads

$$\begin{aligned} O_{\rm RGI} &= \Gamma_O(\mu) Z_O(g, a\mu)\, \left[O(a) - a^{-d}\, O_{\rm sub}\right] = \\ &= \Gamma_O(1/a) Z_O(g, 1)\, \left[O(a) - a^{-d}\, O_{\rm sub}\right]\,, \end{aligned} \tag{2.54}$$

where we could set $\mu = 1/a$ in the last step thanks to scale invariance. Considering that only the dimensionless product

$$\langle O_L \rangle = a^d \langle O(a) \rangle \tag{2.55}$$

can be accessed in a Monte Carlo lattice simulation, and that the lattice size is determined with respect to some reference length scale r_0, then

$$r_0^d \langle O_{\rm RGI}\rangle = \Gamma_O(1/a) Z_O(g,1) \left(\frac{r_0}{a}\right)^d \left[\langle O_L\rangle - \langle O_{\rm sub}\rangle\right] = \\ = \Gamma_O(1/a) Z_O(g,1) \left(\frac{r_0}{a}\right)^d \left[\langle O_L\rangle - \sum_{k=0}^{d-1} \tilde{Z}_{O_k}(g) \langle O_{L,k}\rangle\right] . \qquad (2.56)$$

This is the equation that allows extracting condensates from lattice simulations.

A few remarks are now in order. The quantity $Z_O(g,1)$ is free of any logarithm, and represents a finite renormalisation which goes to 1 in the continuum limit. A similar comment[9] holds for $\Gamma_O(1/a)$, apart from the overall factor $g^{\gamma_{O,1}/b_0}$. It is striking that an equation like

$$O(a) = a^{-d} O_{\rm sub} + \frac{1}{\Gamma_O(\mu) Z_O(g, a\mu)} O_{\rm RGI} = \\ = a^{-d} O_{\rm sub} + g^{-\gamma_{O,1}/b_0} \left(1 + C_1 g^2 + \dots\right) O_{\rm RGI} \qquad (2.57)$$

can be seen as an OPE with $Q \sim 1/a$, where irrelevant operators in the right-hand side would correspond to higher-dimensional terms in the OPE.

2.6 The gluon condensate

The idea of determining the gluon condensate from nonperturbative measurements in lattice gauge theories dates back to the eighties and early nineties [48–54]. These attempts are based on comparing perturbative computations of Wilson loops with the corresponding Monte Carlo determinations. In order to define the gluon condensate, we need to address the problem of renormalising the operator F^2. We will describe the renormalisation properties of F^2 with the background field method, introduced in the next sections.

2.6.1 The background field method

The renormalisation of gauge-invariant operators can be conveniently studied with the *background field method*. We will show that the effective action of a

[9] We note that the relation $g = Z_g(1/a,1) g_R(1/a)$ is also equivalent to a finite renormalisation of the coupling.

theory can be related to the vacuum effective action of the same theory in a classical background. This is an extremely useful property, because in gauge theories it will be possible to preserve gauge invariance with respect to the background field, greatly simplifying the renormalisation procedure. The reader is referred to Refs. [55–58] for some reviews and applications of this method, and for references to the original works. We will now briefly summarise the main aspects of this approach.

The generating functional $Z[J]$ and the connected generating functional $W[J]$ are defined by[10]

$$Z[J] = e^{W[J]} = \int \mathcal{D}A\, e^{-S[A]+JA}\,. \tag{2.59}$$

The derivatives of $Z[J]$ with respect to J generate insertions of A in a correlator,

$$\frac{1}{Z[0]}\frac{\delta}{\delta J(x_1)}\cdots\frac{\delta}{\delta J(x_n)}Z[J]\bigg|_{J=0} = \langle A(x_1)\ldots A(x_n)\rangle\,. \tag{2.60}$$

The effective action generates the one-particle irreducible vertices, and is defined as the Legendre transform respect to the source,

$$\Gamma[\bar{Q}] = W[J_{\bar{Q}}] - J_{\bar{Q}}\,\bar{Q}\,, \tag{2.61}$$

where the inverse of the relation

$$\bar{Q} = \frac{\delta W[J]}{\delta J}\bigg|_{J=J_{\bar{Q}}} = \frac{1}{Z[J]}\frac{\delta Z[J]}{\delta J}\bigg|_{J=J_{\bar{Q}}} = \langle A\rangle_{J_{\bar{Q}}} \tag{2.62}$$

defines the source $J_{\bar{Q}}$ as a function of the conjugated variable. In particular, $J_{\bar{Q}}$ is the source that induces an expectation value of A equal to $\bar{Q}$.

The renormalisation theorem ensures that it is possible to rescale the fields ($\bar{Q} = Z_{\bar{Q}}^{1/2}\bar{Q}_R$) and coupling ($g = Z_g g_R$) so that the renormalised effective action

$$\Gamma_R[\bar{Q}_R; g_R] = \Gamma[Z_{\bar{Q}}^{1/2}\bar{Q}_R; Z_g g_R] \tag{2.63}$$

is finite.

[10] The contraction of all indices (including spacetime indices) is understood: if A is the gauge potential, then

$$JA = \int d^4x \sum_{a,\mu} A^a_\mu(x) J^a_\mu(x) = 2\int d^4x \sum_\mu \mathrm{Tr}\, A_\mu(x) J_\mu(x)\,. \tag{2.58}$$

We consider the partition function obtained by shifting the quantum field with a classical background B, and define

$$Z_B[J] = e^{W_B[J]} = \int \mathcal{D}Q\, e^{-S[B+Q]+JQ}\,, \tag{2.64}$$

where we choose not to couple the background field with the source. It is useful to switch to a new variable $A = B + Q$ to understand the relation between $W_B[J]$ and $W[J]$,

$$e^{W_B[J]} = \int \mathcal{D}A\, e^{-S[A]+J(A-B)} = e^{W[J]-JB}\,. \tag{2.65}$$

The Legendre transform of $W_B[J]$ reads

$$\Gamma_B[\tilde{Q}] = W_B[\mathcal{J}_{\tilde{Q}}] - \mathcal{J}_{\tilde{Q}}\,\tilde{Q}\,, \tag{2.66}$$

where the source $\mathcal{J}_{\tilde{Q}}$ is fixed from

$$\tilde{Q} = \left.\frac{\delta W_B[J]}{\delta J}\right|_{J=\mathcal{J}_{\tilde{Q}}} = \left.\frac{\delta W[J]}{\delta J}\right|_{J=\mathcal{J}_{\tilde{Q}}} - B\,. \tag{2.67}$$

We emphasise that $J_{\bar{Q}}$ and $\mathcal{J}_{\tilde{Q}}$ are used to indicate two different functions: as it can be seen from

$$\left.\frac{\delta W[J]}{\delta J}\right|_{J=J_{\bar{Q}}} = \bar{Q} \qquad \text{and} \qquad \left.\frac{\delta W[J]}{\delta J}\right|_{J=\mathcal{J}_{\tilde{Q}}} = \tilde{Q} + B\,, \tag{2.68}$$

they are related one to the other by

$$J_{\bar{Q}+B} = \mathcal{J}_{\bar{Q}}\,. \tag{2.69}$$

Putting together Eqs. (2.61), (2.65), (2.66), (2.69), it is now straightforward to relate the effective actions with and without background,

$$\Gamma_B[\tilde{Q}] = W_B[J_{\tilde{Q}+B}] - J_{\tilde{Q}+B}\,\tilde{Q} = W[J_{\tilde{Q}+B}] - J_{\tilde{Q}+B}\,(B+\tilde{Q}) = \Gamma[\tilde{Q}+B]\,. \tag{2.70}$$

This is the fundamental equation we were looking for: the original effective action can be computed by summing all vacuum graphs in the theory with background,

$$\Gamma[B] = \Gamma_B[0]\,. \tag{2.71}$$

It is clear that the renormalisation theorem for $\Gamma_B[\tilde{Q}]$ requires the background

field to be renormalised as well[11].

A useful property holds for the derivatives of the effective action with background field. Suppose that λ is some parameter (for example a coupling, or even another source) in the action: the derivative with respect to λ of the vacuum effective action with background is related to the derivative of the connected generating functional,

$$\begin{aligned}\frac{d\Gamma_B[0]}{d\lambda} &= \frac{dW_B[\mathcal{J}_{\tilde{Q}=0}]}{d\lambda} = \\ &= \frac{dW[J_B]}{d\lambda} - \frac{dJ_B}{d\lambda} B = \\ &= \frac{\partial W[J_B]}{\partial\lambda} + \frac{\delta W[J]}{\delta J}\bigg|_{J=J_B} \frac{dJ_B}{d\lambda} - \frac{dJ_B}{d\lambda} B = \\ &= \frac{\partial W[J_B]}{\partial\lambda} \,. \end{aligned} \tag{2.72}$$

In this derivation, we had to take into account that the function J_B inherits a dependence on λ from inverting Eq. (2.62).

2.6.2 Gauge theory effective action with the background field method

One of the most valuable application of the background field method is to gauge theories: indeed, in a gauge theory with background, it is possible to make clever choices for the gauge fixing function in order to retain gauge invariance with respect to the background field[12]. These gauges go under the name of *background field gauges* [55, 57–60]. Having a gauge invariant effective action simplifies incredibly the renormalisation procedure. We will consider a pure gauge theory first, postponing the discussion of the role of fermions to the end of Sect. 2.6.3. A possible renormalisation of the gauge-fixing parameter and of the ghost field can also be neglected in this discussion.

[11] In order to compute $\Gamma_B[0]$, one option is to treat the background field perturbatively. Only diagrams with B in the external legs would be considered: the renormalisation of $\tilde{Q}$ becomes irrelevant, as it appears only in loops.

[12] For example, the action in Eq. (2.64) can be supplied with $G = D_{\text{adj}}(B)Q$ or $G = D_{\text{adj}}(B)(Q - B)$.

Let us focus on the field strength for the background field,

$$F_{\mu\nu} = Z_B^{1/2} \left(\partial_\mu (B_R)_\nu - \partial_\nu (B_R)_\mu + i Z_B^{1/2} [(B_R)_\mu, (B_R)_\nu] \right) , \tag{2.73}$$

where we rescaled $B = Z_B^{1/2} B_R$. Since, in a background gauge, gauge invariance is not broken, Eq. (2.73) will take the gauge-covariant form of a constant times $F_{\mu\nu}$ only if $Z_B^{1/2} = 1$: the field B does not renormalise[13].

The non-renormalisability of the background field has advantageous implications for $\Gamma_B[0; g]$. The bare effective action can be expanded as the integral of a gauge-invariant and parity-conserving Lagrangian density (with possibly nonlocal terms). Renormalisability implies that the divergent part of such Lagrangian is a local polynomial in the background field and its derivatives. By power counting, in Yang-Mills theory the local counterterms needed to cancel the divergences have dimension less or equal to 4 (i.e. no primitive divergence arises from diagrams with 5 or more external legs): since F^2 is the only operator with the correct dimension and symmetries, we can write

$$\Gamma_B[0; g] = -\frac{C(g)}{4g^2} \int d^4x \, F^2(x) + \text{finite terms} \, , \tag{2.74}$$

where $C(g)$ is some divergent constant[14], and

$$F^2(x) = \sum_{a,\mu,\nu} F^a_{\mu\nu}(x) F^a_{\mu\nu}(x) \, . \tag{2.75}$$

The overall normalisation is a convention: at tree level the effective action is simply the action with opposite sign, so with our choice $C(g) = 1 + O(g)$, and the finite terms are also $O(g)$. In case a dimensionful regulator is used, then power divergences should also be considered: these will be dealt with in Sect. 2.6.4. Since B does not renormalise, the renormalisation theorem tells us that

$$(\Gamma_R)_B[0; g_R] = \Gamma_B[0; Z_g g_R] = -\frac{C(g)}{4 Z_g^2 g_R^2} \int d^4x \, F^2(x) + \text{finite terms} \tag{2.76}$$

is finite and hence $C(g) = Z_g^2$ must hold, up to finite terms. This is consistent

[13] As a side remark, if we used for B the normalisation required for perturbation theory, we would find that the renormalisation constant of the background field is related to Z_g. This allows computing conveniently the β-function of the theory from two-point diagrams only.

[14] It should be always kept in mind that the theory has been somehow regularised. Therefore, $C(g)$ depends on the ultraviolet cutoff, which has to be put in a way to preserve gauge invariance (like in lattice gauge theories). In dimensional regularisation, $C(g)$ is a polynomial in $1/\epsilon$, where ϵ goes to zero as the number of dimensions approaches 4.

with the result of Ref. [59].

2.6.3 Renormalisation of F^2

In order to find the renormalisation properties of F^2 [57, 61], it is useful to add a new source J_{F^2} to the generating functional, so that derivatives with respect to J_{F^2} produce insertions of F^2,

$$Z[J, J_{F^2}] = e^{W[J,J_{F^2}]} = \int \mathcal{D}A\, e^{-S[A]+JA+J_{F^2}F^2}\,. \tag{2.77}$$

With a background field, we define

$$Z_B[J, J_{F^2}] = e^{W_B[J,J_{F^2}]} = \int \mathcal{D}Q\, e^{-S[B+Q]+JQ+J_{F^2}F^2_{B+Q}}\,, \tag{2.78}$$

where F^2_{B+Q} stands for the field strength of the field $B+Q$. If only one insertion of F^2 is allowed (with one insertion there is no distinction between connected/disconnected and reducible/irreducible Green functions), the effective action can be defined without taking the Legendre transform with respect to J_{F^2}: thus, the discussion in Sect. 2.6.1 carries on in an analogous way, with the only difference that all functions are decorated with a dependence on J_{F^2}. The quantity we are interested in is the effective action with one insertion of F^2, $\Gamma_{F^2}[B]$: it is related to the connected generating functional thanks to Eq. (2.72),

$$\begin{aligned}\Gamma_{F^2}[B] &= \frac{\delta}{\delta J_{F^2}}\Gamma[B, J_{F^2}]\bigg|_{J_{F^2}=0} = \frac{\delta}{\delta J_{F^2}}\Gamma_B[0, J_{F^2}]\bigg|_{J_{F^2}=0} = \\ &= \frac{\delta W[J_B, J_{F^2}]}{\delta J_{F^2}}\bigg|_{J_{F^2}=0}\,.\end{aligned} \tag{2.79}$$

The renormalisation theorem and the non-renormalisability of the background field imply that

$$(\Gamma_R)_{F^2}[B; g_R] = Z_{F^2}\Gamma_{F^2}[B; Z_g g]\,, \tag{2.80}$$

where the renormalised operator is defined as $(F^2)_R = Z_{F^2}F^2$.

The arguments presented so far are quite general, and apply to any operator. What is special in our case is that F^2 appears in the action, and we can trade

the derivative with respect to J_{F^2} with a derivative with respect to the coupling,

$$\int dx^4 \, \frac{\delta W[J_B, J_{F^2}; g]}{\delta J_{F^2}(x)}\bigg|_{J_{F^2}=0} = -4 \, \frac{\partial W[J_B; g]}{\partial g^{-2}} = -4 \, \frac{d\Gamma_B[0; g]}{dg^{-2}} \,, \tag{2.81}$$

where in the last step we made use of Eq. (2.72) again. Since the bare effective action for the background field has been already computed in Eq. (2.74), by comparing

$$\int dx^4 \, \Gamma_{F^2(x)}[B; g] = \frac{d}{dg^{-2}} \left(\frac{Z_g}{g^2} \right) \int d^4x \, F^2(x) + \text{finite terms} \,. \tag{2.82}$$

with Eq. (2.80) we finally obtain

$$Z_{F^2} = \left(\frac{d}{dg^{-2}} \frac{Z_g}{g^2} \right)^{-1} + \text{finite terms} \,, \tag{2.83}$$

with the corresponding anomalous dimension

$$\gamma_{F^2} = -\frac{1}{Z_{F^2}^{-1}} \frac{d \, Z_{F^2}^{-1}}{d \log \mu} = -\frac{\frac{d}{d \log \mu} \left(\frac{d}{dg^{-2}} \frac{Z_g^2}{g^2} \right)}{\frac{d}{dg^{-2}} \frac{Z_g^2}{g^2}} \,. \tag{2.84}$$

Because Z_g is the only term depending on the renormalisation scale, with the help of

$$\frac{d \, Z_g}{d \log \mu} = -\frac{Z_g}{g_R} \, \beta(g_R) \tag{2.85}$$

we obtain

$$\gamma_{F^2}(g_R) = -\frac{\frac{d}{dg^{-2}} \frac{2 Z_g}{g^2} \left(-\frac{Z_g}{g_R} \beta(g_R) \right)}{\frac{d}{dg^{-2}} \frac{Z_g^2}{g^2}} = 2 \, \frac{\frac{d}{dg^{-2}} \frac{\beta(g_R)}{g_R^3}}{\frac{d}{dg^{-2}} \frac{1}{g_R^2}} = 2 \, \frac{\frac{d}{dg_R} \frac{\beta(g_R)}{g_R^3}}{\frac{d}{dg_R} \frac{1}{g_R^2}} = -g_R^3 \, \frac{d}{dg_R} \frac{\beta(g_R)}{g_R^3} \,. \tag{2.86}$$

We could change variables in the derivatives because the Jacobian simplifies between numerator and denominator. Note that this relation implies that:

- the anomalous dimension of F^2 vanishes at one loop
- the ratio between the anomalous dimension and the β-function is an exact differential,

$$\frac{\gamma_{F^2}(g_R)}{\beta(g_R)} = -\frac{d}{dg_R} \log \frac{\beta(g_R)}{g_R^3} \tag{2.87}$$

- $\frac{\beta(g_R)}{g_R^3}(F^2)_R$ is renormalisation group invariant,

$$\frac{d}{d\log\mu}\frac{\beta(g_R)}{g_R^3}(F^2)_R = \left(\frac{d}{d\log\mu}\frac{\beta(g_R)}{g_R^3}\right)(F^2)_R + \frac{\beta(g_R)}{g_R^3}\frac{d\log Z_{F^2}}{d\log\mu}(F^2)_R = \\ = \beta(g_R)\left(\frac{d}{dg_R}\frac{\beta(g_R)}{g_R^3}\right)(F^2)_R + \frac{\beta(g_R)}{g_R^3}\gamma_{F^2}(g_R)(F^2)_R = \\ = 0\,, \tag{2.88}$$

  and matches, apart from an overall constant, the renormalisation group invariant operator one would get from Eq. (2.53),

$$\Gamma_{F^2}(\mu)(F^2)_R = \exp\left(-\int_0^{g_R(\mu)} dg'\,\frac{\gamma_{F^2}(g')}{\beta(g')}\right)(F^2)_R = \\ = \exp\left(\log\frac{\beta(g)}{g^3}\bigg|_0^{g_R(\mu)}\right)(F^2)_R = -\frac{1}{b_0}\frac{\beta(g_R)}{g_R^3}(F^2)_R\,. \tag{2.89}$$

The renormalisation group invariant quantity that we found is the trace of the energy-momentum tensor [62, 63]. In order to get a normalisation suitable for perturbation theory, the field strength must be rescaled as $F_{\mu\nu} = g\,G_{\mu\nu}$. It is customary to call

$$O_G = -\frac{1}{4\pi^2 b_0}\frac{\beta(g_R)}{g_R^3}(F^2)_R = -\frac{1}{4\pi^2 b_0}\frac{\beta(g_R)}{g_R}(G^2)_R = -\frac{2}{\beta_0}\frac{\beta(\alpha_R)}{\alpha_R}(G^2)_R \tag{2.90}$$

the *gluon condensate*.

In a theory with fermions, the operator F^2 is not the only gauge-invariant parity-conserving operator with dimension 4. In principle, mixing can happen with

- $m\bar\psi\psi$, which vanishes in the massless case,
- $\bar\psi(i\sum_\mu \gamma_\mu D_\mu - m)\psi$, which vanishes when the equation of motion are used,
- $\sum_\mu \partial_\mu(\bar\psi\gamma_\mu\psi)$, which vanishes at zero momentum.

In general, our discussion has to be rephrased in order to take this mixing into account [57, 61]; it turns out that O_G is not even a renormalisation group invariant operator, and it must be combined with $m\bar\psi\psi$ to give a renormalisation group invariant quantity. Since our goal is to investigate theories with massless fermions, such complications do not arise when studying condensates.

2.6.4 F^2 and the gluon condensate on the lattice

To begin, we need to define a renormalised coupling on the lattice. A possible definition is in the minimal subtraction (MS) scheme: on the lattice, this scheme amounts to subtracting only powers of logarithms in the lattice cutoff. The resulting *MS lattice coupling* $g_{\rm latt}$ is

$$g_{\rm latt} = g_R(\mu) = Z_g(g, a\mu)\, g \qquad \text{with} \qquad g_R(1/a) = g\,, \tag{2.91}$$

and satisfies $\beta(g_R) = \beta_L(g_R)$ (see Appendix B).

The analysis in Sect. 2.6.3 applies if the discretisation of the F^2 operator coincides with the corresponding discretisation used in the gauge action. Therefore, for the Wilson action we have to deal with the plaquette operator P, see Eq. (1.20). In the same spirit as the lattice coupling, the finite terms in Eq. (2.83) can be fixed by choosing minimal subtraction, i.e.

$$Z_P(g, a\mu)\big|_{\mu=1/a} = 1\,. \tag{2.92}$$

This choice determines the scheme for renormalising the operator. Moreover, thanks to Eq. (2.87) and the vanishing of the anomalous dimension at one loop, we can readily compute

$$\Gamma_P(1/a) = -\frac{1}{b_0}\frac{\beta(g)}{g^3}\,. \tag{2.93}$$

We can now move on and study the relevant power divergences. It is easy to relate the gluon condensate and the plaquette in the naive continuum limit,

$$a^{-4}P \xrightarrow{a\to 0} \frac{\pi^2}{12N_c}\,O_G = \frac{F^2}{48N_c} = \frac{\pi^2}{12N_c}\left(\frac{\alpha}{\pi}\,G^2\right)\,, \tag{2.94a}$$

$$O_G = \frac{\alpha}{\pi}\,G^2\,[1 + O(\alpha)]\,. \tag{2.94b}$$

In the interacting theory, mixing with operators of lower or equal dimension occurs. In our case, only the identity operator must be considered, since it is the only operator with the same quantum number as F^2. In the limit $a^{-1} \gg \Lambda$ it is possible to build the OPE as in Eq. (2.57), and write

$$a^{-4}P = a^{-4}\tilde{Z}_{\mathbb{1}}(g)\mathbb{1} + \frac{\pi^2}{12N_c}\,C_G(g)O_G + O(a^2\Lambda^6)\,, \tag{2.95}$$

or, for the expectation values,

$$\langle P\rangle = \tilde{Z}_{\mathbb{1}}(g) + \frac{\pi^2}{12N_c}\, C_G(g) a^4 \langle O_G\rangle + O(a^6\Lambda^6)\,, \tag{2.96}$$

where $\tilde{Z}_{\mathbb{1}}(0) = 0$, and the normalisation has been chosen so that $C_G(0) = 1$. By comparing Eqs. (2.57) and (2.95), we can read the Wilson coefficient

$$C_G(g) = \Gamma_P(1/a)^{-1} = -\frac{b_0 g^3}{\beta(g)} = -\frac{\beta_0 \alpha^2}{2\pi\beta(\alpha)}\,. \tag{2.97}$$

Finally, Eq. (2.56) allows the determination of the gluon condensate,

$$\begin{aligned} r_0^4\,\langle O_G\rangle &= \frac{12N_c}{\pi^2}\,\Gamma_P(1/a) Z_P(g,1)\,\left(\frac{r_0}{a}\right)^4\,\Big[\langle P\rangle - \tilde{Z}_{\mathbb{1}}(g)\langle \mathbb{1}\rangle\Big] = \\ &= \frac{12N_c}{\pi^2}\,\left(-\frac{1}{b_0}\frac{\beta(g)}{g^3}\right)\,\left(\frac{r_0}{a}\right)^4\,\Big[\langle P\rangle - \tilde{Z}_{\mathbb{1}}(g)\langle \mathbb{1}\rangle\Big] = \\ &= \frac{12N_c}{\pi^2}\, C_G(g)^{-1}\,\left(\frac{r_0}{a}\right)^4\,\Big[\langle P\rangle - \tilde{Z}_{\mathbb{1}}(g)\langle \mathbb{1}\rangle\Big]\,. \end{aligned} \tag{2.98}$$

We stress again that in this framework the Wilson coefficients are defined in perturbation theory,

$$\tilde{Z}_{\mathbb{1}}(\beta) = \sum_{n=0} p_n \beta^{-(n+1)}\,, \quad C_G(\beta) = 1 + \sum_{n=0} c_n \beta^{-(n+1)}\,, \tag{2.99}$$

and the condensate is affected by the ambiguity discussed in Sect. 2.3.

Chapter 3

Lattice perturbation theory on the computer

The Faddeev-Popov procedure is required for a perturbative approach to non-abelian gauge theories. When a nonperturbative definition is indispensable, one usually relies on lattice gauge theories. Another possibility is provided by the method of *stochastic quantisation*, whose original goal was exactly to overcome the necessity of gauge fixing in perturbation theory, and at the same time to accomplish a nonperturbative definition of non-abelian gauge theories. Indeed Gribov ambiguities, when present, can be seen in all respects as artefacts of a quantisation procedure. As a side effect, it turns out that stochastic quantisation provides also a favourable ground for performing perturbative calculations numerically on a computer.

For many more details about stochastic quantisation and its numerical application to perturbation theory, the reader is referred respectively to the reviews in Ref. [64] and Ref. [65].

3.1 Stochastic quantisation

Stochastic quantisation provides a new way of quantising physical systems which is equivalent to canonical or path integral quantisation. The idea, proposed in Ref. [66], is to introduce a stochastic time t and setup a stochastic process in this new dimension, such that averages performed when the process is at equilibrium

correspond to quantum expectation values. To be more concrete: a generic field $\phi(x)$ is promoted to $\phi(x;t)$, and the evolution in t is given by the Langevin equation

$$\frac{d\phi(x;t)}{dt} = -\frac{\delta S[\phi]}{\delta\phi(x;t)} + \eta(x;t)\,, \tag{3.1}$$

where $S[\phi]$ is the action of the theory, and $\eta(x;t)$ is a Gaussian noise satisfying

$$\langle\eta(x;t)\rangle_\eta = 0\,, \qquad \langle\eta(x;t)\eta(x';t')\rangle_\eta = 2\delta(x-x')\delta(t-t')\,. \tag{3.2}$$

The average of a generic observable $O[\phi]$ must be understood as an average on the noise,

$$\langle O[\phi]\rangle_\eta = \int \mathcal{D}\eta\, P[\eta]O[\phi] \qquad \text{with} \quad P[\eta] = \frac{e^{-\frac{1}{4}\int d^4x\, dt\, \eta^2(x;t)}}{\int \mathcal{D}\eta'\, e^{-\frac{1}{4}\int d^4x'\, dt'\, \eta'^2(x';t')}}\,. \tag{3.3}$$

In the absence of noise, only the first term on the right-hand side of Eq. (3.1), called *drift* or *force term*, would contribute, and the field would be driven towards a stationary point of the action, i.e. on the classical equations of motion. The role of η is to mimic quantum fluctuations: when the stochastic process is in equilibrium, stochastic averages correspond to quantum expectation values,

$$\lim_{t\to+\infty} \langle\phi(x_1;t)\dots\phi(x_n;t)\rangle_\eta = \langle\phi(x_1)\dots\phi(x_n)\rangle\,. \tag{3.4}$$

It is now essential to study and give some motivation to Eq. (3.4), which is the core of stochastic quantisation. From now on we will drop the subscript η in the averages as it will be clear from the context when a quantum or noise average is intended.

Stochastic differential equations

From a realistic point of view, Eq. (3.2) is pathological since the noise has infinite variance. In order to put the Langevin equation on a more solid ground, it is now convenient to introduce briefly stochastic differential equations. Neglecting the spacetime index and focusing on one degree of freedom, we define the integral of the noise

$$\omega(t) = \frac{1}{\sqrt{2}}\int_0^t ds\,\eta(s)\,. \tag{3.5}$$

It is easy to see that this function satisfies

$$\langle \omega(t) \rangle = 0\,, \qquad \langle \omega(t)\omega(t') \rangle = \min(t,t')\,. \tag{3.6}$$

The variance of this process is now finite; in fact, it can be shown that $\omega(t)$ is a well-defined stochastic process[1]. Therefore, starting from a generic Langevin equation

$$\frac{d\phi(t)}{dt} = a(\phi,t) + b(\phi,t)\eta(t)\,, \tag{3.7}$$

it is possible to take its integral form

$$\phi(t) - \phi(0) = \int_0^t ds\, a(\phi,s) + \sqrt{2}\int_0^t d\omega(s)\, b(\phi,s) \tag{3.8}$$

as the definition of the stochastic equation. Still, the interpretation of the stochastic integration on the right-hand side of Eq. (3.8) requires some care. If we partition the interval $[0,t]$, and define the stochastic integral as the limit of a Riemann sum, we soon realise that the final result depends on the intermediate points $\tau_n \in [t_{n-1}, t_n]$ chosen for evaluating the integrand. For example,

$$\left\langle \int_0^t d\omega(s)\, \omega(s) \right\rangle = \sum_n \langle [\omega(t_n) - \omega(t_{n-1})]\, \omega(\tau_n) \rangle = \sum_n (\tau_n - t_{i-1}) = \alpha t\,, \tag{3.9}$$

where $\tau_n = \alpha t_n + (1-\alpha) t_{n-1}$ and $\alpha \in [0,1]$. The prescription $\alpha = 0$ defines the *Itô stochastic integral*, while the midpoint prescription $\alpha = \frac{1}{2}$ defines the *Stratonovich stochastic integral*. It is important to note that the usual rules of calculus lead naturally to the Stratonovich definition: in the previous example,

$$\left\langle \int_0^t d\omega(s)\, \omega(s) \right\rangle = \frac{1}{2}\langle \omega(t)^2 - \omega(0)^2 \rangle = \frac{t}{2}\,. \tag{3.10}$$

The Stratonovich integral also allows for the usual integration by parts. Even though in principle all the choices of α are on the same footing, we will adopt the Stratonovich definition. Indeed, in physical cases Eq. (3.2) is just an idealisation, and the autocorrelation function is not singular. For instance, if time is discretised with a time step ϵ, then one would have

$$\langle \eta(t) \rangle = 0\,, \qquad \langle \eta(t)\eta(t') \rangle = \frac{2}{\epsilon}\,\delta_{tt'}\,. \tag{3.11}$$

[1] In particular, it is a Wiener process.

It can be proved that when $\epsilon \to 0$ the Stratonovich solution of the stochastic equation is recovered [67] (and clearly this holds independently of the way the Dirac delta is regularised).

Interestingly, the Stratonovich prescription fixes the value of the Heaviside step function

$$\Theta(t) = \int_{-\infty}^{t} ds\, \delta(s) \tag{3.12}$$

when the argument is zero. From Eq. (3.9) it is possible to make the noise explicit

$$\frac{1}{2}\left\langle \int_0^t ds\, \xi(s) \int_0^s ds'\, \xi(s') \right\rangle = \int_0^t ds \int_0^s ds'\, \delta(s-s') = \frac{t}{2} \tag{3.13}$$

so that the identity

$$\int_0^s ds'\, \delta(s-s') = \frac{1}{2} \tag{3.14}$$

implies $\Theta(0) = \frac{1}{2}$.

Fokker-Planck equation

We are now in the position to derive the Fokker-Planck equation associated to Eq. (3.1), and prove the assertion of stochastic quantisation. The change in time of the average in Eq. (3.3) is

$$\frac{d}{dt}\langle O[\phi]\rangle = \int d^4x \left\langle \frac{\delta O[\phi]}{\delta\phi(x;t)} \left(-\frac{\delta S[\phi]}{\delta\phi(x;t)} + \eta(x;t) \right) \right\rangle . \tag{3.15}$$

Using the explicit form of $P[\eta]$ and integrating by parts we obtain

$$\begin{aligned} \left\langle \frac{\delta O[\phi]}{\delta\phi(x;t)} \eta(x;t) \right\rangle &= -2 \int \mathcal{D}\eta\, \frac{\delta O[\phi]}{\delta\phi(x;t)}\, \frac{\delta P[\eta]}{\delta\eta(x;t)} = \\ &= 2 \int d^4y \left\langle \frac{\delta^2 O[\phi]}{\delta\phi(x;t)\delta\phi(y;t)}\, \frac{\delta\phi(y;t)}{\delta\eta(x;t)} \right\rangle . \end{aligned} \tag{3.16}$$

In order to compute the derivative of the field with respect to the noise, it is useful to transform Eq. (3.1) into an integral equation

$$\phi(y;t) = \phi(y;0) + \int_0^{+\infty} ds\, \Theta(t-s) \left[-\frac{\delta S[\phi]}{\delta\phi(y;s)} + \eta(y;s) \right] , \tag{3.17}$$

from which it is simple to read

$$\frac{\delta\phi(y;t)}{\delta\eta(x;t)} = \Theta(0)\delta(x-y) = \frac{1}{2}\delta(x-y)\,. \tag{3.18}$$

Clearly the drift term does not participate in the derivative since it depends only on the noise at times $s < t$. Putting everything together, we have found that the time derivative of the stochastic average is

$$\frac{d}{dt}\langle O[\phi]\rangle = \int d^4x \left\langle -\frac{\delta O[\phi]}{\delta\phi(x;t)}\frac{\delta S[\phi]}{\delta\phi(x;t)} + \frac{\delta^2 O[\phi]}{\delta\phi(x;t)^2}\right\rangle . \tag{3.19}$$

Defining the probability of having the field configuration $\phi(x)$ at time t

$$P[\phi;t] = \int \mathcal{D}\eta\, P[\eta] \prod_y \delta(\phi(y;t) - \phi(y))\,, \tag{3.20}$$

allows expressing stochastic averages as

$$\langle O[\phi]\rangle = \int \mathcal{D}\phi\, P[\phi;t] O[\phi]\,. \tag{3.21}$$

This equation can be used for evaluating the averages in Eq. (3.19). It is straightforward to integrate by parts and move on $P[\phi;t]$ all the derivatives acting on the observable. The Fokker-Planck equation that describes the time evolution of the probability density function $P[\phi,t]$ is then

$$\frac{dP[\phi;t]}{dt} = \int d^4x\, \frac{\delta}{\delta\phi(x)}\left[\left(\frac{\delta S[\phi]}{\delta\phi(x)} + \frac{\delta}{\delta\phi(x)}\right) P[\phi;t]\right] , \tag{3.22}$$

and it is evident that a stationary solution is provided by $P_{\rm eq}[\phi] \sim e^{-S[\phi]}$. Whenever

$$\lim_{t\to+\infty} P[\phi,t] = P_{\rm eq}[\phi] = \frac{e^{-S[\phi]}}{\int \mathcal{D}\phi'\, e^{-S[\phi']}}\,, \tag{3.23}$$

then stochastic quantisation is realised: the stochastic average reconstructs the Euclidean path integral. The limit in Eq. (3.23) must be understood in the weak sense, i.e. the limit is done on correlation functions as in Eq. (3.4). The reaching of the correct equilibrium distribution has been proved for several systems; for example, it is not hard to show that it holds when the number of degrees of freedom is finite and $e^{-S[\phi]}$ is integrable. When an infinite number of degrees of freedom is considered, the right-hand side of Eq. (3.22) must be suitably regularised. In the case of gauge theories, it can be argued that the limit in

Eq. (3.23) exists only for gauge-invariant correlation functions.

3.2 Stochastic perturbation theory and NSPT

Before describing stochastic perturbation theory, it is beneficial to make some general consideration. Let us consider a differential equation

$$\mathrm{L}\phi = f + \lambda \mathrm{NL}\phi \tag{3.24}$$

where f is some nonhomogeneous term, L is a linear differential operator and NL is a nonlinear operator, whose significance is controlled by a small parameter λ. Let G be the inverse of L with appropriate boundary conditions, i.e. G is a linear integral operator satisfying $\mathrm{LG} = 1$. We also assume that ϕ has been redefined so that the solution of the homogeneous equation vanishes. If G is known[2], the differential equation (3.24) is suited to a perturbative treatment: first the differential equation is traded for an integral equation,

$$\phi = G(f + \lambda \mathrm{NL}\phi) \tag{3.25}$$

and then ϕ is recursively substituted into the right-hand side of Eq. (3.25). As a simple example, if $\mathrm{NL}\phi = \phi^2$ we have

$$\phi = Gf + \lambda G(Gf)^2 + 2\lambda^2 G\left\{(Gf)\left[G(Gf)^2\right]\right\} + O(\lambda^3)\,. \tag{3.26}$$

The same approach works for a generic $\mathrm{NL}\phi$, that is a combination of monomials in ϕ, derivatives of ϕ and λ. It is also convenient to have a diagrammatic representation of Eq. (3.26), where the kernel of G is the propagator and NL generates vertices; it is easy to see that only tree diagrams are involved, i.e. there cannot be any loop.

It is interesting to note that the same perturbative expansion can be obtained from another perspective: if we plug a formal expansion of the field, $\phi = \sum_n \phi^{(n)}\lambda^n$, into Eq. (3.24), the result is a set of recursive equation that can be solved iteratively. Once the lowest order is found, that solution is used as input for the following equation and so on; only the knowledge of G is necessary. The process can be consistently truncated at an arbitrary order. Going back to

[2] In principle our discussion holds irrespectively of L (NL) being linear (nonlinear), all that matters is knowing how to compute G.

our example $\mathrm{NL}\phi = \phi^2$, up to λ^2 we have

$$\mathrm{L}\phi^{(0)} = f \tag{3.27a}$$
$$\mathrm{L}\phi^{(1)} = (\phi^{(0)})^2 \tag{3.27b}$$
$$\mathrm{L}\phi^{(2)} = 2\phi^{(0)}\phi^{(1)} \,. \tag{3.27c}$$

The system of equations is solved iteratively by applying G to both sides: the final result reconstructs exactly Eq. (3.26),

$$\phi^{(0)} = Gf \tag{3.28a}$$
$$\phi^{(1)} = G(\phi^{(0)})^2 = G(Gf)^2 \tag{3.28b}$$
$$\phi^{(2)} = 2G(\phi^{(0)}\phi^{(1)}) = 2G\left\{(Gf)\left[G(Gf)^2\right]\right\} \,. \tag{3.28c}$$

This technology can be applied straightforwardly to Eq. (3.1): the idea is to consider

$$\mathrm{L}\phi = \frac{d\phi}{dt} + \frac{\delta S_{\mathrm{free}}[\phi]}{\delta\phi(x;t)} \,, \qquad f = \eta \,, \qquad \mathrm{NL}\phi = -\frac{\delta S_{\mathrm{int}}[\phi]}{\delta\phi(x;t)} \,, \tag{3.29}$$

where the action has been split into a free and interaction part, $S[\phi] = S_{\mathrm{free}}[\phi] + S_{\mathrm{int}}[\phi]$, so that we know how to compute G. Stochastic perturbation theory [66] consists in adopting the recipe in Eq. (3.4) to compute correlators, which in turn are computed in perturbation theory with the technique developed so far. First, with an expansion analogous to Eq. (3.26), we write all the diagrams that contribute at a certain order; the Gaussian nature of η entitles to perform Wick contractions and get rid of the noise[3]. Finally, the limit $t \to +\infty$ gives the sought result. For a scalar theory, the contribution of the standard Feynman diagrams is indeed recovered [68]. A complete proof of equivalence between stochastic perturbation theory and the usual perturbative approach from field theory can be accomplished in the Fokker-Planck formalism [69]. We will deal with the complications arising from gauge theories in Sect. 3.4.

Stochastic perturbation theory, written in the form of Eq. (3.27), is appropriate to be handled on a computer. Each of the Langevin equations can be integrated numerically in order to evolve all the $\phi^{(n)}$; the lowest order $\phi^{(0)}$ depends explicitly

[3] In a classical framework, where for example f is some source and L, NL are respectively the free and interaction terms of a field equation, only tree level diagrams can be built. In this respect, the noise is providing quantum fluctuations: it is reassuring that because of the Wick contractions loops can and will appear in the diagrams.

on the noise, while higher $\phi^{(n)}$ depend only on $\phi^{(m)}$ with $m < n$. Under this point of view, the stochastic time t corresponds to the simulation time. Any observable $O[\phi]$ inherits a formal perturbative expansion from ϕ. Performing the Monte Carlo average over the Langevin history of $O[\phi]$, once the stochastic process is at equilibrium, returns the perturbative expansion of $\langle O[\phi] \rangle$. This approach goes under the name of *Numerical Stochastic Perturbation Theory* (NSPT) [70]. Particular attention has to be paid to the field configurations ϕ_{zm} such that

$$\left. \frac{\delta S_{\mathrm{free}}[\phi]}{\delta \phi(x)} \right|_{\phi_{\mathrm{zm}}} = 0 \,. \tag{3.30}$$

We call ϕ_{zm} a *zero mode*. Such configuration is not affected by the drift: it is clear from Eq. (3.27a) that $\phi^{(0)}_{\mathrm{zm}}$ is just the integral of the noise and behaves like a random walk. This kind of fluctuation is zero on average, but its magnitude grows with time, see Eq. (3.6). Given the recursive nature of Eq. (3.28), similar effects are expected in all the perturbative components. In analytical computations this is not a problem, but diverging fluctuations prevent from extracting statistically meaningful signals in numerical applications.

We also mention that the idea of studying the convergence properties of a stochastic process order by order after an expansion in the coupling is actually quite general. In this spirit, we refer to Refs. [71, 72] for the description of other NSPT schemes based on stochastic differential equations different from Langevin.

3.3 NSPT for lattice gauge theories

The Langevin equation can be used to perform Monte Carlo simulations and compute correlation functions [73]. It is also a starting point for simulating lattice gauge theories both nonperturbatively [74, 75] and in perturbation theory [70]. Because the degrees of freedom are the link variables, the Langevin equation must be reformulated for compact Lie groups [76–78]: if $\nabla_{x\mu}$ is the Lie derivative[4] with respect to $U_\mu(x)$, then the desired equation is

$$\frac{d}{dt} U_\mu(x;t) = i \left[-\nabla_{x\mu} S[U] + \eta(x;t) \right] U_\mu(x;t) \,, \tag{3.31}$$

[4] The group theory conventions are explained in detail in Appendix A.

where the Gaussian noise $\eta_\mu(x;t) = T^a \eta^a_\mu(x;t)$ satisfies

$$\left\langle \eta^a_\mu(x;t) \right\rangle = 0\,, \qquad \left\langle \eta^a_\mu(x;t)\eta^b_\nu(x';t') \right\rangle = 2\delta^{ab}\delta_{\mu\nu}\delta_{xx'}\delta(t-t')\,. \tag{3.32}$$

Rather than motivating such result, we will study a discrete Langevin process (suitable for computer simulations) modelled on Eq. (3.31), and check if stochastic quantisation is realised. If stochastic time is discretised as $t_n = n\epsilon$, with $n \in \mathbb{N}$ and time step ϵ, we can integrate numerically Eq. (3.31). A possible choice of an Euler scheme is

$$U_\mu(x;t_{n+1}) = e^{-F_\mu(x;t_n)}\, U_\mu(x;t_n) \tag{3.33}$$

with

$$F_\mu(x;t_n) = i\left[\epsilon \nabla_{x\mu} S[U(t_n)] - \sqrt{\epsilon}\,\eta_\mu(x;t_n)\right] \tag{3.34}$$

and

$$\left\langle \eta^a_\mu(x;t_n) \right\rangle = 0\,, \qquad \left\langle \eta^a_\mu(x;t_n)\eta^b_\nu(x';t_m) \right\rangle = 2\delta^{ab}\delta_{\mu\nu}\delta_{xx'}\delta_{nm}\,. \tag{3.35}$$

Even though in a first-order scheme all powers higher than ϵ^1 should be negligible, having the full exponential in Eq. (3.33) guarantees that the links stay within the group. The factor $\sqrt{\epsilon}$ in front of the noise arises because η must be rescaled with ϵ to become dimensionless, as it is evident from Eq. (3.11).

Instead of considering Eq. (3.33) just as a numerical approximation, the discrete process can be raised to a higher status: indeed, we will show that the associated probability distribution obeys to Eq. (3.23), but the equilibrium action is modified by $O(\epsilon)$ effects. Therefore, such discrete process can be used to compute expectation values, but $O(\epsilon)$ effects are expected. In order to correct for this systematic error, observables must be computed for several values of ϵ and then extrapolated to vanishing time step[5].

In the discrete process, the probability of having the configuration U' at time t_{n+1} can be computed from the probability of having a generic U at time t_n and the probability of the transition $U \to U'$, namely

$$P[U';t_{n+1}] = \int \mathcal{D}U\, P[U;t_n] \left\langle \prod_{x,\mu} \delta\left(U'_\mu(x) - e^{-F_\mu(x;t_n)} U_\mu(x;t_n)\right) \right\rangle . \tag{3.36}$$

Having in mind that the interesting regime is when ϵ is small, we can Taylor

[5] Clearly the extrapolation is linear for small enough values of ϵ.

expand in $F_\mu(x;t_n) = iT^a F^a_\mu(x;t_n)$ the delta function,

$$\begin{aligned}\delta\left(U' - e^{-F(t_n)}U(t_n)\right) = \delta\left(U' - U(t_n)\right) + \\ + \sum_{n=1}^{\infty}\sum_{a_1,\ldots,a_n}\frac{(-1)^n}{n!}F^{a_1}(t_n)\ldots F^{a_n}(t_n)\cdot \\ \cdot\,\nabla^{a_1}_{U(t_n)}\ldots\nabla^{a_n}_{U(t_n)}\delta\left(U' - U(t_n)\right)\,, \end{aligned} \tag{3.37}$$

and integrate by parts the Lie derivatives (the space and Lorentz indices have been temporarily suppressed for clarity). The remaining delta function allows integrating over U, forcing $U'_\mu(x) = U_\mu(x;t_n)$. Dropping the prime, the probability of having the configuration U at time t_n changes at time t_{n+1} by

$$\begin{aligned}P[U;t_{n+1}] - P[U;t_n] = \\ = \sum_{n=1}^{\infty}\sum_{\substack{a_1,\ldots,a_n\\ x_1,\ldots,x_n\\ \mu_1,\ldots,\mu_n}}\frac{1}{n!}\nabla^{a_1}_{x_1\mu_1}\ldots\nabla^{a_n}_{x_n\mu_n}\left[\left\langle F^{a_1}_{\mu_1}(x_1)\ldots F^{a_n}_{\mu_n}(x_n)\right\rangle P[U;t_n]\right]\,.\end{aligned} \tag{3.38}$$

Such expansion is a discrete version of the Kramers–Moyal expansion [79, 80]. For $t \to +\infty$ the process reaches equilibrium and the left-hand side vanishes; this means that the equilibrium distribution satisfies

$$\sum_{n=1}^{\infty}\sum_{\substack{a_1,\ldots,a_n\\ x_1,\ldots,x_n\\ \mu_1,\ldots,\mu_n}}\frac{1}{n!}\nabla^{a_1}_{x_1\mu_1}\ldots\nabla^{a_n}_{x_n\mu_n}\left[\left\langle F^{a_1}_{\mu_1}(x_1)\ldots F^{a_n}_{\mu_n}(x_n)\right\rangle P_{\mathrm{eq}}[U]\right] = 0\,. \tag{3.39}$$

From Eq. (3.39) it is possible to determine P_{eq} order by order in ϵ. In order to see the $O(\epsilon)$ effect, we need

$$\langle F_i\rangle = \epsilon\nabla_i S \tag{3.40a}$$

$$\langle F_iF_j\rangle = \epsilon^2\nabla_i S\nabla_j S + 2\epsilon\delta_{ij} \tag{3.40b}$$

$$\langle F_iF_jF_j\rangle = 2\epsilon^2(\delta_{ij}\nabla_k S + \delta_{ik}\nabla_j S + \delta_{jk}\nabla_i S) + O(\epsilon^3) \tag{3.40c}$$

$$\langle F_iF_jF_kF_l\rangle = 4\epsilon^2(\delta_{ij}\delta_{kl} + \delta_{ik}\delta_{jl} + \delta_{il}\delta_{jk}) + O(\epsilon^3)\,, \tag{3.40d}$$

where i, j, k, l are multi-indices, each one collecting position, Lorentz and colour

indices. The Fokker-Planck equation at equilibrium then reads

$$0 = \sum_{i,j} \nabla_i \left[(\nabla_i S + \nabla_i) P_{\rm eq} \right] + \\ + \epsilon \sum_{i,j} \left[\frac{1}{2} \nabla_i \nabla_j (\nabla_i S \nabla_j S \, P_{\rm eq}) + \nabla_i \nabla^2 (\nabla_i S \, P_{\rm eq}) + \frac{1}{2} \nabla^2 \nabla^2 P_{\rm eq} + \right. \\ \left. - \frac{1}{3} \nabla_i [\nabla_i, \nabla_j] (\nabla_j S \, P_{\rm eq}) + \frac{1}{6} [\nabla_i, \nabla_j] \nabla_i \nabla_j P_{\rm eq} \right] + O(\epsilon^2) \, . \quad (3.41)$$

At the lowest order, we recognise exactly the right-hand side of Eq. (3.22): this implies that

$$\nabla_i P_{\rm eq} = -\nabla_i S P_{\rm eq} + O(\epsilon) \quad (3.42)$$

and that $P_{\rm eq} \propto e^{-S} + O(\epsilon)$ is the desired distribution. The full solution of Eq. (3.41) is needed to understand the impact of a non-zero ϵ. After some algebra[6], it is possible to show that the Fokker-Planck equation can be rewritten as

$$0 = \sum_{i,j} \nabla_i \left[(\nabla_i \bar{S} + \nabla_i) P_{\rm eq} \right] + O(\epsilon^2) \, , \quad (3.43)$$

with a modified action

$$\bar{S}[U] = \left(1 + \frac{\epsilon}{12} C_A \right) S[U] + \frac{\epsilon}{4} \sum_{ax\mu} \left(2 \nabla^a_{x\mu} \nabla^a_{x\mu} S[U] - \nabla^a_{x\mu} S[U] \nabla^a_{x\mu} S[U] \right) \, . \quad (3.44)$$

The equilibrium distribution $P_{\rm eq} \propto e^{-\bar{S} + O(\epsilon^2)}$ yields quantum expectation values in a theory where the action differs by $O(\epsilon)$ from the original one. This is the reason why the extrapolation to $\epsilon = 0$ becomes necessary.

From the early stages of the Langevin technique, it was soon realised that it is possible to reduce the impact of the finite time step, so that $\bar{S} = S + O(\epsilon^2)$: this can be done thanks to a Runge-Kutta integration scheme for non-abelian theories [74, 75]. Recently, this algorithm has been further improved in Ref. [41]. The basic idea is to perform a first Euler step that updates the original configuration and produces a tentative gauge configuration; then the Runge-Kutta step is made of a drift which is computed both from the original and the tentative configurations. The terms proportional to ϵ in Eq. (3.44) are exactly cancelled, whatever the action S is. We will not describe this algorithm in detail, since we will stick with a first-order integration scheme in the following. Even if

[6] Essentially the idea is to substitute Eq. (3.42) into the $O(\epsilon)$ part of Eq. (3.41), in order to move on S the derivatives acting on $P_{\rm eq}$. The commutators can be simplified with $[\nabla^a_{x\mu}, \nabla^b_{y\nu}] = -f^{abc} \nabla^c_{x\mu} \delta_{xy} \delta_{\mu\nu}$ and $\sum_{ab} f^{abc} f^{abd} = C_A \delta^{cd}$.

second-order schemes prove themselves to be very useful in pure gauge theories, subtleties arise when fermions are considered, as we will explain in Sect. 4.4.

NSPT can be applied to this whole procedure in order to perform perturbative calculations in gauge theories. The idea is always the same: we have to expand formally the links around the vacuum, and then plug the expansion into Eq. (3.33) to integrate numerically the Langevin equations governing each perturbative component. Because in lattice gauge theory the action is proportional to the coupling β, a straightforward application of this procedure would lead to an inconsistent solution of Eq. (3.33), as the lowest order would be controlled only by the noise. An easy solution is rescaling the time step with the coupling, $\tau = \epsilon\beta$, so that both the noise and the drift contributions start from the same order $\beta^{-1/2}$. Explicitly, the formal series reads

$$U_\mu(x) = 1 + \sum_{n=1}^{\infty} U_\mu^{(n)}(x)\, \beta^{-n/2}\,, \tag{3.45}$$

where 1 corresponds to the vacuum and the rescaling $\epsilon \to \tau$ requires expanding in $\beta^{-1/2}$ instead of β^{-1}. From this, all the operations are done order by order in perturbation theory: for example, the gauge potential is defined as the logarithm of the link field, and it reads

$$\begin{aligned} A_\mu(x) &= \sum_{n=1}^{\infty} A_\mu^{(n)}(x)\, \beta^{-n/2} = \\ &= -i \log U_\mu(x) = -iU_\mu^{(1)}(x)\beta^{-1/2} - i\left[U_\mu^{(2)}(x) - \frac{1}{2}\left(U_\mu^{(1)}(x)\right)^2\right]\beta^{-1} + \dots\,. \end{aligned} \tag{3.46}$$

All the components $A_\mu^{(n)}(x)$ must be Hermitian and traceless. On the other hand, it is interesting to note that the unitarity requirement on $U_\mu(x)$ leads to nonlinear relations between the $U_\mu^{(n)}(x)$. The force inherits a similar expansion, $F_\mu(x) = \sum_{n=1} F_\mu^{(n)}(x)\beta^{-1/2}$. From Eq. (3.33), a chain of recursive equations follows, the first few of which are

$$U_\mu^{(1)}(x;t_{n+1}) = U_\mu^{(1)}(x;t_n) - F_\mu^{(1)}(x;t_n) \tag{3.47a}$$

$$\begin{aligned} U_\mu^{(2)}(x;t_{n+1}) = U_\mu^{(2)}(x;t_n) - F_\mu^{(2)}(x;t_n) - F_\mu^{(1)}(x;t_n)U_\mu^{(1)}(x;t_n) + \\ + \frac{1}{2}\left(F_\mu^{(1)}(x;t_n)\right)^2\,, \end{aligned} \tag{3.47b}$$

and so on. The noise enters explicitly only in $F^{(1)}$.

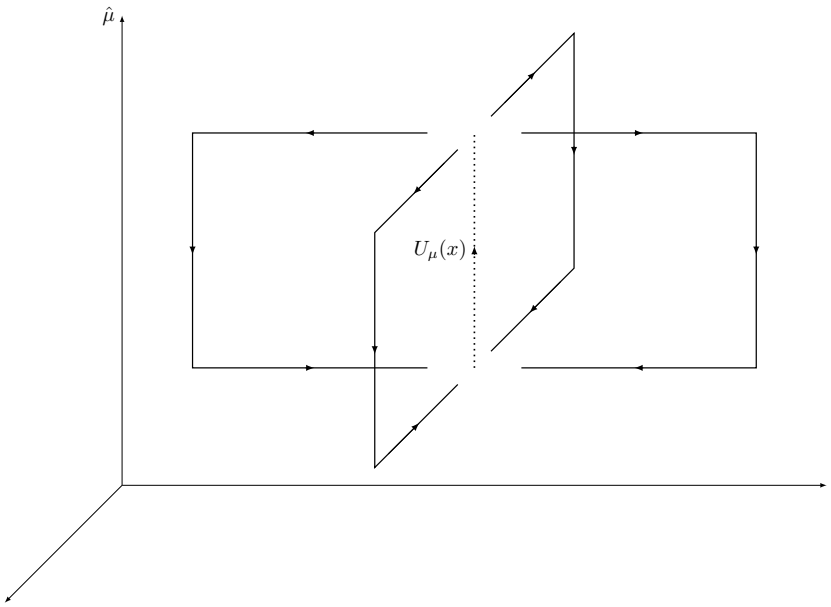

Figure 3.1 *Staples around the link $U_\mu(x)$ needed to evaluate the derivative of the Wilson action.*

The exact form of the drift in the case of the Wilson action of Eq. (1.21) can be derived easily from the Lie derivative of the action, which reads

$$\nabla_{x\mu} S_G[U] = \frac{-i\beta}{2N_c}\,\Pi_{\mathfrak{g}}\left(U_\mu(x)\sum_{\nu\neq\mu} H_{\mu\nu}(x)\right)\,, \tag{3.48}$$

with

$$\begin{aligned} H_{\mu\nu}(x) = {} & U_\nu(x+a\hat{\mu})U_\mu(x+a\hat{\nu})^\dagger U_\nu(x)^\dagger + \\ & + U_\nu(x-a\hat{\mu}+a\hat{\nu})^\dagger U_\mu(x-a\hat{\nu})^\dagger U_\nu(x-a\hat{\nu})\,. \end{aligned} \tag{3.49}$$

The sum in the Lie derivative is pictured in Figure 3.1, and is known as the sum over the *staples*.

It must also be emphasised that lattice gauge theories exhibit two sources of zero modes that spoil the numerical convergence of the stochastic process. We will deal with the gauge zero mode in the following Sect. 3.4; Sect. 4.3 is dedicated to the zero-momentum mode.

3.4 Stochastic gauge fixing

Gauge invariance of the action causes troubles in quantising physical systems: in the path integral formalism, the Faddeev-Popov procedure is needed to factor the integral on the gauge orbits, where the action is constant. The price that is paid is the introduction of a gauge-fixing term and, if the theory is non-abelian, ghosts. From the point of view of perturbation theory, where the Faddeev-Popov procedure is fully consistent, gauge fixing makes the quadratic part of the action invertible. Indeed, without gauge fixing, the longitudinal modes of the gauge field would be unconstrained by the equations of motion; in the language of stochastic quantisation, the force would act only on the transverse components. The longitudinal modes of the gauge field are zero modes: as explained at the end of Sect. 3.1, they are not a problem for gauge-invariant observables in stochastic quantisation (the original goal of the method is precisely to overcome gauge fixing in perturbation theory), but compromise the usefulness of NSPT.

Stochastic gauge fixing [81] provides a nonperturbative procedure for gauge fixing. It consists in adding to the drift a new term which does not affect gauge-invariant quantities but provides a force that keeps limited the norm of the gauge field. In this way, Eq. (3.23) holds not only for gauge-invariant observables, but for a generic correlator: the equivalence with canonical quantisation can then be proved [69].

Evidently, in NSPT the absence of a force for longitudinal A_μ affects the links as well, as U_μ and A_μ are equal at the lowest order. Stochastic gauge fixing can be obtained by exploiting the following freedom in the discrete stochastic process. Let us suppose that after each Langevin step a generic gauge transformation $\Omega(x;t_n)$ is performed: thus Eq. (3.33) is replaced by

$$\begin{aligned}\tilde{U}_\mu(x;t_{n+1}) &= \Omega(x;t_n)\, e^{-F_\mu[U(t_n),\eta(t_n)](x)}\, U_\mu(x;t_n)\, \Omega^\dagger(x+\hat{\mu};t_n) = \\ &= \Omega(x;t_n)\, U_\mu(x;t_{n+1})\, \Omega^\dagger(x+\hat{\mu};t_n)\,, \end{aligned} \tag{3.50}$$

where it was made explicit that the force is computed from the configuration $U(t_n)$ and the noise realisation $\eta(t_n)$. How does this new evolution scheme affect observables? Using the gauge covariance of the force[7], it is clear that

$$F_\mu[\tilde{U}(t_{n+1}),\eta(t_{n+1})](x) = \Omega(x;t_n)\, F_\mu[U(t_{n+1}),\eta^\Omega(t_{n+1})](x)\, \Omega^\dagger(x;t_n)\,, \tag{3.51}$$

[7] The deterministic part of F is made of Wilson loops.

with the new noise

$$\eta^{\Omega}_{\mu}(x;t_{n+1}) = \Omega^{\dagger}(x;t_n)\eta_{\mu}(x;t_{n+1})\Omega(x;t_n)\,. \tag{3.52}$$

The next Langevin step is equivalent to

$$\begin{aligned}\tilde{U}_{\mu}(x;t_{n+2}) &= \Omega(x;t_{n+1})\, e^{-F_{\mu}[\tilde{U}(t_{n+1}),\eta(t_{n+1})](x)}\, \tilde{U}_{\mu}(x;t_{n+1})\, \Omega^{\dagger}(x+\hat{\mu};t_{n+1}) = \\ &= \Omega(x;t_{n+1})\, \Omega(x;t_n)\, e^{-F_{\mu}[U(t_{n+1}),\eta^{\Omega}(t_{n+1})](x)}\,\cdot \\ &\quad \cdot\, U_{\mu}(x;t_{n+1})\, \Omega^{\dagger}(x+\hat{\mu};t_n)\, \Omega^{\dagger}(x+\hat{\mu};t_{n+1})\,,\end{aligned} \tag{3.53}$$

and so on. The new evolution scheme leads to gauge-transformed configurations that have evolved with a noise η^{Ω}. Still, η^{Ω} is again a Gaussian noise and realises a valid Langevin history with the correct asymptotic distribution: therefore, gauge-invariant observables are not affected, and Eq. (3.50) provides a legitimate integration scheme. It is natural to expect that choosing

$$\Omega(x;t_n) = e^{\omega[U(t_{n+1})](x)} \qquad \text{with} \qquad \omega[U](x) = -\alpha\, \Pi_{\mathfrak{g}} \left(\sum_{\mu} \delta^{*}_{\mu} A_{\mu}(x) \right)\,, \tag{3.54}$$

with $\alpha \in (0,1)$, is effectively providing a force acting on the longitudinal components of the gauge field. Indeed, Eq. (3.54) is a gauge transformation that, if iterated, leads to the Landau gauge, as explained in Sect. 5.2.

Finally, we can present the discrete stochastic process that we are going to adopt [70]:

$$U'_{\mu}(x;t_n) = e^{-F_{\mu}(x;t_n)}\, U_{\mu}(x;t_n)\,, \tag{3.55a}$$

$$U_{\mu}(x;t_{n+1}) = e^{w[U'(t_n)](x)} U'_{\mu}(x;t_n) e^{-w[U'(t_n)](x+\hat{\mu})}\,, \tag{3.55b}$$

with

$$\omega[U](x) = -\alpha\, \Pi_{\mathfrak{g}} \left(\sum_{\mu} \delta^{*}_{\mu} U_{\mu}(x) \right)\,. \tag{3.56}$$

The chosen gauge transformation is different from the one in Eq. (3.54), and would not lead to the Landau gauge if iterated: however, it guarantees a force on the longitudinal components of the gauge field (U_{μ} and A_{μ} are equal at the lowest order), and it is cheaper to evaluate numerically (the logarithm needed to compute A_{μ} from the links is avoided).

Chapter 4

Twisted boundary conditions and fermions in NSPT

A perturbative approach for lattice gauge theories defined in a finite volume with periodic boundary condition (PBC) is not completely well defined. The Wilson action has several minima around which a perturbative expansion can be defined: these are called *torons*. It can be shown that not all of these vacua are equivalent, but there are some singular toron configurations around which the weak coupling expansion of the partition function is non-analytic [82–84]. On the other hand, it has been found that clever choices of boundary conditions allow overcoming this problem: in particular, *twisted boundary conditions* (TBC) admit a vacuum which is unique up to similarity transformations and multiplication by an element in the centre of SU (N_c) [85, 86], thus putting a perturbative expansion in finite volume on a solid ground.

TBC have been introduced in pure gauge NSPT for the first time in Refs. [87, 88]. In NSPT the introduction of such boundary conditions has another major motivation: they remove naturally the zero-momentum mode from the theory. We are going to study TBC and their compatibility with fermions; then, we will focus on the implementation of Wilson and staggered fermions in NSPT.

In this chapter $a = 1$.

4.1 Twisted boundary conditions

The usual choice of PBC implies defining the theory on a 4-dimensional torus. In fact, this premise can be relaxed. While the action and observables must be single-valued, the fields have additional freedom. In other words, when a theory is defined in finite volume, in order to avoid boundary terms, the fields can be required to satisfy any boundary conditions that are compatible with the symmetries of the action: since gauge field configurations related by a gauge transformation are physically equivalent, we can actually impose the gauge field to be periodic up to a gauge transformation. These are twisted boundary conditions [89].

Even though it is interesting to consider the general case [86], we will restrict ourselves to constant gauge transformations: TBC in direction $\hat{\nu}$ are

$$U_\mu(x + L\hat{\nu}) = \Omega_\nu U_\mu(x)\Omega_\nu^\dagger \,, \tag{4.1}$$

where $\Omega_\nu \in \mathrm{SU}(N_c)$ are the *twist matrices*. The gauge group has to transform accordingly: given a gauge transformation $\Lambda(x)$, then

$$\Lambda(x + L\hat{\nu}) = \Omega_\nu \Lambda(x)\Omega_\nu^\dagger \tag{4.2}$$

so that a gauge transformed link at the boundary can be evaluated without ambiguity,

$$\begin{aligned}\Lambda(x + L\hat{\nu})U_\mu(x + L\hat{\nu})\Lambda(x + L\hat{\nu} + \hat{\mu})^\dagger &= \Omega_\nu\Lambda(x)\Omega_\nu^\dagger\Omega_\nu U_\mu(x)\Omega_\nu^\dagger\Omega_\nu\Lambda(x + \hat{\mu})^\dagger\Omega_\nu^\dagger = \\ &= \Omega_\nu\Lambda(x)U_\mu(x)\Lambda(x + \hat{\mu})^\dagger\Omega_\nu^\dagger \,. \end{aligned} \tag{4.3}$$

Let us assume that directions $\hat{1}$ and $\hat{2}$ are twisted: since

$$U_\mu(x + L\hat{1} + L\hat{2}) = \Omega_1 U_\mu(x + L\hat{2})\Omega_1^\dagger = \Omega_1\Omega_2 U_\mu(x)\Omega_2^\dagger\Omega_1^\dagger \tag{4.4a}$$

$$U_\mu(x + L\hat{1} + L\hat{2}) = \Omega_2 U_\mu(x + L\hat{1})\Omega_2^\dagger = \Omega_2\Omega_1 U_\mu(x)\Omega_1^\dagger\Omega_2^\dagger \,, \tag{4.4b}$$

consistency requires that

$$U_\mu(x)(\Omega_1\Omega_2)^\dagger\Omega_2\Omega_1 = (\Omega_1\Omega_2)^\dagger\Omega_2\Omega_1 U_\mu(x) \,. \tag{4.5}$$

This means that the matrix $(\Omega_1\Omega_2)^\dagger\Omega_2\Omega_1$ must commute with all the elements of $\mathrm{SU}(N_c)$, i.e. must be in the centre Z_{N_c}. Therefore, the twist matrices cannot be

arbitrary matrices: they must satisfy

$$\Omega_2\Omega_1 = z\Omega_1\Omega_2 \tag{4.6}$$

for some $z = e^{i\frac{2\pi}{N_c}n}$ with $n = 0, \ldots, N_c - 1$. For a general number of twisted directions, the same condition reads

$$\Omega_\nu\Omega_\mu = z_{\mu\nu}\Omega_\mu\Omega_\nu\,, \tag{4.7}$$

with $z_{\mu\nu} = e^{i\frac{2\pi}{N}n_{\mu\nu}}$. The antisymmetric tensor $n_{\mu\nu}$ is called the *twist tensor*, and its components are integers modulo N_c. The elements Ω_μ, Ω_ν, z generate the *twist group*. If only two directions are twisted and $n_{\mu\nu}$ and N_c are coprime integers, it can be proved that the twist matrices are unique up to similarity transformations and multiplication by an element of the centre, i.e. they form an irreducible representation of the twist group (see Ref. [86] and references therein). Moreover, thanks to Schur's lemma, we have that $\Omega_\mu^{N_c}$ is an element of the centre times the identity, since it commutes with all the elements of the twist group.

4.1.1 Twisted action

It is possible to show that the Wilson action with TBC is related by a change of variable to a modified *twisted action* with PBC. We will present the argument here in pure gauge, and we will study later to which extent the equivalence holds in presence of fermions.

The partition function for pure Yang-Mills theory on the lattice is

$$Z = \int \mathcal{D}U\, e^{-S_G[U]}\,, \tag{4.8}$$

where we adopt the Wilson action of Eq. (1.21). TBC affect plaquette $U_{\mu\nu}(x)$ only when x is on the edge of the lattice in a twisted direction (i.e. $x_\mu = L - 1$ for a twisted direction $\hat{\mu}$). Two different cases arise.

x on the edge in one twisted direction: let $\hat{\mu}$, $\hat{\nu}$ be respectively twisted and periodic directions, and x such that $x_\mu = L - 1$. Then

$$U_{\mu\nu}(x) = U_\mu(x)\Omega_\mu U_\nu\left(x - (L-1)\hat{\mu}\right)\Omega_\mu^\dagger U_\mu(x+\hat{\nu})^\dagger U_\nu(x)^\dagger\,. \tag{4.9}$$

x **on the edge in two twisted directions:** let $\hat{\mu}$, $\hat{\nu}$ be two twisted directions, and x such that $x_\mu = x_\nu = L-1$. Then

$$U_{\mu\nu}(x) = U_\mu(x)\Omega_\mu U_\nu\left(x-(L-1)\hat{\mu}\right)\Omega_\mu^\dagger\Omega_\nu U_\mu\left(x-(L-1)\hat{\nu}\right)^\dagger\Omega_\nu^\dagger U_\nu(x)^\dagger\,. \quad (4.10)$$

We can now perform a unitary change of variable in the path integral in order to absorb the twist matrices in the plaquette. As explicitly shown in Refs. [82, 90, 91], new links $\tilde{U}_\mu(x)$ can be defined according to[1]

$$\begin{cases} U_\mu(x) = \tilde{U}_\mu(x)\Omega_\mu^\dagger & \text{if } \hat{\mu} \text{ is a twisted direction and } x_\mu = L-1 \\ U_\mu(x) = \tilde{U}_\mu(x) & \text{otherwise} \end{cases}. \quad (4.11)$$

The effect of the change of variable in the evaluation of the action is the following.

x **on the edge in one twisted direction:** in this case the plaquette is the same as if new variables obeyed PBC,

$$\begin{aligned} U_{\mu\nu}(x) &= \tilde{U}_\mu(x)\Omega_\mu^\dagger\Omega_\mu\tilde{U}_\nu\left(x-(L-1)\hat{\mu}\right)\Omega_\mu^\dagger\Omega_\mu\tilde{U}_\mu(x+\hat{\nu})^\dagger\tilde{U}_\nu(x)^\dagger = \\ &= \tilde{U}_\mu(x)\tilde{U}_\nu\left(x-(L-1)\hat{\mu}\right)\tilde{U}_\mu(x+\hat{\nu})^\dagger\tilde{U}_\nu(x)^\dagger\,. \end{aligned} \quad (4.12)$$

x **on the edge in two twisted directions:** in this case the plaquette is the same, apart from an overall phase, as if new variables obeyed PBC,

$$\begin{aligned} U_{\mu\nu}(x) &= \tilde{U}_\mu(x)\Omega_\mu^\dagger\Omega_\mu\tilde{U}_\nu\left(x-(L-1)\hat{\mu}\right)\Omega_\nu^\dagger\Omega_\mu^\dagger\Omega_\nu\Omega_\mu\tilde{U}_\mu\left(x-(L-1)\hat{\nu}\right)^\dagger\cdot \\ &\quad\cdot\,\Omega_\nu^\dagger\Omega_\nu\tilde{U}_\nu(x)^\dagger = \\ &= z_{\mu\nu}\tilde{U}_\mu(x)\tilde{U}_\nu\left(x-(L-1)\hat{\mu}\right)\tilde{U}_\mu(x+\hat{\nu})^\dagger\tilde{U}_\nu(x)^\dagger\,. \end{aligned} \quad (4.13)$$

All things considered, the partition function reduces to

$$Z_{\mathrm{TEK}} = \int \mathcal{D}U\,\exp\left(-\frac{\beta}{N_c}\sum_x\sum_{\mu<\nu}\mathrm{Re}\,\mathrm{Tr}\left(z_{\mu\nu}(x)U_{\mu\nu}(x)\right)\right), \quad (4.14)$$

where we dropped the tilde over the new links. The link variables now are assumed to be periodic. The phase $z_{\mu\nu}(x)$ is always equal to 1, except when $x_\mu = x_\nu = L-1$: in that case, $z_{\mu\nu}(x) = z_{\mu\nu}$ corresponds to the phase in the twist group. For the plaquettes that have $z_{\mu\nu}(x) \neq 1$, the action corresponds to the one of the

[1] Introducing the *ladders* $\Lambda_\mu = \{U_\mu(x) : x_\mu = L-1\}$, we see that the change of variable affects only the gauge links attached to a ladder in a twisted direction.

twisted Eguchi-Kawai model (TEK) [92, 93].

In conclusion, it can be stated that using explicit TBC is equivalent to have PBC and a twisted action. From the very same argument, other interesting properties follow:

- when $z_{\mu\nu} = 1$ (e.g. when only one direction is twisted, or when commuting twist matrices are used), TBC are not realised
- the vacuum of the TEK action (*twist eater*) can be obtained by setting $U_\mu(x) = 1$ in Eq. (4.11)
- sets of twist matrices with the same twist tensor are equivalent, and the corresponding partition functions are related to each other via the change of variable in Eq. (4.11).

4.2 Fermions with twisted boundary conditions

The partition function for a gauge theory coupled with fermions is

$$Z = \int \mathcal{D}[U, \psi, \bar{\psi}]\, e^{-S_G[U] - S_F[U,\psi,\bar{\psi}]}\,, \tag{4.15}$$

where, in addition to the lattice gauge action, we are considering a Wilson or staggered fermion action as in Eqs. (1.30) and (1.37) (for simplicity, only one flavour is considered).

4.2.1 Adjoint representation

Dealing with fermions in the adjoint representation and TBC does not pose any particular issue, because in this case fermions share the same transformation law as the gauge links. In this representation, it is more convenient to describe the fermion field with a $N_c \times N_c$ traceless matrix $\psi(x)$ defined by $\psi = \psi^a T^a$, see Appendix A. Using

$$\left((U_{\text{adj}})_\mu(x)\right)_{ab} = 2\,\text{Tr}\left(T^a U_\mu(x) T^b U_\mu(x)^\dagger\right)\,, \tag{4.16}$$

it is easy to rewrite the fermion action as a trace: for example, focusing on the colour structure only,

$$\bar{\psi}^a(x)\left(U_\mu^{\text{adj}}(x)\right)_{ab}\psi^b(x+\hat{\mu}) = 2\,\text{Tr}\left(\bar{\psi}(x)U_\mu(x)\psi(x+\hat{\mu})U_\mu(x)^\dagger\right)\,. \tag{4.17}$$

Imposing that the field configurations are periodic up to a gauge transformation requires care, because gauge invariance holds only if the fermions undergo a gauge transformation as well. This means that, in addition to Eq. (4.1), we require (in the matrix representation of the field)

$$\psi(x+L\hat{\nu}) = \Omega_\nu\psi(x)\Omega_\nu^\dagger\,. \tag{4.18}$$

Note that Eq. (4.7) is sufficient to make the twist well defined.

We can now try to build a twisted action. Since both Wilson and staggered actions have nearest neighbours interactions, like in Eq. (4.17), TBC have an effect only when x is on the edge of the lattice ($x_\mu = L-1$) and μ is a twisted direction: but that is also the only case in which the change of variable of Eq. (4.11) is switched on, therefore

$$\begin{aligned}\bar{\psi}(x)U_\mu(x)\psi(x+\hat{\mu})U_\mu(x)^\dagger &= \bar{\psi}(x)U_\mu(x)\Omega_\mu\psi(x-(L-1)\hat{\mu})\Omega_\mu^\dagger U_\mu(x)^\dagger = \\ &= \bar{\psi}(x)\tilde{U}_\mu(x)\Omega_\mu^\dagger\Omega_\mu\psi(x-(L-1)\hat{\mu})\Omega_\mu^\dagger\Omega_\mu\tilde{U}_\mu(x)^\dagger\,.\end{aligned} \tag{4.19}$$

After taking the trace it is evident that the new link variables absorb the twist in the fermion sector; in the new variables, the fermion field can be considered periodic[2]. We have found that a lattice gauge theory with Wilson or staggered fermions in the adjoint representation and TBC is equivalent to a theory with PBC and a twisted action for the gauge sector.

4.2.2 Fundamental representation

The inclusion of fermions in the fundamental representation is not straightforward; indeed, the gauge transformation for the fermions when translated by a

[2] Periodic is in the sense that it does not undergo a gauge transformation after L sites. If the field had other constraints (for example antiperiodicity in the time direction), those will stay.

multiple of the lattice size reads

$$\psi(x + L\hat{\nu}) = \Omega_\nu \psi(x)\,, \tag{4.20}$$

leading to an ambiguous definition of $\psi(x + L\hat{\mu} + L\hat{\nu})$. An idea to overcome this problem, proposed in Ref. [94, 95] and implemented e.g. in Ref. [96], is to introduce a new quantum number so that fermions exist in different copies, or *smells*, which transform into each other according to the antifundamental representation of SU(N_c). The theory has a new global symmetry, but physical observables are singlets under the smell group. Thus, configurations related by a smell transformations are equivalent, and in finite volume we are free to substitute Eq. (4.20) with

$$\psi(x + L\hat{\nu})_{ir} = \sum_{j,s} \big(\Omega_\nu\big)_{ij} \psi(x)_{js} \big(\Lambda_\nu^\dagger\big)_{sr}\,, \tag{4.21}$$

where $\Lambda_\nu \in \mathrm{SU}(N_c)$. It is useful to think of the fermion field as a matrix in colour-smell space. If the transformation matrices in smell space satisfy the same relations as in Eq. (4.7), then twisted boundary conditions are well defined. In particular, we will always choose $\Lambda_\mu = \Omega_\mu$.

It is worth pointing out that the change of variable in Eq. (4.11) does not allow formulating a twisted action. If x is on the edge of the lattice and μ is a twisted direction, then the action has a contribution that goes like

$$\begin{aligned}\bar{\psi}(x) U_\mu(x) \psi(x + \hat{\mu}) &= \bar{\psi}(x) U_\mu(x) \Omega_\mu \psi(x - (L-1)\hat{\mu}) \Omega_\mu^\dagger = \\ &= \bar{\psi}(x) \tilde{U}_\mu(x) \Omega_\mu^\dagger \Omega_\mu \psi(x - (L-1)\hat{\mu}) \Omega_\mu^\dagger\,,\end{aligned} \tag{4.22}$$

where the field $\psi(x)$ is regarded as a matrix in colour-smell space. Since only one link participate in Eq. (4.22), not all the twist matrices are absorbed, even after taking the trace. A redefinition of $\psi(x)$ would spoil other contributions to the action in the inner region of the lattice. Thus, the explicit transformation of Eq. (4.21) is required when fermions in the fundamental representation with smell are considered.

4.3 Zero-momentum mode in NSPT

When dealing with gauge theories in NSPT, we have already mentioned the existence of zero-mode sources. The problem of the gauge zero mode has been

already tackled in Sect. 3.4. Here we want to study the zero-momentum mode: indeed, it is evident that the Fourier mode of the gauge potential with $k = 0$ is not affected by the Langevin drift, and satisfies Eq. (3.30). In other words, the force originating from the gauge action does not act on constant gauge configurations (the free field strength in Eq. (1.11) is made of derivatives acting on the gauge potential). This issue survives in the lattice formulation, since the link field and the gauge potential are equal at the lowest order; the diverging fluctuations propagate to higher perturbative orders as well. The zero-momentum problem can also be seen in finite-volume lattice perturbation theory: the gluon propagator has a pole at $k = 0$, and gives a divergent contribution when a quantised gluon momenta with PBC is summed over. A quick solution amounts to neglecting such mode [97]: in NSPT this means that, at each evolution step, the condition

$$\sum_x A_\mu^{(n)}(x) = 0 \tag{4.23}$$

must be enforced at all orders. The theory simulated in this way is nonlocal, as it is a gauge theory with an additional constraint which becomes irrelevant in the infinite-volume limit only. New nonperturbative effects due to the lack of this mode are introduced: these invalidate the finite-volume OPE developed in Ref. [98].

On the other hand, TBC can be used in finite-volume lattice perturbation theory to remove the zero-momentum mode without imposing any additional constraint. To understand why this happens, first we have to work out the Fourier decomposition with TBC. Such decomposition will turn out to be useful also when simulating fermions in NSPT.

If $f(x)$ is a periodic function defined on the L^4 lattice, its Fourier transform and inverse are

$$f(x) = \frac{1}{L^4} \sum_{p_\parallel} e^{ip_\parallel x} \tilde{f}(p_\parallel)\,, \qquad \tilde{f}(p_\parallel) = \sum_x e^{-ip_\parallel x} f(x)\,, \tag{4.24}$$

where $p_\parallel$ is the quantised vector $p_\parallel = \frac{2\pi}{L}(n_1, n_2, n_3, n_4)$, and the sum is to be read $\sum_{p_\parallel} = \sum_{n_1,n_2,n_3,n_4=0}^{L-1}$. Antiperiodicity in the direction $\hat{\nu}$ would lead again to Eq. (4.24) but with a quantised momentum $(p_\parallel)_\mu = \frac{2\pi}{L} n_\mu + \frac{\pi}{L}\delta_{\mu\nu}$.

Twisted boundary conditions on a plane

Let us consider some $N_c \times N_c$ matrix $M(x)$ (which for example can be a gauge link or the vector potential seen as matrices in colour space, or a fundamental fermion field seen as a matrix in colour-smell). We impose twisted boundary condition in the $\hat{1}, \hat{2}$ plane so that

$$M(x + L\hat{1}) = \Omega_1 M(x) \Omega_1^\dagger \,, \qquad M(x + L\hat{2}) = \Omega_2 M(x) \Omega_2^\dagger \,, \tag{4.25}$$

with $\Omega_2 \Omega_1 = z \Omega_1 \Omega_2$, $z = z_{12} \in Z_{N_c}$. If we had just (anti)periodic boundary conditions, we would treat the matrix as N_c^2 independent scalar functions; twisted boundary conditions actually couple the different components, therefore in order to expand $M(x)$ in plane waves we need to find a good basis for the matrix space. It can be proved (see Refs. [91, 93, 99]) that the Fourier transform and its inverse are

$$M(x) = \frac{1}{N_c L^4} \sum_{p_\parallel, p_\perp} e^{ipx} \, \Gamma_{p_\perp} \tilde{M}(p_\parallel)_{p_\perp} \,, \qquad \tilde{M}(p_\parallel)_{p_\perp} = \sum_x e^{-ipx} \, \mathrm{Tr} \, \Gamma_{p_\perp}^\dagger M(x) \,, \tag{4.26}$$

where $p = p_\parallel + p_\perp$, $p_\perp$ is the quantised vector $p_\perp = \frac{2\pi}{N_c L}(\tilde{n}_1, \tilde{n}_2, 0, 0)$, and the sum is to be read $\sum_{p_\perp} = \sum_{\tilde{n}_1, \tilde{n}_2 = 0}^{N_c - 1}$. The matrices $\Gamma_{p_\perp}$ form the sought basis in the matrix space: assuming a twist with $z = \exp(2\pi i / N_c)$, we can choose for example

$$\Gamma_{p_\perp} = \Omega_1^{\tilde{n}_2} \Omega_2^{-\tilde{n}_1} \,. \tag{4.27}$$

A different choice for z would have somehow reshuffled the exponents in Eq. (4.27). We see that the Fourier transform of $M(x)$ is a scalar function $\tilde{M}(p_\parallel)_{p_\perp}$, but momentum has a finer resolution compared to (anti)periodic boundary conditions: spatial and colour degrees of freedom mix in momentum space. We can now see that traceless matrices naturally do not have a zero mode, because

$$\tilde{M}(p_\parallel)_{p_\perp = 0} = \sum_x e^{-ip_\parallel x} \, \mathrm{Tr} \, M(x) \,. \tag{4.28}$$

Therefore the gauge potential does not have any zero-momentum component.

It is also useful to report a few properties satisfied by the matrices defined in

Eq. (4.27),

$$\operatorname{Tr}\Gamma_{p_\perp} = N_c\,\delta_{p_\perp,0} \tag{4.29a}$$

$$\Gamma^\dagger_{p_\perp} = f(p_\perp,p_\perp)\Gamma_{-p_\perp} \tag{4.29b}$$

$$\Gamma_{p_\perp}\Gamma_{p'_\perp} = f(p_\perp,p'_\perp)\Gamma_{p_\perp+p'_\perp}\,, \tag{4.29c}$$

where we defined the phase

$$f(p_\perp,p'_\perp) = z^{-\tilde{n}_1\tilde{n}'_2}\,. \tag{4.30}$$

Twisted boundary conditions in three directions

The conditions in Eq. (4.25) are supplemented by

$$M(x+L\hat{3}) = \Omega_3 M(x)\Omega_3^\dagger\,, \tag{4.31}$$

with $\Omega_3 = \Omega_1^\rho\Omega_2^\sigma$ and ρ,σ span all the possible twist choices. It can be shown that Eq. (4.26) still holds, but with a fine momentum $p_\perp = \frac{2\pi}{N_cL}(\tilde{n}_1,\tilde{n}_2,\tilde{n}_3,0)$. The component $\tilde{n}_3$ is not a new degree of freedom but depends on the values of $\tilde{n}_1,\tilde{n}_2$. For example, in the case $z=\exp(2\pi i/N_c), \rho=\sigma=1$, then $\tilde{n}_3 = (\tilde{n}_1+\tilde{n}_2)$ mod N_c. Other choices of z,ρ,σ just give a new relation between $\tilde{n}_3$ and $z,\tilde{n}_1,\tilde{n}_2$.

Numerical implementation

The Fast Fourier Transform (FFT) algorithm encodes Eq. (4.24), $\mathrm{FFT}[f(x)] = \tilde{f}(p)$. It is not possible to apply the FFT directly to each matrix element of $M(x)$, because the Fourier expansion has a dependence on $p_\perp x$. First, we need to project onto one of the $p_\perp$,

$$\hat{M}(x)_{p_\perp} = e^{-ip_\perp x}\operatorname{Tr}\Gamma^\dagger_{p_\perp}M(x) = \frac{1}{L^4}\sum_{p_\parallel} e^{ip_\parallel x}\tilde{M}(p_\parallel)_{p_\perp}\,, \tag{4.32}$$

and then to each of these we apply the FFT,

$$\tilde{M}(p_\parallel)_{p_\perp} = \mathrm{FFT}[\hat{M}(x)_{p_\perp}]\,. \tag{4.33}$$

At the end, N_c^2 projections and N_c^2 FFTs have been performed. The inverse transform will be simply

$$\hat{M}(x)_{p_\perp} = \mathrm{FFT}^{-1}[\tilde{M}(p_\parallel)_{p_\perp}] \tag{4.34}$$

followed by

$$M(x) = \frac{1}{N_c} \sum_{p_\perp} e^{ip_\perp x}\, \Gamma_{p_\perp} \hat{M}(x)_{p_\perp}\,. \tag{4.35}$$

Note that $\tilde{M}(p_\parallel)_{p_\perp}$ is a scalar function but the dependence on $p_\perp$ is through $\tilde{n}_1, \tilde{n}_2$, where each integer runs from 0 to $N_c - 1$: this allows a representation of the Fourier transform again with a $N_c \times N_c$ matrix field, $\big(M(p_\parallel)\big)_{\tilde{n}_1\tilde{n}_2}$. Of course this has to be understood only as a useful representation of the momentum degrees of freedom, not as a matrix in colour space.

4.4 Fermion drift in NSPT

If $S_F[U, \psi, \bar{\psi}] = \sum_{x,y} \bar{\psi}(x) M[U]_{x,y} \psi(y)$ is the action of a single fermion, then dynamical fermions can be included in NSPT thanks to a new term in the drift, as shown in Refs. [75, 100]. The determinant arising from N_f degenerate fermions can be rewritten as

$$\det(M)^{N_f} = \exp\left(N_f \,\mathrm{Tr} \log M\right)\,, \tag{4.36}$$

and can be taken into account by considering the effective action

$$S_{\mathrm{eff}}[U] = S_G[U] - N_f \,\mathrm{Tr} \log M\,. \tag{4.37}$$

From the Lie derivative of the additional term, and recalling that a rescaled time step $\tau = \epsilon/\beta$ is used in the Euler update, we obtain the new contribution

$$F_\mu^f(x) = -i\, \frac{\tau N_f}{\beta} \sum_a T^a \,\mathrm{Tr}(\nabla^a_{x\mu} M) M^{-1} \tag{4.38}$$

to be added to the pure gauge drift of Eq. (3.34). It is important to note that the coefficient of iT^a is purely real because the Wilson operator is γ_5-Hermitian and the staggered operator is antihermitian: this is consistent with the drift being an element of the algebra. The trace can be evaluated stochastically: Eq. (4.38) is

replaced by

$$F^f_\mu(x) = -i\frac{\tau N_f}{\beta}\sum_a T^a \,\mathrm{Re}\,\xi^*(\nabla^a_{x\mu}M)M^{-1}\xi \tag{4.39}$$

thanks to the introduction of a new complex Gaussian noise ξ satisfying[3]

$$\langle \xi^*(y)_{\beta ir}\xi(z)_{\gamma js}\rangle = \delta_{yz}\delta_{\beta\gamma}\delta_{ij}\delta_{rs}\,. \tag{4.40}$$

The real part must be enforced, otherwise the drift would be guaranteed to be in the algebra only on average, and the dynamics would lead the links out of the group.

The stochastic process defined in this way is driven by two random sources, η and ξ: retracing the same steps presented in Sect. 3.3, it is easy to see that the equilibrium distribution is the desired one up to $O(\epsilon)$. The pure-gauge Runge-Kutta algorithms developed in Refs. [41, 75] are able to remove $O(\epsilon)$ effects only if the fermion contribution is evaluated exactly; this is because it would hold, trivially, $\big\langle F^f_\mu(x)F^f_\nu(y)\big\rangle = \big\langle F^f_\mu(x)\big\rangle\big\langle F^f_\nu(y)\big\rangle$. Since the drift originating from the fermion action is evaluated stochastically, higher-order integration schemes need to take into account the presence of two random sources: this means that, calling $\mathrm{Re}\,\xi^*(\nabla_{x\mu}M)M^{-1}\xi = \xi^*A_{x\mu}\xi$, it is

$$\begin{aligned}\big\langle F^f_\mu(x)F^f_\nu(y)\big\rangle &= -\epsilon^2 N_f^2\langle \xi^*A_{x\mu}\xi\,\xi^*A_{y\nu}\xi\rangle = \\ &= -\epsilon^2 N_f^2\,(\mathrm{Tr}\,A_{x\mu}\,\mathrm{Tr}\,A_{y\nu} + \mathrm{Tr}\,A_{x\mu}A_{y\nu}) = \\ &= \big\langle F^f_\mu(x)\big\rangle\big\langle F^f_\nu(y)\big\rangle - \epsilon^2 N_f^2\,\mathrm{Tr}\,A_{x\mu}A_{y\nu}\,.\end{aligned} \tag{4.41}$$

The additional term in Eq. (4.41) is a *non-integrable term* that prevents from defining an equilibrium distribution for the Fokker-Planck equation. Such term arises from the connected contribution of the four-point Gaussian correlator[4]. Even though it is possible to build more sophisticated Runge-Kutta schemes where the non-integrable terms are removed [101, 102], they turn out to be computational expensive and not practical [103]. Having this in mind, the choices in the literature have been either to remove the $O(\epsilon)$ effects partially, by adopting a naive Runge-Kutta integrator and leaving the non-integrable terms, or to use simply an Euler scheme; we will always stick to the latter option in the following.

[3] Obviously ξ does not have any Dirac structure in the staggered case. The noise can be built from the independent generation of real and imaginary part with zero mean and variance 1/2.

[4] An additional non-integrable term would be present in the case of a non-Gaussian fermion noise, see Sect. 4.4.5.

In NSPT, the Dirac operator inherits a formal perturbative expansion from the links, $M = \sum_{n=0}^{\infty} \beta^{-n} M^{(n)}$, so the inverse $\psi = M^{-1}\xi$ can be computed efficiently from the knowledge of the inverse free operator via the recursive formula

$$\psi^{(0)} = {M^{(0)}}^{-1} \xi \tag{4.42a}$$

$$\psi^{(n)} = -{M^{(0)}}^{-1} \sum_{j=0}^{n-1} M^{(n-j)} \psi^{(j)} \,. \tag{4.42b}$$

The inverse of the free operator is conveniently applied in Fourier space. It is important to remember that the massless fermion propagator has a pole for vanishing momentum, and one must be careful when applying ${M^{(0)}}^{-1}$: the component with zero momentum must be excluded from the Fourier decomposition of ξ. Clearly this is only a matter of existence of the inverse Dirac operator, and is a problem unrelated to the issue of convergence of the stochastic process. Indeed, a fundamental fermion with smell (seen as matrix in colour-smell space) is not required to be traceless, thus its Fourier zero-mode does not vanish. Therefore, fermions are always required to have antiperiodic boundary conditions in time direction. Twisted boundary conditions in time direction are also avoided because, in the massless case, it might happen for the free fermion propagator to develop a pole at some particular momenta.

If fermions have smell, then the rescaling $N_f \to N_f/N_c$ is required in order to have N_f flavours in the infinite-volume limit. In other words, this is the same as considering the N_cth root of the determinant of the fermion operator. In principle such rooted determinant could come from a nonlocal action, because twisted boundary conditions break the invariance under smell transformations. Nevertheless, this rooting procedure is sound since we know in advance that in the infinite-volume limit all the dependence on boundary conditions will be lost, and the determinant will factorise as the fermion determinant of a single smell times the identity in smell space. It is also possible to show with arguments similar to those presented in Ref. [10] that, if the theory without smell is renormalisable, this operation leads to a perturbatively renormalisable theory as well. Below, when describing Wilson and staggered fermions in the fundamental representation, we explicitly rescale $N_f \to N_f/N_c$.

4.4.1 Wilson fermions

The Wilson Dirac operator and its Lie derivative are

$$M_{y\beta ir,z\gamma js} = (m+4)\delta_{rs}\delta_{yz}\delta_{\beta\gamma}\delta_{ij} + \sum_{\mu}\left[D(\mu) + \gamma_5 D(\mu)^\dagger \gamma_5\right]_{y\beta ir,z\gamma js} \tag{4.43a}$$

$$\nabla^a_{x\mu} M_{y\beta ir,z\gamma js} = i\delta_{xy}[T^a D(\mu)]_{y\beta ir,z\gamma js} - i\delta_{xz}[\gamma_5 D(\mu)^\dagger \gamma_5 T^a]_{y\beta ir,z\gamma js}\,, \tag{4.43b}$$

where the non-diagonal term has been expressed through

$$D(\mu)_{y\beta ir,z\gamma js} = -\frac{1}{2}\delta_{rs}\delta_{y,z-\hat{\mu}}(1-\gamma_\mu)_{\beta\gamma}U_\mu(y)_{ij}\,. \tag{4.44}$$

It is easy to see that this operator reconstructs the action in Eq. (1.30). We must give a perturbative structure to the mass $m = \sum_{n=0}^{\infty}\beta^{-n}m^{(n)}$ to account for an additive mass renormalisation, see Sect. 5.1. The stochastic evaluation of the trace leads to

$$\xi^*(\nabla^a_{x\mu}M)M^{-1}\xi = i\,\mathrm{Tr}\,T^a\sum_{\beta}\left(\varphi^{(\mu)}(x)_\beta\,\xi(x)^\dagger_\beta - \psi(x)_\beta\,\tilde{\varphi}^{(\mu)}(x)^\dagger_\beta\right)\,, \tag{4.45}$$

where $\varphi^{(\mu)} = D(\mu)\psi$, $\tilde{\varphi}^{(\mu)} = \gamma_5 D(\mu)\gamma_5\xi$ and the fermion fields have been represented as matrices in colour-smell space. After taking the real part, the fermion drift can be finally written as

$$\begin{aligned} F^f_\mu(x)_{ij} &= \frac{1}{2}\frac{N_f}{N_c}\frac{\tau}{\beta}\sum_a T^a_{ij}\,\mathrm{Tr}\,T^a\sum_\beta\left[\left(\varphi^{(\mu)}(x)_\beta\,\xi(x)^\dagger_\beta - \psi(x)_\beta\,\tilde{\varphi}^{(\mu)}(x)^\dagger_\beta\right) - \mathrm{h.c.}\right] = \\ &= \frac{1}{2}\frac{N_f}{N_c}\frac{\tau}{\beta}\,\Pi_{\mathfrak{g}}\left[\sum_\beta\left(\varphi^{(\mu)}(x)_\beta\,\xi(x)^\dagger_\beta + \tilde{\varphi}^{(\mu)}(x)_\beta\,\psi(x)^\dagger_\beta\right)\right]_{ij}\,. \end{aligned} \tag{4.46}$$

In Sect. 4.4.3 the actual implementation of the fermion drift is described (only one of the two terms in Eq. (4.46) is actually needed).

With the Fourier transform described in Sect. 4.3, the inverse free Wilson operator with twisted boundary conditions is diagonal in momentum space and can be expressed as

$$M^{(0)^{-1}}_{k,p} = \delta_{k_\parallel p_\parallel}\delta_{k_\perp p_\perp}\frac{2\sum_\mu \sin^2\frac{k_\mu}{2} + m^{(0)} - i\sum_\mu \gamma_\mu \sin k_\mu}{\left(2\sum_\mu \sin^2\frac{k_\mu}{2} + m^{(0)}\right)^2 + \sum_\mu \sin^2 k_\mu}\,. \tag{4.47}$$

4.4.2 Staggered fermions

We implemented for the first time staggered fermions in NSPT. The staggered field has no Dirac structure and describes four physical fermions in the continuum limit. Therefore, we rescale $N_f \to N_f/4$ and the staggered operator is understood to be rooted when the number of flavour is not a multiple of four[5]. The staggered Dirac operator and its Lie derivative are

$$M_{yir,zjs} = m\delta_{rs}\delta_{yz}\delta_{ij} + \sum_{\mu} \left[D(\mu) - D(\mu)^\dagger\right]_{yir,zjs} \tag{4.48a}$$

$$\nabla^a_{x\mu} M_{yir,zjs} = i\delta_{xy}[T^a D(\mu)]_{yir,zjs} + i\delta_{xz}[D(\mu)^\dagger T^a]_{yir,zjs}\,, \tag{4.48b}$$

where the non-diagonal term has been expressed through

$$D(\mu)_{yir,zjs} = \frac{1}{2}\alpha_\mu(y)\delta_{rs}\delta_{y,z-\hat{\mu}}U_\mu(y)_{ij}\,. \tag{4.49}$$

This operator reconstructs the staggered action in Eq. (1.37). The stochastic evaluation of the trace is analogous to the Wilson fermion case and Eq. (4.45) becomes

$$\xi^*(\nabla^a_{x\mu}M)M^{-1}\xi = i\,\mathrm{Tr}\,T^a\left(\varphi^{(\mu)}(x)\,\xi(x)^\dagger - \psi(x)\,\tilde{\varphi}^{(\mu)}(x)^\dagger\right)\,, \tag{4.50}$$

with $\varphi^{(\mu)} = D(\mu)\psi$ and $\tilde{\varphi}^{(\mu)} = -D(\mu)\xi$, leading to the final expression

$$F^f_\mu(x)_{ij} = \frac{1}{2}\frac{N_f}{4N_c}\frac{\tau}{\beta}\,\Pi_{\mathfrak{g}}\left(\varphi^{(\mu)}(x)\,\xi(x)^\dagger + \tilde{\varphi}^{(\mu)}(x)\,\psi(x)^\dagger\right)_{ij}\,. \tag{4.51}$$

Again, the actual implementation of the staggered drift is shown in Sect. 4.4.3.

With the Fourier transform described in Sect. 4.3, the inverse free staggered operator with twisted boundary conditions is found to be

$$M^{(0)\,-1}_{k,p} = \delta_{k_\perp p_\perp}\frac{m\delta_{k_\parallel p_\parallel} - i\sum_\mu \sin k_\mu\,\bar{\delta}(k_\parallel + \pi\bar{\mu} - p_\parallel)}{\sum_\mu \sin^2 k_\mu + m^2}\,, \tag{4.52}$$

where $\bar{1} = 0$, $\overline{\mu+1} = \bar{\mu} + \hat{\mu}$ and $\bar{\delta}$ is the periodic Kronecker delta, with support in $0 \mod 2\pi$. The propagator is not diagonal in momentum space because the

[5] As rooting does not pose any issue in perturbation theory, the use of naive fermions would have been acceptable as well. However, staggered fermions are the choice to be preferred because they are cheaper to simulate and because, in order to compare perturbative and nonperturbative physics, we can exploit results of several nonperturbative simulations performed in the past.

action depends explicitly on the position through $\alpha_\mu(x)$, but it is simple enough to avoid a complete matrix multiplication over all the degrees of freedom. If we aim to compute ${M^{(0)}}^{-1}v$ for some field v in momentum space, it is useful to represent $v(p_\parallel)_{p_\perp}$ as matrices $N_c \times N_c$ with indices $\tilde{n}_1, \tilde{n}_2$ defined at each $p_\parallel$ site (n_1, n_2, n_3, n_4). Then the non-diagonal terms become diagonal when shifting iteratively v by $L/2$ in the $p_\parallel$ space. Incidentally, we must consider L to be even so that at the same time $L/2$ is well defined and (in the massless case) no spurious pole is hit when Eq. (4.52) is evaluated in finite volume: this stems from the fact that the staggered action is only invariant under translation of two lattice spacings, therefore twisted boundary conditions would be inconsistent for L odd.

4.4.3 Drift optimisation

A useful optimisation consists in improving on Eqs. (4.46) and (4.51) so that it becomes numerically cheaper to evaluate the fermion drift. Considering for example Wilson fermions, we notice that it is possible to simplify the trace

$$\begin{aligned}\mathrm{Tr}(\nabla^a_{x\mu} M)M^{-1} &= i\tilde{\mathrm{Tr}}\left[\left(T^a D(\mu)M^{-1}\right)_{x,x} - \left(\gamma_5 D(\mu)^\dagger \gamma_5 T^a M^{-1}\right)_{x,x}\right] = \\ &= i\sum_{y,\beta,i,r}\left(\delta_{x,y}[T^a D(\mu)M^{-1}]_{y\beta ir,y\beta ir} - \text{h.c.}\right), \end{aligned} \tag{4.53}$$

where $\tilde{\mathrm{Tr}}$ is tracing all indices but the position one, and we used the fact that the inverse Wilson operator is γ_5-Hermitian. For staggered fermions the simplification is analogous because the inverse staggered operator is antihermitian. The step must be done before the stochastic evaluation of the trace: once the random sources are introduced, cyclic invariance gets broken and will be restored only on average. Using Eq. (4.53) as a starting point, we obtain a drift which is already in the algebra (no need of taking the real part),

$$F^f_\mu(x)_{ij} = \frac{N_f}{N_c}\frac{\tau}{\beta}\,\Pi_{\mathfrak{g}}\left(\sum_\beta \varphi^{(\mu)}(x)_\beta\,\xi(x)^\dagger_\beta\right)_{ij} \qquad \text{(Wilson fermions)} \tag{4.54a}$$

$$F^f_\mu(x)_{ij} = \frac{N_f}{4N_c}\frac{\tau}{\beta}\,\Pi_{\mathfrak{g}}\left(\varphi^{(\mu)}(x)\,\xi(x)^\dagger\right)_{ij} \qquad \text{(staggered fermions)}\,. \tag{4.54b}$$

In a similar fashion, it could be possible to show that also

$$F^f_\mu(x)_{ij} = \frac{N_f}{N_c}\frac{\tau}{\beta}\,\Pi_{\mathfrak{g}}\left(\sum_\beta \tilde{\varphi}^{(\mu)}(x)_\beta\,\psi(x)^\dagger_\beta\right)_{ij} \qquad \text{(Wilson fermions)} \tag{4.55a}$$

$$F^f_\mu(x)_{ij} = \frac{N_f}{4N_c}\frac{\tau}{\beta}\,\Pi_{\mathfrak{g}}\left(\tilde{\varphi}^{(\mu)}(x)\,\psi(x)^\dagger\right)_{ij} \qquad \text{(staggered fermions)} \tag{4.55b}$$

are legitimate expressions for the drift. Even though all these new formulae are numerically different from those in Eqs. (4.46) and (4.51), they lead to the same results on average; clearly the advantage is that only half of the Lie derivative has to be computed.

4.4.4 Adjoint representation

The whole construction presented so far can be adapted to the case of fermions in the adjoint representation. Thanks to Eq. (4.16), the Lie derivative of a link in the adjoint representation can be recast as a trace involving links in the fundamental representation,

$$\nabla^a_{x\mu}((U_{\text{adj}})_\mu(x))_{bc} = 2i\,\mathrm{Tr}\,T^a[U_\mu(x)T^cU_\mu(x)^\dagger, T^b]\,. \tag{4.56}$$

A Gaussian noise satisfying

$$\left\langle \xi^*(y)^a_\beta\,\xi(z)^b_\gamma\right\rangle = \delta_{yz}\delta_{\beta\gamma}\delta^{ab} \tag{4.57}$$

is introduced for the stochastic evaluation of the fermion trace (no Dirac structure is given to ξ in the staggered case). The matrix representation $\xi = \sum_a \xi^a T^a$ can be conveniently used. The previous calculations carry on in an analogous way, with the following minor modifications:

- an overall factor of 2, due to the different normalisation that arises from using the matrix representation for the field
- the outer products $\varphi\,\xi$ and $\tilde{\varphi}\,\psi$ are replaced by commutators
- the operator $D(\mu)$ acts in the adjoint representation, e.g. for staggered fermions $D(\mu)\psi(x) = \frac{1}{2}\alpha_\mu(x)U_\mu(x)\psi(x+\hat{\mu})U_\mu(x)^\dagger$.

Eqs. (4.46) and (4.51) become respectively

$$F_\mu^f(x)_{ij} = \frac{N_f}{N_c}\frac{\tau}{\beta}\,\Pi_{\mathfrak{g}}\left[\sum_\beta\left([\varphi^{(\mu)}(x)_\beta,\xi(x)^\dagger_\beta] + [\tilde{\varphi}^{(\mu)}(x)_\beta,\psi(x)^\dagger_\beta]\right)\right]_{ij} \tag{4.58}$$

and

$$F_\mu^f(x)_{ij} = \frac{N_f}{4N_c}\frac{\tau}{\beta}\,\Pi_{\mathfrak{g}}\left([\varphi^{(\mu)}(x),\xi(x)^\dagger] + [\tilde{\varphi}^{(\mu)}(x),\psi(x)^\dagger]\right)_{ij}\,. \tag{4.59}$$

In this formulation, it must also be emphasised that the Dirac operator is not linear in the links, as link multiplication $U\psi$ is replaced by $U\psi U^\dagger$; the perturbative structure of the Dirac operator is found by expanding in the coupling both U and $U^\dagger$, and thus becomes slightly more involved.

4.4.5 A better estimator of the trace

It was assumed that the white noise employed to evaluate stochastically the fermion trace was coming from a normal distribution. In fact, this hypothesis can be relaxed. We will prove now that when ξ is drawn from a Z_2 distribution, the variance of the estimator in Eq. (4.39) is minimum. Even though we have ascertained numerically that the use of a Z_2 estimator reduces the variances of signals in NSPT, this is still a topic that has not been investigated thoroughly. In the results we present in Chapter 5 and Chapter 6, a Gaussian ξ is still used. Definitely, using a Z_2 noise represents a promising feature to be added in future simulations.

A small summary on random variables

Let a be a real random variable, then $\langle f(a)\rangle = \int P(a)f(a)da$, where $P(a)$ is the probability density[6] associated to a. For some $n \in \mathbb{N}$, the moments of the probability distribution are defined as

$$\hat{\sigma}_n = \int P(a)a^n da\,. \tag{4.60}$$

$P(a)$ is chosen to be even, so that all odd moments vanish (in particular, the expectation value of a is zero). Without loss of generality, we also take $\hat{\sigma}_2 = 1$,

[6]Thus $P(a) \geq 0$, $\int P(a)da = 1$. If a is discrete, then $P(a)$ is some linear combination of delta functions and the integral becomes a sum.

which corresponds to a choice for the normalisation of the random variable. If a_1, a_2 are two such variables, then it is possible to define a new complex random variable

$$\xi = \frac{1}{\sqrt{2}} (a_1 + i a_2) \ . \tag{4.61}$$

We can restrict ourselves to expectation values of $|\xi|$, because averages $\langle (\xi^*)^i (\xi)^j \rangle$ with $i \neq j$ vanish. The moments are defined as

$$\sigma_n = \langle |\xi|^n \rangle \, , \tag{4.62}$$

and our previous choice of normalisation fixes $\sigma_2 = 1$. Note that, given some function $f(a)$, Lyapunov's inequality

$$\langle |f(a)|^s \rangle^{1/s} \leq \langle |f(a)|^t \rangle^{1/t} \quad \text{with} \quad 0 < s \leq t \tag{4.63}$$

implies

$$\langle |f(a)|^t \rangle \geq \langle |f(a)|^s \rangle^{t/s} \quad \text{with} \quad 0 < s \leq t \, , \tag{4.64}$$

and gives the *moment monotonicity*

$$\langle |\xi|^t \rangle \geq \langle |\xi|^s \rangle^{t/s} \quad \text{with} \quad 0 < s \leq t \, . \tag{4.65}$$

In particular $\sigma_{2n} \geq \sigma_n^2$. When having a vector of independent complex random variables, it always possible to split the expectation value $\langle \xi_i^* \dots \xi_j^* \xi_k \dots \xi_l \rangle$ in connected and disconnected components. For example,

$$\langle \xi_i^* \xi_j \rangle = \sigma_2 \delta_{ij} = \delta_{ij} \tag{4.66a}$$

$$\begin{aligned} \langle \xi_i^* \xi_j^* \xi_k \xi_l \rangle &= \langle \xi_i^* \xi_k \rangle \langle \xi_j^* \xi_l \rangle + \langle \xi_i^* \xi_l \rangle \langle \xi_j^* \xi_k \rangle + \\ &\quad + [\langle \xi_i^* \xi_i^* \xi_i \xi_i \rangle - \langle \xi_i^* \xi_k \rangle \langle \xi_j^* \xi_l \rangle - \langle \xi_i^* \xi_l \rangle \langle \xi_j^* \xi_k \rangle] \delta_{ij} \delta_{jk} \delta_{kl} = \\ &= \delta_{ik} \delta_{jl} + \delta_{il} \delta_{jk} + (\sigma_4 - 2) \delta_{ij} \delta_{jk} \delta_{kl} \, . \end{aligned} \tag{4.66b}$$

In the case of Gaussian variables, $P(a) = \frac{1}{\sqrt{2\pi}} e^{-\frac{a^2}{2}}$, the moments are $\sigma_{2n} = n!$ and $\sigma_{2n+1} = \frac{(2n+1)!!}{2^{n+1}} \sqrt{\pi}$. The four-point function can be written in terms of two-point function,

$$\langle \xi_i^* \xi_j^* \xi_k \xi_l \rangle = \delta_{ik} \delta_{jl} + \delta_{il} \delta_{jk} \, . \tag{4.67}$$

This is true also for all expectation values (Wick theorem).

In the case of Z_2 variables, it is $P(a) = \frac{1}{2}[\delta(a-1) + \delta(a+1)]$, therefore $a = \pm 1$

with equal probability. Here obviously $|\xi| = 1$ implies $\sigma_n = 1$. This distribution is saturating all the bounds set by moment monotonicity: therefore Eq. (4.65) is the strongest bound that can be put on the moments of a generic distribution.

Stochastic estimation of a trace

The goal is to estimate $\operatorname{Tr} A$ for some matrix A. It is possible to use a complex vector of independent random variable ξ to evaluate stochastically the trace,

$$\langle \xi^* A \xi \rangle = \operatorname{Tr} A \,. \tag{4.68}$$

The variance of such estimator is

$$\begin{aligned} \operatorname{Var}(\xi^\dagger A \xi) &= \left\langle \left(\xi^\dagger A \xi - \operatorname{Tr} A\right) \left(\xi^\dagger A \xi - \operatorname{Tr} A\right)^* \right\rangle = \\ &= \langle \xi^\dagger A \xi \, \xi^\dagger A^\dagger \xi \rangle - |\operatorname{Tr} A|^2 = \\ &= \sum_{ijkl} A_{ik} A^\dagger_{jl} \langle \xi_i^* \xi_j^* \xi_k \xi_l \rangle - |\operatorname{Tr} A|^2 \,. \end{aligned} \tag{4.69}$$

From Eq. (4.66b), we see that

$$\begin{aligned} \operatorname{Var}(\xi^\dagger A \xi) &= |\operatorname{Tr} A|^2 + \operatorname{Tr} A A^\dagger + (\sigma_4 - 2) \sum_i |A_{ii}|^2 - |\operatorname{Tr} A|^2 = \\ &= \operatorname{Tr} A A^\dagger + (\sigma_4 - 2) \sum_i |A_{ii}|^2 \,, \end{aligned} \tag{4.70}$$

and with $\sigma_4 \geq \sigma_2^2 = 1$ we set the bound

$$\operatorname{Var}(\xi^\dagger A \xi) \geq \operatorname{Tr} A A^\dagger - \sum_i |A_{ii}|^2 \,. \tag{4.71}$$

For Gaussian noise, the variance is $\operatorname{Var}(\xi^\dagger A \xi) = \operatorname{Tr} A A^\dagger$; on the other hand, for Z_2 noise the bound is saturated, $\operatorname{Var}(\xi^\dagger A \xi) = \operatorname{Tr} A A^\dagger - \sum_i |A_{ii}|^2$. The estimator with Z_2 noise is called Hutchinson's estimator [104], and minimises the variance of $\xi^\dagger A \xi$: this means that any other noise can have at best the same variance as Z_2. In order to further reduce the variance, it is therefore needed to improve the estimator itself.

Chapter 5

The critical mass of Wilson fermions

We have seen in Sect. 1.3 that in order to simulate fermions on the lattice one is forced to give up some properties at finite lattice spacing: in the case of Wilson fermions, this property is chiral symmetry. To keep the fermion mass under control, an additive renormalisation of the mass is required. In this chapter we describe how NSPT can be used to determine such renormalisation constant order by order in perturbation theory. Some results presented here are published in Refs. [1, 2].

5.1 Critical mass in lattice perturbation theory

The inverse of the Wilson fermion propagator in momentum space can be expressed as

$$\begin{aligned} a\Gamma(ap, am, \beta^{-1}) &= aS(ap, am, \beta^{-1})^{-1} = \\ &= i \sum_{\mu} \gamma_{\mu} \overline{(ap_{\mu})} + \frac{1}{2} \widehat{(ap)}^{\,2} + am - a\Sigma(ap, am, \beta^{-1}) \,, \end{aligned} \tag{5.1}$$

where $\bar{v}_{\mu} = \sin v_{\mu}$, $\hat{v}_{\mu} = 2\sin(\frac{v_{\mu}}{2})$ and $\Sigma(ap, am, \beta^{-1})$ is the self energy. Wilson fermions are not equipped with chiral symmetry when the bare mass m vanishes: the self energy at zero momentum is affected by a power divergence a^{-1}, which has to be cured by an additive renormalisation. In an on-shell renormalisation

scheme, the critical value of the bare mass, m_c, for which the lattice theory describes massless fermions, is given by the solution of

$$am_c - a\Sigma(ap = 0, am_c, \beta^{-1}) = 0\,. \tag{5.2}$$

As observed in Ref. [105], this prescription matches the one obtained by requiring the chiral Ward identity to hold in the continuum limit. Expanding Eq. (5.2) defines the critical mass order by order in perturbation theory. The perturbative expansion of the inverse propagator is

$$a\Gamma(ap, am, \beta^{-1}) = \sum_{n=0} \Gamma^{(n)}\,(ap, am)\,\beta^{-n}\,, \tag{5.3}$$

where we have indicated explicitly the dependence of the coefficients on the bare mass am. The functions $\Gamma^{(n)}(ap, am)$ are matrices in Dirac space; since we are interested in the small momentum region and $\Gamma^{(n)}(0, am)$ is proportional to the identity, we consider $\Gamma^{(n)}(ap, am)$ as scalar functions: when $ap \neq 0$ a projection onto the identity is understood. Plugging the perturbative expansion of the critical mass

$$am_c = \sum_{n=1} m_c^{(n)} \beta^{-n} \tag{5.4}$$

into Eq. (5.3) results in

$$a\Gamma(ap, am_c, \beta^{-1}) = \sum_{n=0} \gamma^{(n)}\,(ap)\,\beta^{-n} = \sum_{n=0} \left[m_c^{(n)} + \chi^{(n)}\,(ap)\right] \beta^{-n}\,, \tag{5.5}$$

where the dependence of $\gamma^{(n)}$ on $m_c^{(n)}$ has been made explicit and $\chi^{(n)}$ depends only on $m_c^{(0)}, \ldots, m_c^{(n-1)}$. Therefore, the renormalisation condition in Eq. (5.2) becomes order by order

$$\gamma^{(n)}(0) = 0 \qquad \text{or} \qquad m_c^{(n)} = -\chi^{(n)}(0)\,. \tag{5.6}$$

For illustration, we can compute the recursive solution of Eq. (5.2). By virtue of a Taylor expansion in the mass, the renormalisation condition can be written as

$$\sum_{n=0} \Gamma^{(n)}\,(0, am_c)\,\beta^{-n} = \sum_{n=0} \sum_{k=0} \frac{1}{k!}\,\frac{\partial^k \Gamma^{(n)}\,(0, am)}{\partial (am)^k}\bigg|_{am=0} (am_c)^k\,\beta^{-n} = 0\,, \tag{5.7}$$

Figure 5.1 *Feynman diagrams contributing to the fermion self energy at order* β^{-1}.

where m_c needs to be further expanded as in Eq. (5.4) and

$$\left.\frac{\partial^k \Gamma^{(0)}\left(0, am\right)}{\partial (am)^k}\right|_{am=0} = \delta_{k,1}\,. \tag{5.8}$$

For the first two non-trivial orders, this condition yields

$$\gamma^{(1)}(0) = \Gamma^{(1)}(0,0) + m_c^{(1)} = 0 \tag{5.9a}$$

$$\gamma^{(2)}(0) = m_c^{(1)} \left.\frac{\partial \Gamma^{(1)}}{\partial (am)}\right|_{ap=0, am=0} + \Gamma^{(2)}(0,0) + m_c^{(2)} = 0\,. \tag{5.9b}$$

Both results are familiar from analytical calculations of the critical mass. The first equation encodes the fact that the mass counterterm at first order in perturbation theory is given by the one-loop diagrams computed at zero bare mass. The second equation states that the second-order correction is given by summing two-loop diagrams evaluated at vanishing bare mass, and one-loop diagrams with the insertion of the $O\left(\beta^{-1}\right)$ counterterm[1], see e.g. Ref. [106].

Critical masses have been computed analytically up to two loops [106, 107], and in NSPT at three and four loops [108, 109]. We computed the one-loop critical mass at finite volume in twisted lattice perturbation theory. The Feynman diagrams involved are shown in Figure 5.1, and they have to be computed according to the Feynman rules described in Appendix C. It should also be noted that, when working in finite volume, momenta are quantised. Unless periodic boundary conditions are used, $p = 0$ is not an allowed value for the momentum of the states in a box. If the computation is performed analytically, the condition in Eq. (5.2) can be imposed by setting artificially the external momentum to zero; when trying

[1] Derivatives with respect to the mass generate counterterm insertions: for example, for a scalar propagator,

$$-m^2 \frac{\partial}{\partial m^2} \frac{1}{k^2+m^2} = \frac{1}{k^2+m^2}\, m^2\, \frac{1}{k^2+m^2}\,. \tag{5.10}$$

to determine the critical mass numerically from NSPT, we will have to measure the inverse propagator at some non-vanishing momenta and then extrapolate to $p = 0$. The detailed implementation is discussed below in Sect. 5.3.

5.2 Gauge fixing in NSPT

Even though the critical mass is gauge-independent at all orders [110], the inverse propagator Γ depends on the gauge when $ap \neq 0$. If we want to measure the perturbative expansion of Γ from NSPT, the problem of how to fix a gauge must be addressed.

In the continuum, the Landau gauge is defined by the condition $\sum_\mu \partial_\mu A_\mu(x) = 0$. On the lattice, it is possible to fix a discretised version of this gauge by applying iteratively a clever choice of gauge transformation [111].

The absolute value of the trace of a $\mathrm{SU}(N_c)$ matrix lies always between 0 and N_c; in particular, the trace of a $\mathrm{SU}(N_c)$ matrix is equal to N_c if and only if the matrix is the identity. Given some configuration $U_\mu(x)$, we can study how to move within the gauge orbit in order to maximise the real part of the trace of the field: in this way, the configuration can be considered as "perturbative", since it is brought as close as possible to the identity. To achieve this, the functional

$$F[\Omega] = 2 \sum_{x\mu} \mathrm{Re}\,\mathrm{Tr}\; \Omega(x) U_\mu(x) \Omega(x+\hat{\mu})^\dagger \tag{5.11}$$

must be maximised. For gauge transformations $\Omega(x) = e^{i\omega(x)}$ not far from the identity, it is possible to perform a Taylor expansion

$$F\left[e^{i\omega}\right] = F[\mathbb{1}] + \sum_{ax} \omega^a(x) \nabla^a_{\Omega(x)} F[\Omega]\big|_{\Omega=\mathbb{1}} + O(\omega^2)\,, \tag{5.12}$$

where the Lie derivative is

$$\begin{aligned} \nabla^a_{\Omega(x)} F[\Omega]\big|_{\Omega=\mathbb{1}} &= 2 \sum_\mu \mathrm{Re}\,\mathrm{Tr}\left[iT^a \Omega(x) U_\mu(x) \Omega(x+\hat{\mu})^\dagger + \right. \\ &\qquad \left. - \Omega(x-\hat{\mu}) U_\mu(x-\hat{\mu}) \Omega(x)^\dagger i T^a \right]\Big|_{\Omega=\mathbb{1}} = \\ &= -2 \sum_\mu \mathrm{Im}\,\mathrm{Tr}\, T^a \delta^*_\mu U_\mu(x) = i \sum_\mu \mathrm{Tr}\, T^a \delta^*_\mu \left[U_\mu(x) - U_\mu(x)^\dagger \right] . \end{aligned} \tag{5.13}$$

With the particular choice

$$\omega(x) = i\alpha \sum_{a\mu} T^a \operatorname{Tr} T^a \delta^*_\mu \left(U_\mu(x) - U_\mu(x)^\dagger \right) = i\alpha \sum_\mu \Pi_{\mathfrak{g}} \left(\delta^*_\mu U_\mu(x) \right) , \qquad (5.14)$$

where $\alpha > 0$ is a small parameter, we see that the functional F is driven towards larger values[2],

$$F\left[e^{i\omega}\right] - F[\mathbb{1}] = \alpha \sum_{ax\mu} \left| \operatorname{Tr} T^a \delta^*_\mu \left(U_\mu(x) - U_\mu(x)^\dagger \right) \right|^2 + O(\omega^2) \, . \qquad (5.15)$$

Therefore, by iterating the gauge transformation built from Eq. (5.14), the functional F follows a steepest descent path towards a local maximum characterised by

$$\nabla^a_{\Omega(x)} F[\Omega]\big|_{\Omega=\mathbb{1}} = i \sum_\mu \operatorname{Tr} T^a \delta^*_\mu \left[U_\mu(x) - U_\mu(x)^\dagger \right] = 0 \, . \qquad (5.16)$$

This stationary condition corresponds to fixing the Landau gauge: indeed, expanding perturbatively $U_\mu = e^{iA_\mu}$,

$$i \sum_\mu \operatorname{Tr} T^a \delta^*_\mu \left[U_\mu(x) - U_\mu(x)^\dagger \right] = -2 \sum_\mu \operatorname{Tr} T^a \delta^*_\mu A_\mu(x) + O(A^3) \, , \qquad (5.17)$$

and the minimum is realised when $\sum_\mu \delta^*_\mu A_\mu = 0$.

This algorithm can be used in a nonperturbative formulation of lattice gauge theories, and leads to the correct result in the continuum limit. In NSPT this is not enough, and we need to adapt the technique in order to have the Landau condition fixed at each perturbative order (i.e. at all values of the lattice spacing) [112]. Since, in the continuum limit, the Landau gauge is the gauge where the potential has minimum norm, we can try to look in the gauge orbit for a configuration that minimises the norm of the potential, instead of maximising the trace of the links. Because $A_\mu(x) = -i \log U_\mu(x)$, the minimisation of the norm of $A_\mu(x)$ is realised when the new functional

$$F'[\Omega] = \sum_{x\mu} \operatorname{Tr} \log \left(\Omega(x) U_\mu(x) \Omega(x+\hat{\mu})^\dagger \right) \left[\log \left(\Omega(x) U_\mu(x) \Omega(x+\hat{\mu})^\dagger \right) \right]^\dagger \qquad (5.18)$$

is minimum. To understand the structure of F' for gauge transformations close to the identity, we define $\Omega(x) = e^{i\omega(x)}$ and expand in ω. Thanks to the

[2] It is important to remind that Eq. (5.13) gives a purely real number.

Baker–Campbell–Hausdorff formula, we have

$$\log \Omega(x) U_\mu(x) \Omega(x+\hat{\mu})^\dagger = \log e^{i\omega(x)} e^{iA_\mu(x)} e^{-i\omega(x+\hat{\mu})} = \\ = iA_\mu(x) + i\omega(x) - i\omega(x+\hat{\mu}) + \cdots + O(\omega^2)\,, \quad (5.19)$$

where the dots represent terms involving commutators of one ω with one or more A. With this in hand, it is possible to expand F',

$$F'[\Omega] = \sum_{x\mu} \mathrm{Tr}\left(iA_\mu(x) + i\omega(x) - i\omega(x+\hat{\mu}) + \cdots + O(\omega^2)\right) \cdot \\ \cdot \left(iA_\mu(x) + i\omega(x) - i\omega(x+\hat{\mu}) + \cdots + O(\omega^2)\right)^\dagger = \\ = \sum_{x\mu} \mathrm{Tr}\, A_\mu(x) A_\mu(x) + 2 \sum_{x\mu} \mathrm{Tr}\, \omega(x) \delta^*_\mu A_\mu(x) + O(\omega^2)\,, \quad (5.20)$$

and read the Lie derivative

$$\nabla^a_{\Omega(x)} F'[\Omega]\big|_{\Omega=\mathbb{1}} = 2 \sum_\mu \mathrm{Tr}\, T^a \delta^*_\mu A_\mu(x) = \sum_\mu \delta^*_\mu A^a_\mu(x)\,. \quad (5.21)$$

The terms in the dots do not contribute: they have to be necessarily combined with $A_\mu(x)$ to give an $O(\omega)$ contribution, and thus the trace of $A_\mu(x)$ times a commutator involving $A_\mu(x)$ and a single ω vanishes thanks to the cyclic property of the trace. With the particular choice

$$\omega(x) = -\alpha \sum_\mu \delta^*_\mu A_\mu(x) = i\alpha \sum_\mu \delta^*_\mu \log U_\mu(x)\,, \quad (5.22)$$

where $\alpha > 0$ is a small parameter, we see that F' is driven towards smaller values,

$$F'\left[e^{i\omega}\right] - F'[\mathbb{1}] = -2\alpha \sum_{x\mu} \mathrm{Tr}\left(\delta^*_\mu A_\mu(x)\right)^2 + O(\omega^2)\,. \quad (5.23)$$

Therefore, by iterating the gauge transformation built from Eq. (5.22), the functional F' follows a steepest descent path towards a local minimum corresponding exactly to the Landau gauge,

$$\nabla^a_{\Omega(x)} F'[\Omega]\big|_{\Omega=\mathbb{1}} = \sum_\mu \delta^*_\mu A^a_\mu(x) = 0\,. \quad (5.24)$$

Since the Landau condition is realised without perturbative corrections, this result holds in NSPT as well: the matrix ω inherits a perturbative structure from the links and, for each perturbative order, the iterated gauge transformation leads to

a vanishing divergence for each perturbative order. In particular, by expanding the first variation of F',

$$2\sum_{x\mu}\mathrm{Tr}\,\omega(x)\delta^*_\mu A_\mu(x) = 2\sum_{x\mu}\sum_{n=1}^{+\infty}\beta^{-n/2}\sum_{l=1}^{n-1}\mathrm{Tr}\,\omega^{(l)}(x)\delta^*_\mu A^{(n-l)}_\mu(x)\,, \tag{5.25}$$

we see that the order by order stationary condition amounts to

$$\sum_{l=1}^{n-1}\sum_{\mu}\delta^*_\mu A^{a\,(n-l)}_\mu(x) = 0\,. \tag{5.26}$$

With the choice $\omega^{(n)} = -\alpha\sum_\mu \delta^*_\mu A^{(n)}_\mu$, the Landau gauge propagates in cascade from the lowest to the highest order.

The techniques described so far suffer by critical slowing-down: the number of iterations needed to reach the Landau gauge grows with the number of lattice sites. To avoid this issue, we also implemented a Fourier accelerated version of this algorithm [113]. The underlying idea can be exposed more clearly by studying the Landau gauge fixing in the continuum for an abelian theory. The potential is updated with the rule

$${}^{(n+1)}A_\mu = {}^{(n)}A_\mu + \alpha\sum_\nu \partial_\mu\partial_\nu\,{}^{(n)}A_\mu\,, \tag{5.27}$$

where ${}^{(n)}A_\mu$ is the potential after n iterations of the gauge transformation defined in Eq. (5.22), and has a divergence equal to

$$\sum_\mu \partial_\mu\,{}^{(n+1)}A_\mu = (1+\alpha\partial^2)\sum_\mu\partial_\mu\,{}^{(n)}A_\mu = (1+\alpha\partial^2)^n\sum_\mu\partial_\mu\,{}^{(0)}A_\mu\,. \tag{5.28}$$

Denoting a Fourier transform with $\mathrm{FT}[\,\cdot\,]$, we see that for a large number of iterations we can write

$$\mathrm{FT}\left[\sum_\mu \partial_\mu\,{}^{(n+1)}A_\mu\right] = (1-\alpha p^2)^n\,\mathrm{FT}\left[\sum_\mu\partial_\mu\,{}^{(0)}A_\mu\right] \simeq e^{-\alpha p^2 n}\,\mathrm{FT}\left[\sum_\mu\partial_\mu\,{}^{(0)}A_\mu\right]. \tag{5.29}$$

The convergence is slower for smaller momenta: the idea of the Fourier acceleration is to correct for this behaviour by compensating the slower convergence with

a larger step size α. With the choice

$$\omega(x) = -\,\mathrm{FT}^{-1}\left[\frac{\alpha}{p^2}\,\mathrm{FT}\left[\sum_\mu \delta^*_\mu A_\mu(x)\right]\right]\,, \tag{5.30}$$

all the momentum components of the divergence of the potential converge with the same rate, and the number of iterations is independent of the volume. Clearly there is an additional burden introduced by the Fourier transform: nevertheless, the dependence of the cost of a FFT on the number of lattice points is found to be mild. With TBC, the Fourier transform is understood to be performed as explained in Sect. 4.3.

5.3 Critical mass in NSPT: zero-momentum extrapolation and valence twist

High-order perturbation theory with massless Wilson fermions requires the tuning of the critical mass at the same order in β^{-1}, and it is possible to determine this renormalisation using NSPT. Let us illustrate the strategy in detail. We begin by collecting configurations for different time steps τ of the stochastic process; for each configuration the gauge is fixed to the Landau gauge [111–113]. The propagator at momentum p is computed by applying the inverse Dirac operator to a point source in momentum space,

$$S(p)_{\alpha\beta} = \sum_{q\gamma} M\,[U]^{-1}_{pq,\alpha\gamma}\,\delta_{qp}\delta_{\gamma\beta}\,. \tag{5.31}$$

The average over all the configurations gives the Monte Carlo estimate of $S(p)$. For each simulation at a given value of τ, the error bars are computed as detailed in Appendix D. The propagator with periodic boundary conditions is a (diagonal) matrix in colour and momentum space and has a Dirac structure; it is important to stress again that with TBC there is not a colour structure any more and the momentum has a finer quantisation. We can now extrapolate the stochastic time step to zero and invert the propagator to obtain $S(p)^{-1}$. Finally, the inverse propagator is projected onto the identity in Dirac space. The errors can be estimated by bootstrapping the whole procedure. All these operations are performed order by order in perturbation theory keeping in mind that, after the measure of the propagator, all perturbative orders $\beta^{-k/2}$ with an odd k are

discarded, since the expansion in powers of $\beta^{-1/2}$ is an artefact of NSPT. We check that these odd orders give contributions that are zero on average, with a variance that increases with the perturbative order.

The legacy of this process is the measure of the functions $\gamma^{(n)}(ap)$, as it is clear from Eq. (5.5). The renormalisation condition in Eq. (5.6) must then be imposed: this can be done iteratively one order after the other. When all the coefficients up to some $m_c^{(n)}$ are included in the simulation, all the γ functions up to $\gamma^{(n)}(ap)$ extrapolate to zero; on the other hand, from $\gamma^{(n+1)}(0)$ we can read $-m_c^{(n+1)}$. In order to move on and compute the following coefficient of the critical mass, a new set of configurations where $m_c^{(n+1)}$ is taken into account must be generated.

The procedure we described is well defined and even theoretically clean, since it enlightens the status of our m_c as a perturbative additive renormalisation: once it is plugged in at a given order, the renormalised mass turns out to be zero at the prescribed order. On the other hand, it is not at all the only possible procedure. The prescription of the authors of Ref. [72] is to expand the solution of the stochastic process both in the coupling and in the mass counterterm. This is in the same spirit of Ref. [114]: the solution of the stochastic process can be expanded in more than one parameter and once a precise power counting is in place, the resulting hierarchy of equations can be exactly truncated at any given order. There are pros and contras for both approaches, i.e. the one we followed and the double expansion. The latter can provide a better handle on estimating errors due to the critical mass value; however, it is expected to be numerical more demanding. All in all, we did not push Wilson fermions to very high orders: moving to the staggered formulation was by far the most natural option for the purpose of this work.

Since in finite volume it is possible to measure $\Gamma(ap)$ only for discretised non-zero momenta, the data need to be extrapolated to zero momentum using a suitable functional form. The strategy adopted in the literature – see for example Eqs. (13) and (14) in Ref. [109] – is based on expanding the quantities of interest in powers of ap. In the infinite-volume limit, such an expansion leads to a hypercubic symmetric Taylor expansion composed of invariants in ap, logarithms of ap and ratios of invariants; an explicit one-loop computation to order a^2 is shown e.g. in Eq. (24) of Ref. [115]. The ratios and the logarithms arise because we are expanding a non-analytic function of the lattice spacing: infrared divergences appear when expanding the integrands in ap. On the other hand, thanks to TBC we can work consistently in finite volume, where no infrared divergences arise:

expressions for $\gamma^{(n)}(ap)$ will be just sums of ratios of trigonometric functions, which we can expand in ap obtaining simply a combination of polynomial lattice invariants[3].

Still, this is not enough for a reliable extrapolation to vanishing momenta, with a reasonable χ^2 value. In order to understand better the range of momenta that allow a safe extrapolation, we computed $\gamma^{(1)}(ap)$ in twisted lattice perturbation theory (see Appendix C). As a cross-check of our calculation we verified that $\gamma^{(1)}(0)$, which correspond to the one-loop critical mass, is gauge-independent [110]. From the analytic expansion of $\gamma^{(1)}(ap)$, it can be seen that even the lowest momentum allowed on our finite-size lattices, $ap_{1,2,3} = 0$, $ap_4 = \pi/L$, is far from the convergence region of this series. This happens even for reasonably big lattices, $L \lesssim 32$. In order to increase the range of available momenta, we use θ-boundary conditions [116] for the valence fermions,

$$\psi(x + L\hat{4}) = e^{i\theta}\psi(x)\,, \tag{5.32}$$

thereby reaching momenta $p_4 = \theta/L$ which are within the convergence radius of the ap-expansion. The hypercubic series becomes just a polynomial in $(ap_4)^2$ by setting all the other components to zero.

The agreement between data and the analytic finite-volume calculations for $N_c = 2$, $N_f = 2$ can be seen in Figure 5.2. It is worthwhile to emphasise that measuring such low momenta requires a careful analysis of the thermalisation. At the lowest order we can check directly when the measures agree with the theoretical predictions. At higher orders, it is necessary to wait until the statistical average has clearly stabilised, as shown in Figure 5.3. This kind of analysis is computationally intensive: in the case at hand, we performed up to $5 \cdot 10^6$ lattice sweeps, saving one propagator every 10^3 sweeps. The first $2 \cdot 10^3$ configurations have been discarded in the analysis.

5.4 An attempt for $\mathrm{SU}(3)$ with $N_f = 2$

We determined the first 7 coefficients of the critical mass for $N_c = 3$ and $N_f = 2$ on a 16^4 lattice with twisted boundary conditions on a plane. The twist matrices

[3]Expanding in ap and sending the lattice size to infinity are operations that do not commute; in particular this gives rise to different series in the finite- and infinite-volume cases.

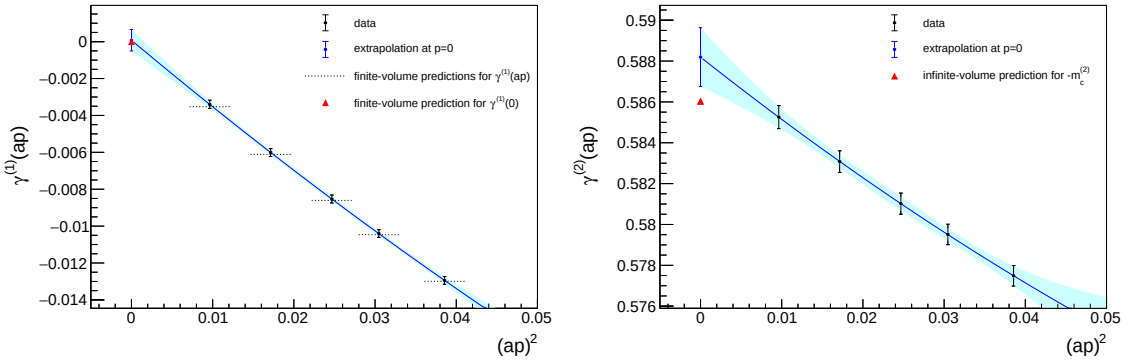

Figure 5.2 *Measure of $\gamma^{(1)}(ap)$ (left panel) and $\gamma^{(2)}(ap)$ (right panel) for a 12^4 lattice with TBC on a plane, $N_c = 2$ and $N_f = 2$ Wilson fermions. The analytic finite-volume critical mass $m_c^{(1)}$ is included in the simulation. A second-order polynomial in $(ap)^2$ is used for fitting. Most analytic finite-volume predictions have been drawn as lines to help the eye in the comparison. The difference with the prediction in the right panel is to be ascribed to the fact that we are able to resolve finite-volume effects.*

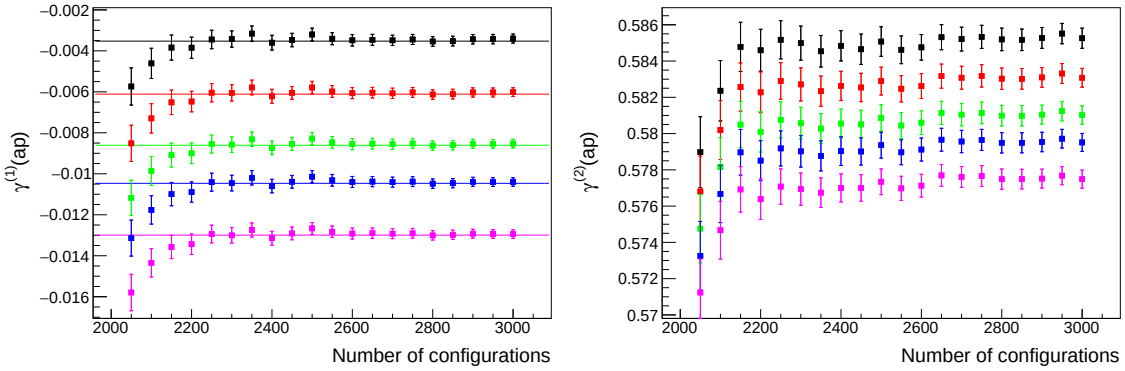

Figure 5.3 *Same as Figure 5.2 with data drawn as a function of the number of configurations included in the analysis. Each colour corresponds to a different momentum. Horizontal lines are the analytical predictions.*

are

$$\Omega_1 = \begin{pmatrix} e^{-i\frac{2\pi}{3}} & 0 & 0 \\ 0 & 1 & 0 \\ 0 & 0 & e^{i\frac{2\pi}{3}} \end{pmatrix} \qquad \Omega_2 = \begin{pmatrix} 0 & 1 & 0 \\ 0 & 0 & 1 \\ 1 & 0 & 0 \end{pmatrix}, \tag{5.33}$$

corresponding to $z_{12} = \exp\left(i\frac{2\pi}{3}\right)$. Configurations are collected at three different time steps, $\tau = 0.005,\ 0.008,\ 0.01$. Because the volume and the number of colours are large compared to the former test in Figure 5.2, it is computationally too expensive to replicate the same statistics at all orders: we settled for $5 \cdot 10^5$ sweeps at the smallest τ, measuring the propagator every $r = 10^3$ sweeps. At larger time steps, we rescale these numbers to keep the product $r \cdot \tau$ constant. The propagator is measured at the smallest available momentum, which has θ/L in the time component and vanishes elsewhere; we choose three different values for the phase of the valence twist, $\theta = \pi/2,\ 2\pi/3,\ 4\pi/5$. Extrapolations to zero momentum are performed using a linear fit in $(ap)^2$. The analysis is performed on different subsets of the data[4] to estimate systematic errors. The total error is the sum in quadrature of half the spread around the central value among the different fits and the largest error from the fits.

The procedure described in Sect. 5.3, even though well-defined, is found to be numerically unstable at high orders. The number of propagators required to reach a clear plateau, like the ones shown in Figure 5.3, is beyond what it can be reasonably collected with the current NSPT implementations. Therefore, we decided to proceed with a smaller statistics and to add a new systematic uncertainty for the extrapolated coefficients, as explained below. It has to be emphasised that once a coefficient of the critical mass is determined, only the central value is used as input for the following runs: even if we could collect enough statistics and manage to reduce the error, that is not included in the simulations. This makes the impact of the uncertainty of $m_c^{(n)}$ on $m_c^{(n+1)}$ and higher hard to assess; also, performing simulations for several values of each coefficient is not feasible. To be conservative, we adopted the following strategy. Once a critical mass $m_c^{(n)}$ is determined and put in the next-order simulation, the corresponding $\gamma^{(n)}(ap)$ should extrapolate to zero. If it extrapolates to ϵ_n, we take $|\epsilon_n/m_c^{(n)}|$ as an estimate of the relative systematic error to be added in quadrature to the determination of all the higher-order critical masses.

Despite these instabilities, the lower-order results are close to the known

[4] The different subsets are built by varying the number of initial configurations that are excluded in the analysis and by rejecting data at different rates.

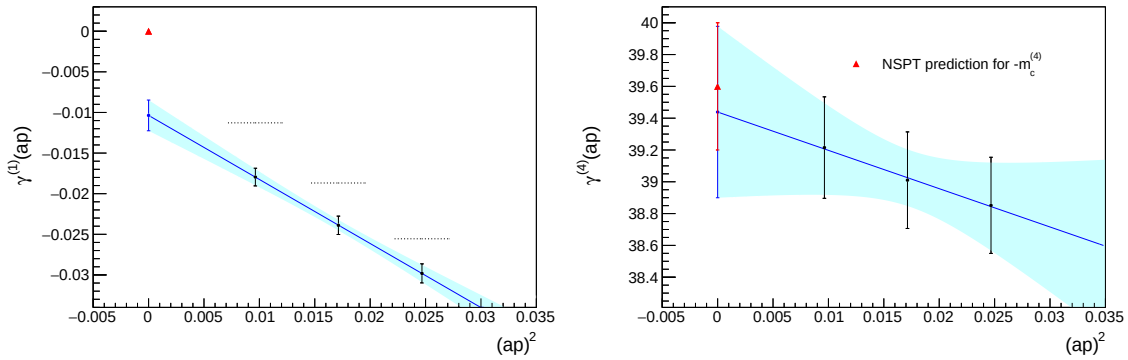

Figure 5.4 *Determination of the coefficient $m_c^{(4)}$. Although $\gamma^{(1)}(ap)$ does not extrapolate to zero, the extrapolation of $\gamma^{(4)}(ap)$ is compatible with the value known from Ref. [109]. Notation as in Figure 5.2.*

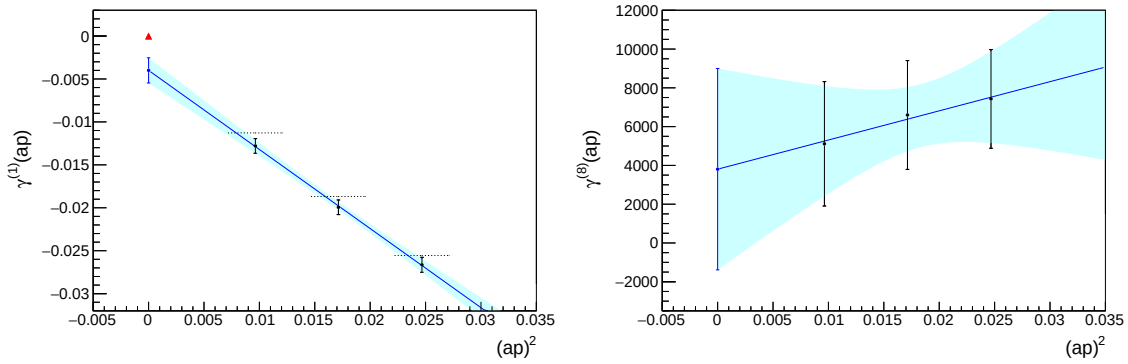

Figure 5.5 *Determination of the coefficient $m_c^{(8)}$. The errors overshadow the value of the critical mass, which is compatible with zero. Notation as in Figure 5.2.*

coefficients (keeping in mind that we might resolve finite-volume effects), as it can be seen for example in Figure 5.4. We stopped the procedure at $m_c^{(8)}$, when the errors started dominating over the central value of the coefficient, see Figure 5.5. Our results are summarised in Table 5.1. A comparison between the critical mass obtained by summing the first n orders of its finite-volume perturbative series and the nonperturbative Monte Carlo determination is presented in Table 5.2 for two particular values of the coupling β.

Table 5.1 *Critical masses for $N_c = 3$, $N_f = 2$ Wilson fermions determined with NSPT on a 16^4 lattice with twisted boundary condition on a plane, compared with the known values in infinite volume. The $n = 1$ coefficient has been determined analytically in twisted lattice perturbation theory; many digits have been used in the actual simulation.*

n	$-m_c^{(n)}$ on 16^4	$-m_c^{(n)}$ in infinite volume	Refs.
1	$2.61083\ldots$	$2.60571\ldots$	-
2	4.32(3)	4.293(1)	[106, 107]
3	$1.21(1) \cdot 10^1$	$1.178(5) \cdot 10^1$	[108, 109]
4	$3.9(2) \cdot 10^1$	$3.96(4) \cdot 10^1$	[109]
5	$1.7(2) \cdot 10^2$	-	-
6	$5(1) \cdot 10^2$	-	-
7	$2(1) \cdot 10^3$	-	-

Table 5.2 *Critical mass determined by summing the first n orders of its finite-volume perturbative series, compared to the nonperturbative Monte Carlo value [106, 117, 118].*

n	m_c at $\beta = 5.5$	m_c at $\beta = 5.6$
2	-0.618(1)	-0.604(1)
3	-0.690(1)	-0.673(1)
4	-0.733(2)	-0.713(2)
5	-0.767(5)	-0.743(4)
6	-0.785(6)	-0.760(5)
7	-0.798(9)	-0.771(8)
Monte Carlo	-0.8975	-0.8446

Chapter 6

Perturbative expansion of the plaquette

A nonperturbative determination of the gluon condensate from lattice gauge theories has been a long-standing challenge, begun with the attempts of Refs. [48–54]. The adopted strategy is always to study the OPE for the plaquette, and try to disentangle the contribution of the identity operator from the one of the condensate. The contribution associated to the identity operator turns out to be ill-defined: it can be computed in perturbation theory, but such series diverges, as discussed in Sect. 2. The prescription chosen to define the sum of the series produces an intrinsic ambiguity in the definition of the condensate itself. There is no need to say that the whole procedure requires to have the asymptotic behaviour of the series of the plaquette well under control. This is why only after the development of NSPT it was possible to systematically address the issue: one can subtract from a nonperturbative (Monte Carlo) measurement of the plaquette the sum of the perturbative series computed in NSPT, and repeat the procedure at different values of the coupling in order to find the signature of a quantity of mass dimension four. Thanks to NSPT, many studies aimed to determine the perturbative expansion of the plaquette and the gluon condensate were prompted [37, 38, 40, 119–125]. The first conclusions were contrasting, since some results suggested the existence of an unexpected dimension-2 operator. Only the computation of really high orders allowed keeping the asymptotic behaviour under control and settle this issue. The first evidence of renormalons were presented in Refs. [41, 88], followed by the determination of the gluon condensate in pure gluodynamics in Refs. [98, 126]. NSPT has also been recently applied

with success for the computation of Wilson loops in the TEK model [127], and high-order results could come also from this direction.

In this chapter we provide a first estimate from NSPT of the perturbative expansion of the plaquette and of the gluon condensate in massless QCD, i.e. in a gauge theory with two massless fermions in the fundamental representation. Some results presented here are published in Refs. [2, 3].

6.1 Analytical results and gluon chain in finite volume

On a finite lattice, from Eq. (1.20) it is useful to define the average plaquette

$$P = \frac{1}{6N_c L^4} \sum_{\square} \mathrm{Re}\,\mathrm{Tr}\,(1 - U_{\square}) \,, \tag{6.1}$$

whose value ranges between 0, when all link variables are equal to the identity, and 1. From Eq. (2.99), the plaquette expectation value has the perturbative expansion

$$\langle P \rangle_{\mathrm{pert}} = \tilde{Z}_{\mathbb{1}}(\beta) = \sum_{n=0}^{\infty} p_n \, \beta^{-(n+1)} \,. \tag{6.2}$$

We will now inspect how the lowest orders of this series arise in perturbation theory, with a special focus on finite-volume effects from twisted lattice perturbation theory [128], see Appendix C for the conventions adopted here. A possible way to proceed is to write

$$W_{\mu\nu}(x) = \frac{1}{N_c} \big\langle \mathrm{Re}\,\mathrm{Tr}\, U_\mu(x) U_\nu(x+\hat{\mu}) U_\mu(x+\hat{\nu})^\dagger U_\nu(x)^\dagger \big\rangle \,, \tag{6.3}$$

expand $U_\mu(x) = e^{igA_\mu\left(x+\frac{\hat{\mu}}{2}\right)}$, and then evaluate the correlators in perturbation theory; the result is a sum of gluon n-point Green functions[1]. We remark that, when doing perturbative calculations, it is customary to define the potential at the midpoint of the link, in order to simplify the Feynman rules for the vertices[2]. $W_{\mu\nu}(x)$ is obviously invariant under translations; on the other hand, different

[1] The free energy is related to the derivative of the partition function with respect to the coupling: to simplify the calculation, it would be actually easier to compute the sum of all the connected vacuum diagrams, see e.g. Ref. [54]. In our discussion we can avoid using this trick, as we will focus on a very small number of diagrams.

[2] This choice has also a nice graphical interpretation, see e.g. Figure 6.1.

orientations of the plaquette are not equivalent because of TBC. From the average over all the plaquette orientations,

$$W = \frac{1}{6}\sum_{\mu>\nu} W_{\mu\nu} = \sum_{n=0}^{\infty} W^{(n)}\,\beta^{-n} = 1 - \sum_{n=0}^{\infty} p_n\,\beta^{-(n+1)}\,, \tag{6.4}$$

one can define the coefficients p_n in finite volume. For p_0, it is enough to expand $W_{\mu\nu}(x)$ in terms of tree-level 2-point functions. For p_1, contributions come from 3- and 4-point functions at tree level, and from 2-point functions at one loop; the contribution of the fermions falls in the latter category.

The terms involving 2-point functions only are, for a plaquette with orientation $\mu\nu$,

$$\begin{aligned} W_{\mu\nu}^{\text{2-point}}(x) = \frac{(ig)^2}{N_c}\,\mathrm{Re}\,\mathrm{Tr}\,\Bigg\{ & \frac{1}{2}\left\langle A_\mu\left(x+\frac{\hat\mu}{2}\right) A_\mu\left(x+\frac{\hat\mu}{2}\right)\right\rangle + \\ & + \frac{1}{2}\left\langle A_\nu\left(x+\frac{\hat\nu}{2}+\hat\mu\right) A_\nu\left(x+\frac{\hat\nu}{2}+\hat\mu\right)\right\rangle + \\ & + \frac{1}{2}\left\langle A_\mu\left(x+\frac{\hat\mu}{2}+\hat\nu\right) A_\mu\left(x+\frac{\hat\mu}{2}+\hat\nu\right)\right\rangle + \\ & + \frac{1}{2}\left\langle A_\nu\left(x+\frac{\hat\nu}{2}\right) A_\nu\left(x+\frac{\hat\nu}{2}\right)\right\rangle + \\ & - \left\langle A_\mu\left(x+\frac{\hat\mu}{2}\right) A_\mu\left(x+\frac{\hat\mu}{2}+\hat\nu\right)\right\rangle + \\ & - \left\langle A_\nu\left(x+\frac{\hat\nu}{2}+\hat\mu\right) A_\nu\left(x+\frac{\hat\nu}{2}\right)\right\rangle + \\ & + \left\langle A_\mu\left(x+\frac{\hat\mu}{2}\right) A_\nu\left(x+\frac{\hat\nu}{2}+\hat\mu\right)\right\rangle + \\ & - \left\langle A_\mu\left(x+\frac{\hat\mu}{2}\right) A_\nu\left(x+\frac{\hat\nu}{2}\right)\right\rangle + \\ & - \left\langle A_\nu\left(x+\frac{\hat\nu}{2}+\hat\mu\right) A_\mu\left(x+\frac{\hat\mu}{2}+\hat\nu\right)\right\rangle + \\ & + \left\langle A_\mu\left(x+\frac{\hat\mu}{2}+\hat\nu\right) A_\nu\left(x+\frac{\hat\nu}{2}\right)\right\rangle\Bigg\}\,. \end{aligned} \tag{6.5}$$

Momentum conservation implies that $\langle A_\mu(p) A_\nu(q)\rangle \propto \delta_{p,-q}$, as shown in

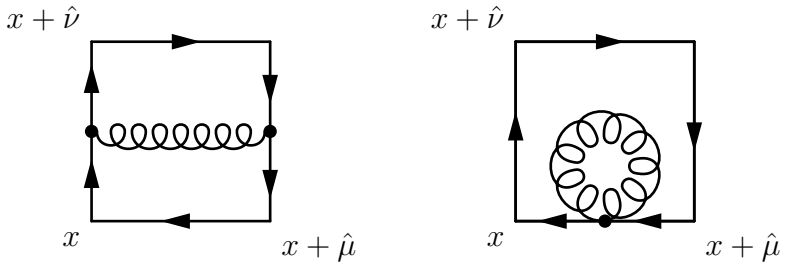

Figure 6.1 *Feynman diagrams contributing to p_0 in Feynman gauge.*

Eq. (C.5), thus it is possible to simplify

$$\langle A_\mu(x)A_\nu(y)\rangle = \sum\!\!\!\!\!\!\int_p e^{i(x-y)p}\,\frac{\Gamma_{p_\perp}\Gamma_{-p_\perp}}{N_cL^4}\,\langle A_\mu(p)A_\nu(-p)\rangle = \\ = \sum\!\!\!\!\!\!\int_p e^{i(x-y)p}\,\frac{f(p_\perp,p_\perp)^*}{N_cL^4}\,\langle A_\mu(p)A_\nu(-p)\rangle\mathbb{1}\,, \tag{6.6}$$

and obtain

$$W^{2\text{-point}}_{\mu\nu}(x) = -\frac{g^2}{2}\sum\!\!\!\!\!\!\int_p \frac{f(p_\perp,p_\perp)^*}{N_cL^4}\Big\{\hat{p}^2_\nu\big\langle A_\mu\big(p\big)A_\mu(-p)\big\rangle + \hat{p}^2_\mu\langle A_\nu(p)A_\nu(-p)\rangle + \\ - 2\hat{p}_\mu\hat{p}_\nu\langle A_\mu(p)A_\nu(-p)\rangle\Big\}\,. \tag{6.7}$$

Plugging in the tree-level gluon propagator, one obtains the leading-order correction to the plaquette,

$$p_0 = -W^{(1)} = \frac{1}{6}\sum_{\mu>\nu}\frac{N_c}{2}\sum\!\!\!\!\!\!\int_p (1-\delta_{p_\perp,0})\,\frac{\hat{p}^2_\mu+\hat{p}^2_\nu}{\hat{p}^2} = \frac{N_c^2-1}{4}\,. \tag{6.8}$$

In Feynman gauge, the lowest-order evaluation of Eq. (6.7) can be pictured with the diagrams in Figure 6.1. Remarkably, the average over all the orientations is volume independent [128]. Different orientations have nonetheless different expectation values, as we explicitly verified in NSPT (see Figure 6.2). It is worth to note that, as shown in Appendix C, on general grounds $\langle A_\mu(p)A_\nu(q)\rangle \propto N_cL^4 f(p_\perp,p_\perp)$, so the corresponding factor in Eq. (6.7) is always cancelled; indeed, such phase depends on the convention chosen and in principle could be eliminated.

The lowest-order fermion contribution comes from considering the vacuum polarisation correction of the free gluon propagator; this is made of the two

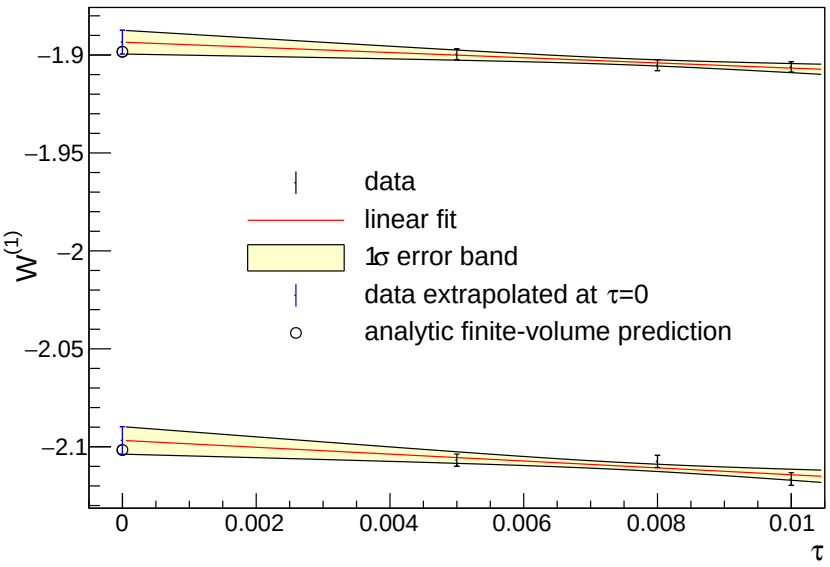

Figure 6.2 *Measure of $W_{\mu\nu}$ at order β^{-1} for a 2^4 lattice with triple TBC at three different time-steps τ of the stochastic process, and $N_c = 3$. The lower measures correspond to the average of the plaquette in the three planes identified by two twisted directions, the upper ones correspond to the average in the three planes identified by one twisted direction and one periodic direction; the size of the lattice has been chosen to enhance the difference of the plaquette value between these two groups of planes. The finite-volume prediction is taken from Eq.* (6.8)*, without averaging over all planes.*

diagrams pictured in Figure 6.3,

$$\Pi_{\mu\nu}(p) = \Pi_{\mu\nu}(p)_{\text{vac. pol.}} + \Pi_{\mu\nu,\text{tadpole}} \,. \tag{6.9}$$

In the infinite-volume limit, the tadpole diagram cancels the divergence arising from the vacuum polarisation at zero momentum (one expects that as a consequence of renormalisability); in finite volume we cannot rely on such simplification, because the cancellation does not happen. Both diagrams must be considered explicitly. We can also be more general and consider the insertion of n fermion bubbles $\Pi_{\mu\nu}(p)$ into the gluon propagator (*gluon chain*), which gives the leading contribution in the large-N_f limit. The n bubbles are joined by $n+1$ propagators: in Feynman gauge, it is

$$\langle A_\mu(p) A_\nu(-p) \rangle_{n \text{ bubbles}} = \frac{N_c L^4}{2} f(p_\perp, p_\perp)(1 - \delta_{p_\perp,0}) \frac{1}{\hat{p}^2} \left(-g^2 N_f \frac{1}{2\hat{p}^2} \right)^n [\Pi(p)^n]_{\mu\nu} \,. \tag{6.10}$$

Note that each propagator attached to a bubble would come with a phase factor $f(p_\perp, p_\perp)$: that phase is cancelled exactly by the phase from the diagrams, which

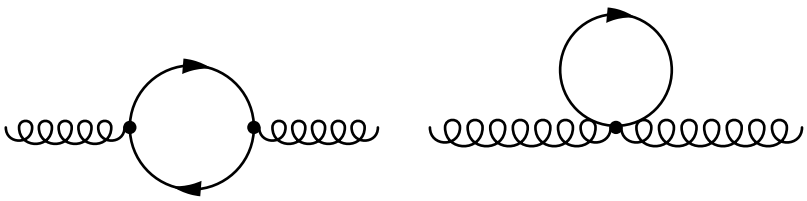

Figure 6.3 *Fermion contribution to the first-order correction of the gluon propagator.*

is $f(p_\perp, p_\perp)^*$. Moreover, the minus sign for the fermionic loop has been factored out. The final result reads

$$\begin{aligned} W^{\text{2-point}}_{\mu\nu,n\text{ bubbles}} &= -\frac{g^2}{2}\sum\!\!\!\!\!\!\int_p (1-\delta_{p_\perp,0})\,\frac{1}{2\hat{p}^2}\left(-g^2 N_f \frac{1}{2\hat{p}^2}\right)^n \cdot \\ &\qquad \cdot \left\{\hat{p}_\nu^2\left[\Pi(p)^n\right]_{\mu\mu} + \hat{p}_\mu^2\left[\Pi(p)^n\right]_{\nu\nu} - 2\hat{p}_\mu\hat{p}_\nu\left[\Pi(p)^n\right]_{\mu\nu}\right\} = \\ &= \frac{N_f^n}{2}\left(-\frac{N_c}{\beta}\right)^{n+1}\sum\!\!\!\!\!\!\int_p (1-\delta_{p_\perp,0})\,\frac{1}{(\hat{p}^2)^{n+1}}\cdot \\ &\qquad \cdot \left\{\hat{p}_\nu^2\left[\Pi(p)^n\right]_{\mu\mu} + \hat{p}_\mu^2\left[\Pi(p)^n\right]_{\nu\nu} - 2\hat{p}_\mu\hat{p}_\nu\left[\Pi(p)^n\right]_{\mu\nu}\right\}, \end{aligned} \tag{6.11}$$

and must be averaged over all the orientations of the Wilson loop,

$$W^{\text{2-point}}_{n\text{ bubbles}} = \frac{1}{6}\sum_{\mu>\nu} W^{\text{2-point}}_{\mu\nu,n\text{ bubbles}}\,. \tag{6.12}$$

In the case of staggered fermions, it must be rescaled $N_f \to N_f/4$ in order for N_f to represent the number of physical flavours; if fermions have smell, the further rescaling $N_f \to N_f/N_c$ is understood. For completeness, the explicit form of the $\Pi_{\mu\nu}(p)$ in the staggered case can be found in Ref. [129]. In Figure 6.4, it is shown the ratio p_n/p_{n-1}, where the finite-volume coefficients p_n have been computed numerically in the gluon-chain approximation, i.e. from $W^{\text{2-point}}_{n\text{ bubbles}}$. It is evident that an exponential behaviour is exhibited, in agreement with the phenomenon described in Sect. 2.4.

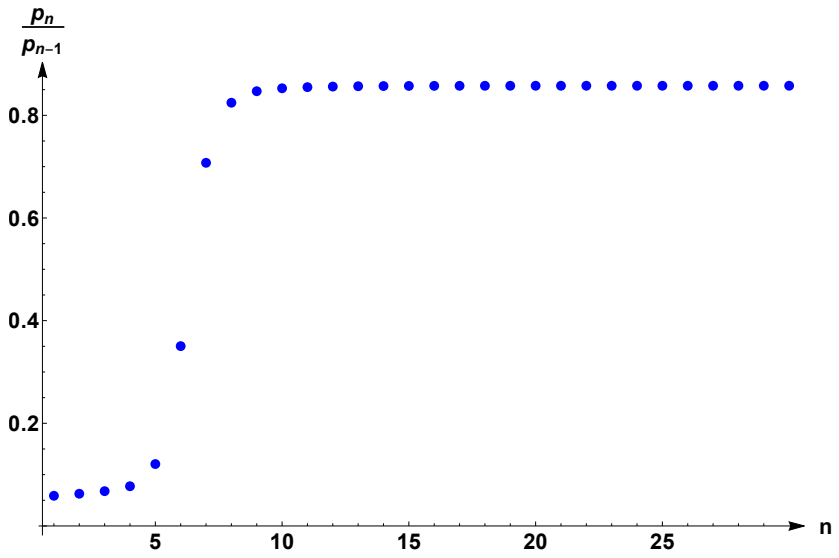

Figure 6.4 *Ratio p_n/p_{n-1} computed in the gluon-chain approximation in finite volume, $L^4 = 18^4$, for two flavours of staggered fermions in the fundamental representation. It is understood that the N_f dependence is trivial, and influences the scale of vertical axis only.*

6.2 The plaquette in massless QCD

We run NSPT simulations of an SU(3) gauge theory with $N_f = 2$ massless staggered fermions in the fundamental representation, measuring the average plaquette after each Langevin update. Twisted boundary conditions are imposed on a plane, with twist matrices chosen as in Eq. (5.33). These simulations have been mostly run with the GridNSPT code on KNL and Skylake nodes provided by the Cambridge Service for Data Driven Discovery (CSD3); simulations on the smallest lattice have been run on the Skylake nodes on the Marconi system provided by CINECA in Bologna. The main features of our code are described in Appendix E. We simulate 24^4, 28^4, 32^4, 48^4 volumes up to order β^{-40} in the expansion of the links. We gradually switch on higher orders when the plaquette at lower orders is thermalised. Because of the instabilities discussed in Sect. 6.2.1, results are presented only up to the order shown in Table 6.1. All simulations are run independently at three different time steps, and we have at least $5 \cdot 10^3$ measures for the largest order at the smallest time step. The length of the runs at larger time steps is rescaled to have approximately the same Langevin time history for all τ.

Table 6.1 *Summary of the ensembles collected for $N_c = 3$ and $N_f = 2$ staggered fermions. The order n_{max} is the highest order at which the plaquette p_n has been measured.*

L	τ	$n_{\max}$
	0.005	35
24	0.0075	35
	0.01	35
	0.005	29
28	0.008	35
	0.01	35
	0.005	33
32	0.008	35
	0.01	35
	0.005	35
48	0.008	35
	0.01	35

6.2.1 Numerical instabilities

The study of the NSPT hierarchy of stochastic processes is not trivial. While there are general results for the convergence of the generic correlation function of a finite number of perturbative components of the fields [65, 130], the study of variances is more involved, and many results can only come from direct inspection of the outcome of numerical simulations. In particular, one should keep in mind that in the context of (any formulation of) NSPT, variances are not an intrinsic property of the theory under study; in other words, they are not obtained as field correlators of the underlying theory. Big fluctuations and correspondingly huge variances were observed at (terrifically) high orders in toy models [130]: signals are plagued by several spikes and it is found by inspection that a fluctuation at a given order is reflected and amplified at higher orders. All in all, variances increase with the perturbative order (not surprisingly, given the recursive nature of the equations of motion). Moving to more realistic theories, a robust rule of thumb is that, as expected on general grounds, the larger the number of degrees of freedom, the less severe the problems with fluctuations are. In particular, we have not yet found (nor has anyone else reported) big problems with fluctuations in the computation of high orders in pure Yang-Mills theory.

We now found that the introduction of fermions indeed causes instabilities at

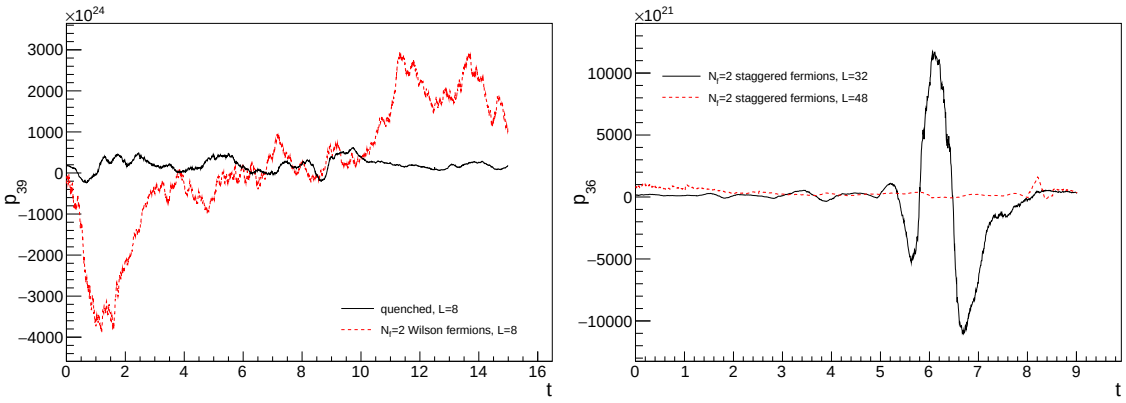

Figure 6.5 *In the left panel, signal samples of the coefficient p_{39} taken from a 8^4 lattice with TBC in three directions. The simulation with Wilson fermions has been performed for illustrative reasons and the bare mass has been set to zero. In the right panel, signal samples of the coefficient p_{36} with TBC on a plane and staggered fermions. In both panels $\tau = 0.005$ and the origin of t is set arbitrarily. It is evident that in the quenched case we could extract the plaquette coefficient even from a small volume, while fermions introduce instabilities that can be mitigated by considering bigger lattices. While we have chosen these two particular examples for illustration purposes, the appearance of spikes is a general phenomenon that we observe for orders approximately ≥ 30 on the volumes under study.*

orders as high as the ones we are considering in this work. Once again, this effect can be tamed by working on increasingly large volumes. Once a fluctuation takes place, the restoring force would eventually take the signal back around its average value but in practice this mechanism is not always effective. At high orders the instabilities can be so frequent and large that the signal is actually lost, and the average value of the plaquette becomes negligible compared to its standard deviation, as it is illustrated in Figure 6.5. The order at which the signal is lost is pushed to higher values by increasing the volume, but eventually uncontrolled fluctuations will dominate. Moreover, we find that spikes tend to happen more frequently at smaller τ. Roughly speaking, this does not come as a surprise, since at smaller time steps one has to live with a larger number of sweeps, thereby increasing the chances of generating large fluctuations when computing the force fields. In Table 6.1 the orders available at each volume and time step are shown in detail.

6.2.2 Extracting the p_n

The lowest coefficients have already been computed analytically. In particular, we remind that, from lattice perturbation theory, $p_0 = 2$ is volume independent [128]. The infinite-volume value of p_1 can be obtained adding to the pure gauge contribution [131],

$$p_{1,g} = 4N_c^2(N_c^2 - 1)\left(0.0051069297 - \frac{1}{128N_c^2}\right), \tag{6.13}$$

the contribution due to staggered fermions [132],

$$p_{1,f} = -1.2258(7) \cdot 10^{-3}\,(N_c^2 - 1)2N_cN_f\,. \tag{6.14}$$

For the specific case $N_c = 3, N_f = 2$, we find $p_1 = 1.10312(7)$. We also computed the fermion contribution to p_1 in twisted lattice perturbation theory[3]. The finite-volume result is $p_1 = 1.10317022\ldots$ at $L = 8$, therefore we expect finite volume effects to be negligible in the lattices we are employing. In particular, we improved the determination of $p_{1,f}$ in Eq. (6.14) using the finite volume calculations at $L = 16$ as the central value, and the variation between $L = 16$ and $L = 14$ as an estimate of its uncertainty, leading to $p_{1,f} = -0.0587909(3)N_f$ for $N_c = 3$, and hence $p_1 = 1.1032139(6)$ for $N_f = 2$. Trying to extract p_0 and p_1 from our data at $L = 48$, we realise that even τ^2 effects in the extrapolation must be considered because of the very high precision of the measurements. For these two coefficients, a dedicated study with additional simulations at time steps $\tau = 0.004$ and $\tau = 0.0065$ has been performed; the agreement with the analytic calculations is found to be excellent, see Figure 6.6.

Therefore, p_0 and p_1 are set to their infinite-volume values and excluded from the analysis of the numerical simulations. The remaining orders are obtained from NSPT. The value $p_{n,\tau}$ for the plaquette at order n and time step τ is computed from the average of the fields generated by the stochastic process, after discarding a number of thermalisation steps. The moving averages result to be stable, as can be seen in the two examples of Figure 6.7. In order to exploit all the available data, the thermalisation is set differently at different orders. The covariance $\mathrm{Cov}(n,m)_\tau$ between $p_{n,\tau}$ and $p_{m,\tau}$ is computed taking into account autocorrelations and cross-correlations, as explained in detail in Appendix D. Clearly there is no correlation

[3]We are grateful to M. García Pérez and A. González-Arroyo for providing us the gluon contribution in finite volume.

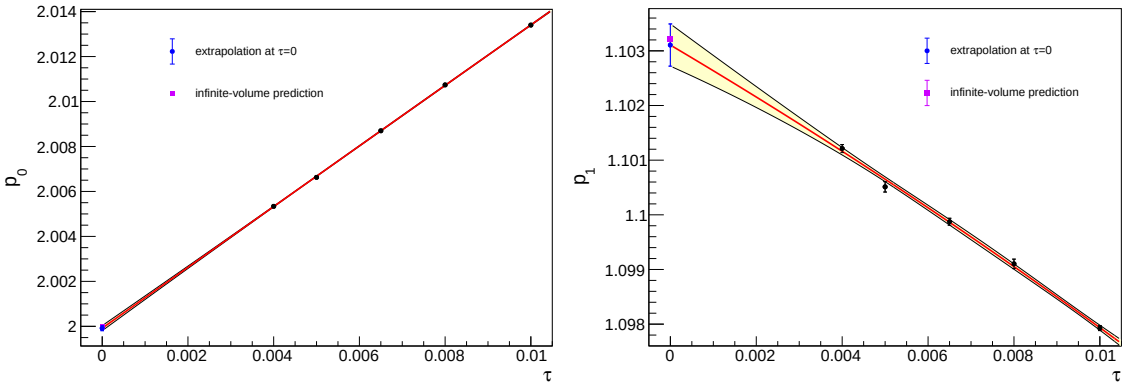

Figure 6.6 *Determination of p_0, p_1 at $L = 48$. Dedicated simulations for these two coefficients have been performed at $\tau = 0.004$ and $\tau = 0.0065$. We extrapolate to zero time step with a second order polynomial in τ. The extrapolated values are $p_0 = 1.9999(1)$ and $p_1 = 1.1031(4)$ with reduced χ^2 respectively equal to 1.710 and 1.477.*

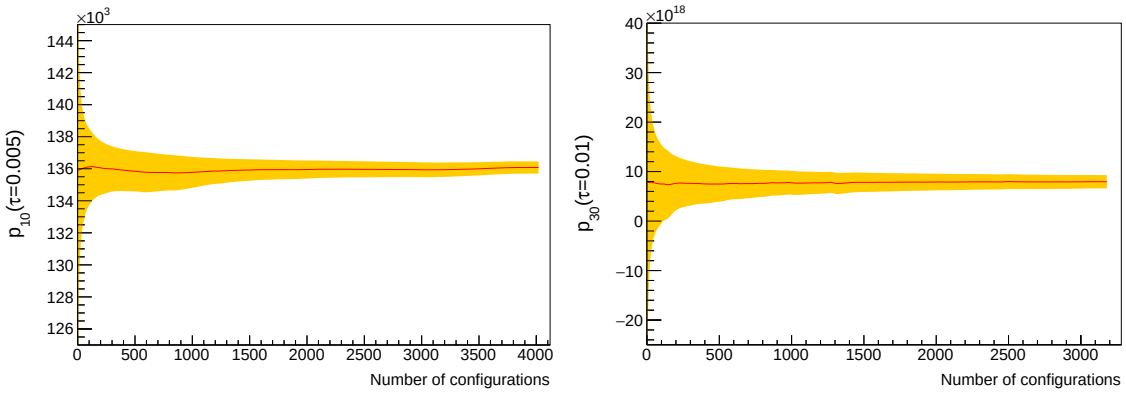

Figure 6.7 *Average of two plaquette coefficients at $L = 48$ as a function of the number of configurations. The error band corresponds to the standard deviation of the sample.*

between different τ. In order to estimate the covariance when two orders have different thermalisation, we take into account only the largest set of common values where both are thermalised. This pairwise estimation of the covariance matrix does not guarantee positive definiteness, therefore we rely on Higham's algorithm, which we describe in Appendix F, to find the nearest positive definite covariance matrix; the procedure introduces some dependence on a tolerance δ. The extrapolation to vanishing time step is performed by minimising

$$\chi^2 = \sum_{n,m}^{n_{max}} \sum_{\tau} (p_{n,\tau} - a_n \tau - p_n) \, \mathrm{Cov}^{-1}(n,m)_\tau \, (p_{m,\tau} - a_m \tau - p_m) \,, \tag{6.15}$$

where the coefficients a_n are the slopes of the combined linear fits. The interesting fit results are the values of the extrapolated plaquettes p_n and their covariance matrix $\mathrm{Cov}(n,m)$. In general, because of the available statistics and the intrinsic fluctuations of the observable, the lower-order values are measured more accurately compared to the higher-order ones; the same holds for the estimate of the entries the covariance matrix. Since, in principle, the plaquette at a certain order could be extracted without any knowledge about its higher-order values, we can get the best estimate for a p_n by implementing the fit iteratively, increasing n_{max} from 0 to the maximum available order. At each iteration, we determine the order with the minimum number of measures $N_{\min}$ and rescale the entries of the covariance matrix so that there is a common normalisation ($N = N_{\min}$ in Eq. (D.3)) for all the matrix elements. In this way, all the data are exploited for the determination of the covariance of the process, and the non-positive definiteness of the covariance of the averages arises only from the presence of autocorrelations and cross-correlations. Higham's algorithm is then applied to $\mathrm{Cov}(n,m)_\tau$ restricted to n_{max} orders. At this stage, minimising the χ^2 allows us to extract $p_{n_{max}}$ with $\mathrm{Cov}(n_{max}, m)$ for $m \leq n_{max}$. The tolerance of Higham's algorithm is tuned so that the covariance matrix is able to represent our data, i.e. so that the reduced chi-squared is close to 1. The combined fit determines also the plaquettes at orders lower than n_{max}, which are always checked and found to be in agreement, within errors, with their previous determination at smaller n_{max}. An example of a correlation matrix extracted with this procedure is in Figure 6.8, where clear structures of correlated and anticorrelated coefficients are visible. The results of the combined extrapolations are summarised in Table 6.2.

In the following, we are going to study the asymptotic behaviour of the coefficients p_n determined in the previous section and discuss the implications for the

Table 6.2 *Plaquette coefficients from the combined fit for $L = 24$, 28, 32, 48. The tolerance δ is given only when the covariance matrix is found not to be positive definite.*

$L = 24$				$L = 28$			
n	p_n	χ^2/dof	δ	n	p_n	χ^2/dof	δ
2	2.536(1)	2.178	–	2	2.537(1)	0.032	–
3	7.622(6)	1.079	0.1	3	7.639(7)	1.136	0.625
4	$2.626(3) \cdot 10^1$	0.735	0.1	4	$2.636(3) \cdot 10^1$	0.648	0.5
5	$9.84(1) \cdot 10^1$	0.615	0.1	5	$9.89(2) \cdot 10^1$	0.853	0.1
6	$3.906(6) \cdot 10^2$	0.828	0.01	6	$3.934(7) \cdot 10^2$	0.593	0.1
7	$1.615(3) \cdot 10^3$	0.529	0.01	7	$1.630(4) \cdot 10^3$	0.480	0.1
8	$6.89(2) \cdot 10^3$	0.581	0.01	8	$6.97(2) \cdot 10^3$	0.707	0.1
9	$3.021(9) \cdot 10^4$	0.421	0.01	9	$3.05(1) \cdot 10^4$	0.927	0.1
10	$1.357(5) \cdot 10^5$	0.861	0.01	10	$1.366(5) \cdot 10^5$	0.753	0.1
11	$6.09(3) \cdot 10^5$	0.940	0.01	11	$6.21(3) \cdot 10^5$	0.599	0.1
12	$2.80(2) \cdot 10^6$	0.753	0.01	12	$2.87(1) \cdot 10^6$	0.512	0.1
13	$1.302(9) \cdot 10^7$	0.690	0.01	13	$1.338(7) \cdot 10^7$	0.443	0.1
14	$6.14(4) \cdot 10^7$	0.570	0.01	14	$6.31(4) \cdot 10^7$	0.401	0.1
15	$2.94(2) \cdot 10^8$	0.652	0.01	15	$3.01(2) \cdot 10^8$	0.360	0.1
16	$1.41(1) \cdot 10^9$	0.797	0.01	16	$1.44(1) \cdot 10^9$	1.012	0.01
17	$6.79(6) \cdot 10^9$	0.758	0.01	17	$6.96(7) \cdot 10^9$	0.998	0.01
18	$3.31(3) \cdot 10^{10}$	0.730	0.01	18	$3.36(3) \cdot 10^{10}$	0.972	0.01
19	$1.65(2) \cdot 10^{11}$	0.678	0.01	19	$1.63(2) \cdot 10^{11}$	0.953	0.01
20	$8.3(1) \cdot 10^{11}$	0.732	0.01	20	$8.0(1) \cdot 10^{11}$	0.884	0.01
21	$4.15(7) \cdot 10^{12}$	0.755	0.01	21	$3.89(6) \cdot 10^{12}$	0.829	0.01
22	$2.08(5) \cdot 10^{13}$	0.590	0.1	22	$1.91(3) \cdot 10^{13}$	0.821	0.01
23	$10.0(4) \cdot 10^{13}$	0.569	0.1	23	$9.5(2) \cdot 10^{13}$	0.873	0.01
24	$5.0(2) \cdot 10^{14}$	0.543	0.1	24	$4.7(1) \cdot 10^{14}$	0.851	0.01
25	$2.5(1) \cdot 10^{15}$	0.485	0.1	25	$2.34(6) \cdot 10^{15}$	0.764	0.01
26	$1.34(4) \cdot 10^{16}$	1.140	0.01	26	$1.14(3) \cdot 10^{16}$	0.695	0.01
27	$6.6(2) \cdot 10^{16}$	1.054	0.01	27	$5.7(2) \cdot 10^{16}$	0.687	0.01
28	$3.2(2) \cdot 10^{17}$	0.479	0.1	28	$2.8(1) \cdot 10^{17}$	0.671	0.01
29	$1.6(1) \cdot 10^{18}$	1.124	0.01	29	$1.5(1) \cdot 10^{18}$	0.462	0.01
30	$7.6(7) \cdot 10^{18}$	0.836	0.01	30	$7.1(7) \cdot 10^{18}$	0.855	0.001
31	$3.6(6) \cdot 10^{19}$	0.456	0.01	31	$4.2(7) \cdot 10^{19}$	0.663	0.001
32	$1.8(4) \cdot 10^{20}$	0.443	0.01	32	$2.0(4) \cdot 10^{20}$	0.661	0.001
33	$9(3) \cdot 10^{20}$	0.445	0.01	33	$10(3) \cdot 10^{20}$	0.651	0.001
34	$5(2) \cdot 10^{21}$	0.432	0.01	34	$4(2) \cdot 10^{21}$	0.516	0.001
35	$3(1) \cdot 10^{22}$	0.425	0.01	35	$2(1) \cdot 10^{22}$	0.519	0.001

$L = 32$				$L = 48$			
n	p_n	χ^2/dof	δ	n	p_n	χ^2/dof	δ
2	2.5370(8)	0.249	–	2	2.5354(7)	2.745	–
3	7.627(4)	1.182	–	3	7.615(3)	1.454	0.01
4	$2.633(2) \cdot 10^1$	2.412	–	4	$2.623(1) \cdot 10^1$	1.428	0.1
5	$9.882(9) \cdot 10^1$	1.378	0.5	5	$9.826(6) \cdot 10^1$	1.673	0.1
6	$3.926(5) \cdot 10^2$	1.015	0.1	6	$3.897(3) \cdot 10^2$	1.653	0.1
7	$1.626(2) \cdot 10^3$	0.730	0.1	7	$1.613(2) \cdot 10^3$	1.338	0.1
8	$6.96(1) \cdot 10^3$	0.929	0.01	8	$6.88(1) \cdot 10^3$	1.194	0.1
9	$3.050(6) \cdot 10^4$	0.772	0.01	9	$3.007(6) \cdot 10^4$	1.079	0.1
10	$1.367(4) \cdot 10^5$	0.638	0.01	10	$1.341(3) \cdot 10^5$	0.998	0.1
11	$6.22(2) \cdot 10^5$	0.963	0.01	11	$6.08(1) \cdot 10^5$	0.925	0.1
12	$2.86(1) \cdot 10^6$	0.645	0.1	12	$2.793(6) \cdot 10^6$	1.108	0.01
13	$1.337(6) \cdot 10^7$	0.771	0.1	13	$1.297(3) \cdot 10^7$	0.978	0.01
14	$6.29(3) \cdot 10^7$	0.861	0.1	14	$6.08(2) \cdot 10^7$	0.883	0.01
15	$3.00(2) \cdot 10^8$	0.952	0.1	15	$2.87(1) \cdot 10^8$	1.067	0.01
16	$1.438(9) \cdot 10^9$	1.012	0.1	16	$1.370(5) \cdot 10^9$	1.013	0.01
17	$6.94(5) \cdot 10^9$	0.996	0.1	17	$6.57(3) \cdot 10^9$	0.951	0.01
18	$3.34(3) \cdot 10^{10}$	1.000	0.1	18	$3.16(1) \cdot 10^{10}$	0.930	0.01
19	$1.63(2) \cdot 10^{11}$	0.965	0.1	19	$1.530(6) \cdot 10^{11}$	0.938	0.01
20	$7.90(8) \cdot 10^{11}$	1.053	0.01	20	$7.45(3) \cdot 10^{11}$	0.890	0.01
21	$3.86(4) \cdot 10^{12}$	0.995	0.01	21	$3.65(1) \cdot 10^{12}$	0.824	0.01
22	$1.90(2) \cdot 10^{13}$	0.957	0.01	22	$1.796(9) \cdot 10^{13}$	0.748	0.01
23	$9.4(1) \cdot 10^{13}$	0.949	0.01	23	$8.88(5) \cdot 10^{13}$	0.691	0.01
24	$4.74(9) \cdot 10^{14}$	0.979	0.01	24	$4.41(3) \cdot 10^{14}$	0.636	0.01
25	$2.39(5) \cdot 10^{15}$	0.967	0.01	25	$2.19(2) \cdot 10^{15}$	0.575	0.01
26	$1.22(3) \cdot 10^{16}$	0.921	0.01	26	$1.09(1) \cdot 10^{16}$	0.548	0.01
27	$6.3(2) \cdot 10^{16}$	0.871	0.01	27	$5.46(9) \cdot 10^{16}$	0.538	0.01
28	$3.2(1) \cdot 10^{17}$	0.849	0.01	28	$2.74(6) \cdot 10^{17}$	0.523	0.01
29	$1.63(9) \cdot 10^{18}$	0.812	0.01	29	$1.38(4) \cdot 10^{18}$	0.511	0.01
30	$8.6(7) \cdot 10^{18}$	0.779	0.01	30	$7.0(3) \cdot 10^{18}$	0.492	0.01
31	$4.5(9) \cdot 10^{19}$	0.743	0.01	31	$3.5(2) \cdot 10^{19}$	0.494	0.01
32	$1.9(3) \cdot 10^{20}$	0.723	0.01	32	$1.7(1) \cdot 10^{20}$	0.503	0.01
33	$9(2) \cdot 10^{20}$	0.723	0.01	33	$8.3(7) \cdot 10^{20}$	1.062	0.001
34	$5(1) \cdot 10^{21}$	0.702	0.01	34	$5.2(6) \cdot 10^{21}$	1.090	0.001
35	$1(1) \cdot 10^{22}$	0.663	0.01	35	$2.3(6) \cdot 10^{22}$	0.486	0.01

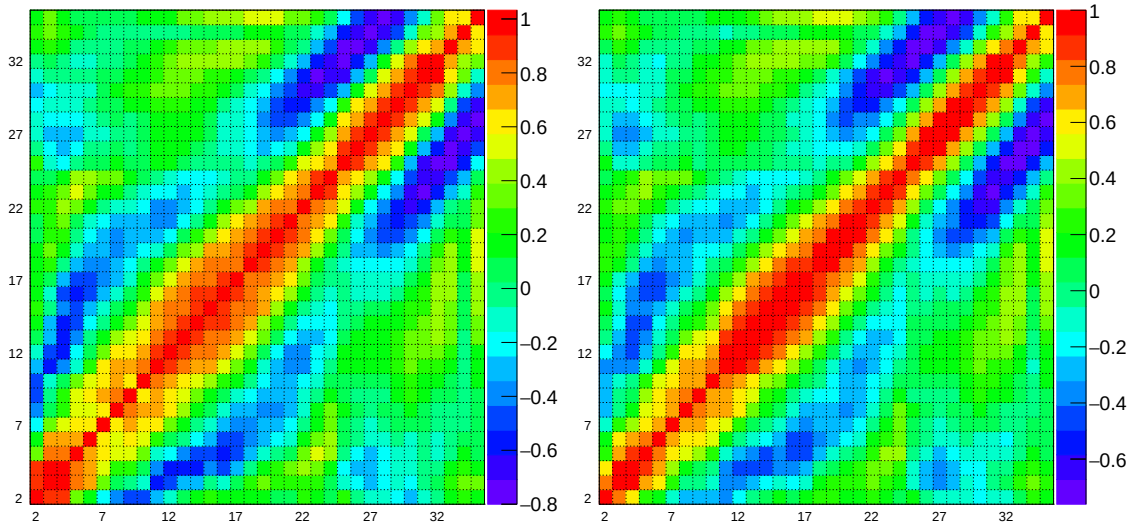

Figure 6.8 *In the left panel, correlation matrix between the coefficients $p_2, \ldots, p_{35}$ at $L = 48$ extracted from the combined fit procedure. The entrances can be bigger than 1 because the matrix is not positive definite. In the right panel, the nearest correlation matrix obtained with Higham's algorithm ($\delta = 10^{-10}$).*

definition of the gluon condensate in massless QCD.

6.2.3 Growth of the coefficients

From the analysis in Sect. 2.4 (in the hypothesis of using the Wilson action with $N_c = 3$), assuming that the plaquette series has a fixed-sign factorial divergence whose corresponding singularity in the Borel plane is the source of an ambiguity that can be absorbed by redefining the condensate, it is possible to predict that for large n it is $p_n = C\, z_0^{-n-1}\, \Gamma(n+1+\gamma)$ with $z_0 = 16\pi^2/(3\beta_0)$, $\gamma = 2\beta_1/\beta_0^2$, and that the ratio $p_n/(np_{n-1})$ behaves as

$$\frac{p_n}{np_{n-1}} = \frac{3\beta_0}{16\pi^2}\left[1 + \frac{2\beta_1}{\beta_0^2}\frac{1}{n} + O\left(\frac{1}{n^2}\right)\right]. \tag{6.16}$$

The scheme-dependent coefficient β_2, not known for staggered fermions, would be needed to go further in the $1/n$ expansion.

In Figure 6.9 and Figure 6.10, the comparison between Eq. (6.16) and our data at different volumes is shown. How finite-volume effects influence the values of the coefficients p_n has already been studied in the literature [40, 98]. From a standard renormalon-based analysis, the value of the loop momenta that contribute the

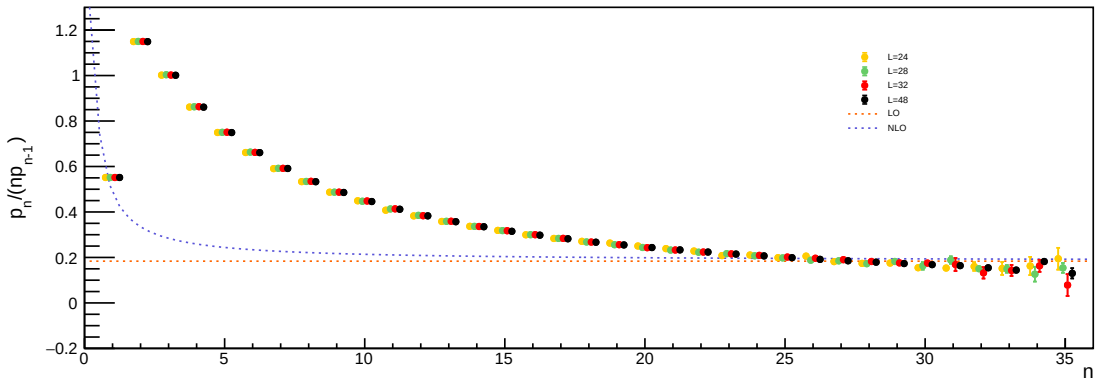

Figure 6.9 *Ratio $p_n/(np_{n-1})$ extracted from our data at $L = 24, 28, 32, 48$. In order to be visible, points referring to different volumes are placed side by side. The leading order (LO) prediction refers to the $n \to \infty$ limit, while the next-to-leading order (NLO) one includes the first $1/n$ correction.*

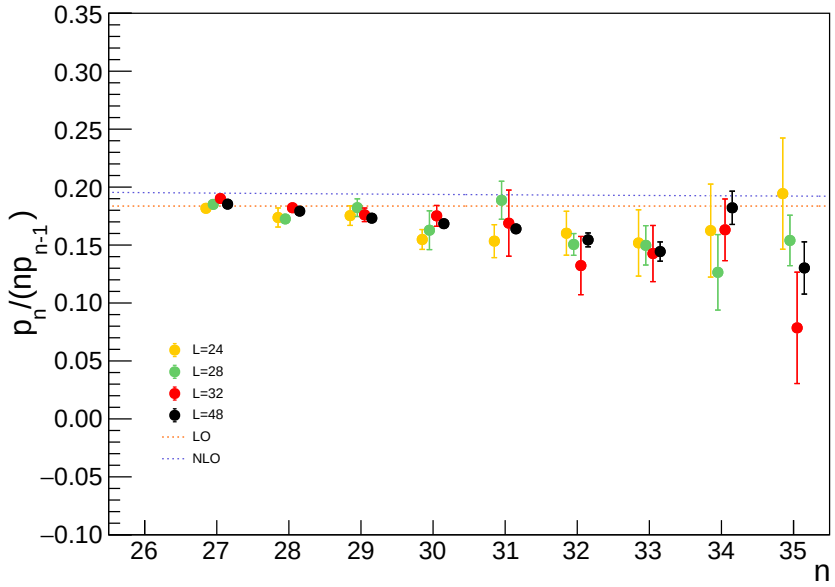

Figure 6.10 *Same as Figure 6.9, but the region at large n is enlarged.*

most to p_n decreases exponentially with n. Since the finite size of the lattice provides a natural infrared cutoff, we expect finite-volume effects to be larger at larger perturbative orders. The dependence of p_n on the lattice size N can be modelled with a finite-volume OPE, exploiting the separation of scales $a^{-1} \gg (Na)^{-1}$: the leading correction is [98]

$$\sum_{n=0} p_n(N)\beta^{-(n+1)} = \sum_{n=0} p_n\beta^{-(n+1)} - \frac{1}{N^4}\, C_G(\beta) \sum_{n=0} f_n \alpha((Na)^{-1})^{n+1} + O\left(\frac{1}{N^6}\right), \tag{6.17}$$

where $\alpha((Na)^{-1})$ must be expressed in terms of the coupling β at the scale a^{-1} using Eq. (1.13). We do not attempt to take into account $1/N^4$ effects, as our

data do not allow performing a reliable combined fit. Apparently no significant finite-volume effects are visible where they would be expected the most, i.e. at larger n. This is shown in the two examples of Figure 6.11. A similar behaviour has been observed in Ref. [98], where the data points computed on comparable volumes show little dependence on the lattice size. In that study, a detailed analysis with a large number of volumes was needed in order to be able to fit the finite-volume corrections. The overall effect is found to be an increase of the ratio $p_n/(np_{n-1})$, see e.g. Figure 6 in Ref. [98]. In our case, data in finite volume do cross the theoretical expectation; still, considering the spread between points at different volumes in Figure 6.10 as a source of systematic error, we could consider our measurements to be compatible with the asymptotic behaviour of Eq. (6.16). We also ascertain the existence of an inversion point when resumming the perturbative series, as explained in Sect. 6.4. Despite this encouraging behaviour, any definite conclusion about the existence of the expected renormalon can only be drawn after performing an appropriate infinite-volume study. We emphasise that in this work the discrepancies in the determination of the p_n from different volumes must be interpreted as part of our systematic uncertainty, being this an exploratory study. A precise assessment of the finite-volume effects will be sought for a precise determination of the gluon condensate; we are currently planning a set of dedicated simulations in the near future to settle this issue.

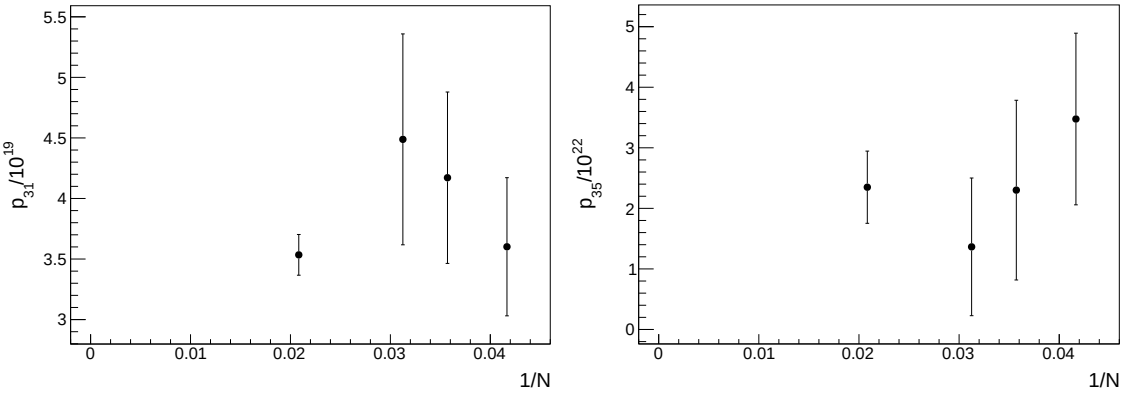

Figure 6.11 *Coefficients p_{31} and p_{35} drawn as a function of the volume. No significant finite-volume effects are observed at our level of precision.*

6.3 Chiral extrapolation of the nonperturbative values of the plaquette

Nonperturbative values for the SU(3) plaquette with $N_f = 2$ (rooted) staggered fermions can be found in Ref. [132], where data are collected from Refs. [133, 134]. For each value of the bare coupling, the physical scale is provided via the Sommer parameter r_0 [135]. The data are given for several values of the fermion bare mass, and need to be extrapolated to the chiral limit for our purposes. A reasonable assumption (for example adopted and verified also in Ref. [136] for the ratio r_0/a) is that the plaquette and the ratio r_0/a have a polynomial behaviour at small masses. We performed fits with linear to cubic polynomials and varied the fit ranges to exclude points at larger values of the masses, but in many cases the fits did not return a satisfactory description of the data with sensible values of χ^2/dof. Because we are using results from past simulations, it is difficult to track accurately the systematic errors in the data. For this reason, we decided to choose the fit with smaller χ^2/dof among those we tried and if $\chi^2/\text{dof} > 1$ the errors in the data were rescaled by a common factor in order to have a reduced chi-squared equal to 1. The fits resulting from this approach are shown in Figure 6.12; the extrapolated values for plaquettes and r_0/a are in Table 6.3. Another approach consists in considering the average between the largest and smallest extrapolated values among all the different fits we tried (without rescaled errors and with reduced chi-squared smaller than some reasonable threshold) and assigning an error equal to the sum in quadrature between the largest error from the fits and half the difference between the largest and smallest extrapolated values. In this way we obtain results compatible (both for central values and errors) with those in Table 6.3, confirming that the chiral extrapolation is sound and the error bars conservative enough. Note that in this work we do not aim at a precise determination of the condensate, and therefore we can be satisfied with an inflated error on the Monte Carlo data points.

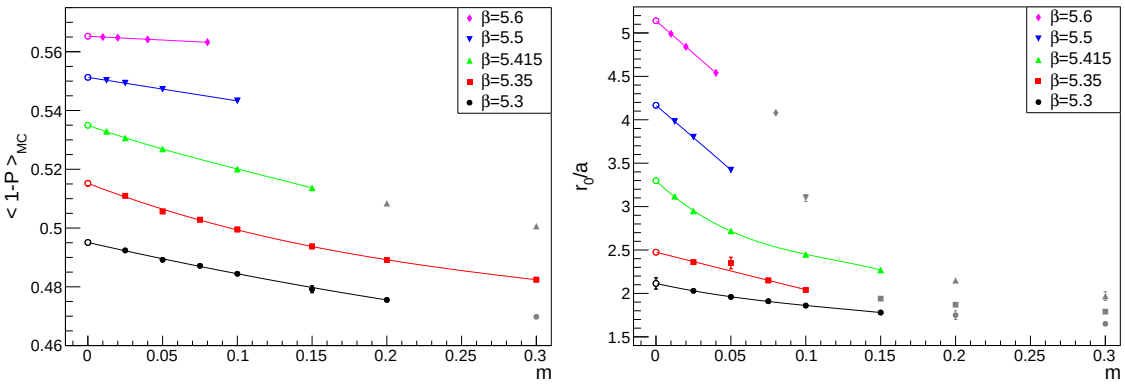

Figure 6.12 *Chiral extrapolation of the nonperturbative plaquette (left panel) and the ratio r_0/a (right panel) at five different values of β. The grey points are available from Ref. [132] but are excluded because of our fit procedure. In most cases the error bar is smaller than the symbol. The orders of the polynomials used in the fits are in Table 6.3.*

Table 6.3 *Results of the chiral extrapolation for the plaquette and the scale. The order of the polynomials used in the fits is indicated.*

β	$\langle 1-P\rangle_{\rm MC}$	pol. ord.	r_0/a	pol. ord.
5.3	0.4951(4)	2	2.11(7)	3
5.35	0.5152(9)	3	2.47(3)	1
5.415	0.5350(3)	3	3.30(3)	3
5.5	0.55128(3)	1	4.17(2)	1
5.6	0.56526(5)	1	5.14(1)	1

6.4 Optimal truncation and the gluon condensate

The *optimal truncation* prescription, that consists in summing a series up to the order of its minimal term, can be adopted to define the perturbative contribution associated to the plaquette [126]. The ambiguity in doing so is of the same order of the ambiguity associated to a Borel resummation.

Let us go back to the example of Sect. 2.1, where a series $R_{\rm pert}(\alpha) = \sum_{n=0}^{\infty} r_n \alpha^{n+1}$ has factorially divergent positive coefficients $r_n = K a^n \Gamma(n+1+\gamma)$. In order to

find $\bar{n}$ such that $r_{\bar{n}}\alpha^{\bar{n}+1}$ is minimum, we look for a zero of the derivative

$$\frac{\partial}{\partial n}\left(r_n\alpha^{n+1}\right) \simeq K\alpha\sqrt{2\pi}\frac{\partial}{\partial n}\left((a\alpha)^n\, n^{\frac{1}{2}+n+\gamma}\, e^{-n}\right) = \\ = K\alpha\sqrt{2\pi}\,(a\alpha)^n\, n^{\frac{1}{2}+n+\gamma}\, e^{-n}\left(\frac{\frac{1}{2}+\gamma}{n} + \log a\alpha n\right). \tag{6.18}$$

If $\bar{n}$ is large, which we have already assumed when using Stirling's approximation for the gamma function, the minimum term is obtained approximately when $\bar{n}$ is the integer closest to $1/(a\alpha)$: we write simply $\bar{n} \sim 1/(a\alpha)$. Comparing the size of the minimum term,

$$r_{\bar{n}}\alpha^{\bar{n}+1} \simeq K\alpha\sqrt{2\pi}\,(a\alpha)^{\bar{n}}\,\bar{n}^{\frac{1}{2}+\bar{n}+\gamma}\, e^{-\bar{n}} = \sqrt{\frac{2}{\bar{n}\pi}}\,\frac{\pi K}{a}\,\frac{e^{-1/(a\alpha)}}{(a\alpha)^\gamma}\,, \tag{6.19}$$

with Eq. (2.7), we see that the ambiguity of the Borel sum is exactly equal to $\sqrt{\bar{n}\pi/2}\, r_{\bar{n}}\alpha^{\bar{n}+1}$.

Since the ambiguity in the case of renormalons has been already computed explicitly in Eq. (2.34), in this case we can read directly the smallest term

$$\frac{c^{\mathrm{ren}}_{\bar{n}}}{\beta^{\bar{n}+1}} = \sqrt{\frac{2}{\bar{n}\pi}}\,\pi C\,(2N_c z_0)^\gamma\,\left(\frac{\Lambda}{Q}\right)^{2\sigma}. \tag{6.20}$$

It is interesting to examine this equation under the lattice perspective, where the continuum limit must be reached for $\beta \to +\infty$, or $Q \sim 1/a \to +\infty$. In the case of optimal truncation, as the coupling β increases the inversion point $\bar{n}$ increases as well, and more and more terms are included in the sum: eventually, it is evident from Eq. (6.20) that the reminder $a^{-2\sigma}c^{\mathrm{ren}}_{\bar{n}}\beta^{-\bar{n}-1}$ is bound to vanish. This is the feature that allows a consistent, even though limited to a specific prescription, definition of the condensate; we recall that, on the other hand, if the series were truncated sharply at some fixed order, the reminder would diverge in the continuum limit.

We can now apply this prescription to our numerical data. The determination of the minimal term and the summation of the series are performed separately for each volume. According to the optimal truncation, we define $\tilde{Z}_{\mathbb{1}}(\beta)$ by performing the sum up to the order $\bar{n}$ such that the term $p_n\beta^{-n-1}$ is minimum,

$$\tilde{Z}_{\mathbb{1}}(\beta) = \sum_{n=0}^{\bar{n}} p_n\beta^{-(n+1)}\,. \tag{6.21}$$

Table 6.4 *Summation up to the minimal term of the perturbative series of the plaquette.*

β	L	$S_P(\beta)$	$\bar{n}$	$p_{\bar{n}}\beta^{-(\bar{n}+1)}$
5.3	24	0.47515(9)	25	$3.70 \cdot 10^{-4}$
	28	0.4767(1)	30	$2.52 \cdot 10^{-4}$
	32	0.4775(4)	35	$5.23 \cdot 10^{-5}$
	48	0.47665(7)	33	$1.97 \cdot 10^{-4}$
5.35	24	0.46718(8)	25	$2.90 \cdot 10^{-4}$
	28	0.46843(9)	30	$1.88 \cdot 10^{-4}$
	32	0.4690(3)	35	$3.73 \cdot 10^{-5}$
	48	0.46826(5)	33	$1.43 \cdot 10^{-4}$
5.415	24	0.4587(1)	33	$1.06 \cdot 10^{-4}$
	28	0.45844(7)	30	$1.29 \cdot 10^{-4}$
	32	0.4588(2)	35	$2.42 \cdot 10^{-5}$
	48	0.45822(4)	33	$9.51 \cdot 10^{-5}$
5.5	24	0.44663(9)	33	$6.22 \cdot 10^{-5}$
	28	0.44651(6)	30	$7.98 \cdot 10^{-5}$
	32	0.4466(1)	35	$1.38 \cdot 10^{-5}$
	48	0.44627(4)	33	$5.60 \cdot 10^{-5}$
5.6	24	0.43384(6)	34	$3.32 \cdot 10^{-5}$
	28	0.43380(5)	30	$4.57 \cdot 10^{-5}$
	32	0.43383(6)	35	$7.21 \cdot 10^{-6}$
	48	0.43357(3)	33	$3.03 \cdot 10^{-5}$

Our results for all combinations of L and β are summarised in Table 6.4. The order $\bar{n}$ at which the series starts to diverge depends only on the central value of the coefficients p_n and not on their errors: in order to check that the inversion point determined by our procedure is stable, we bootstrapped the procedure by generating an ensemble of sets of coefficients $\{p_n\}$. For each set, the coefficients p_n are drawn from a Gaussian probability, whose mean and covariance are taken from the fit procedure described in Sect. 6.2.2. We then determine $\bar{n}$ for each of these sets. The inversion point turns out to be stable, as shown in Figure 6.13 for the case $L = 48$, and $\beta = 5.3$. This particular case is shown for illustration purposes, and the same features are seen in all other combinations of L and β.

The gluon condensate is then determined from Eq. (2.98): for $N_c = 3$, it is

$$r_0^4 \langle O_G \rangle = \frac{36}{\pi^2} C_G(g)^{-1} \left(\frac{r_0}{a}\right)^4 \left[\langle P \rangle - \tilde{Z}_{\mathbb{1}}(\beta)\right] , \tag{6.22}$$

with the Wilson coefficient defined in Eq. (2.97) and computed in perturbation

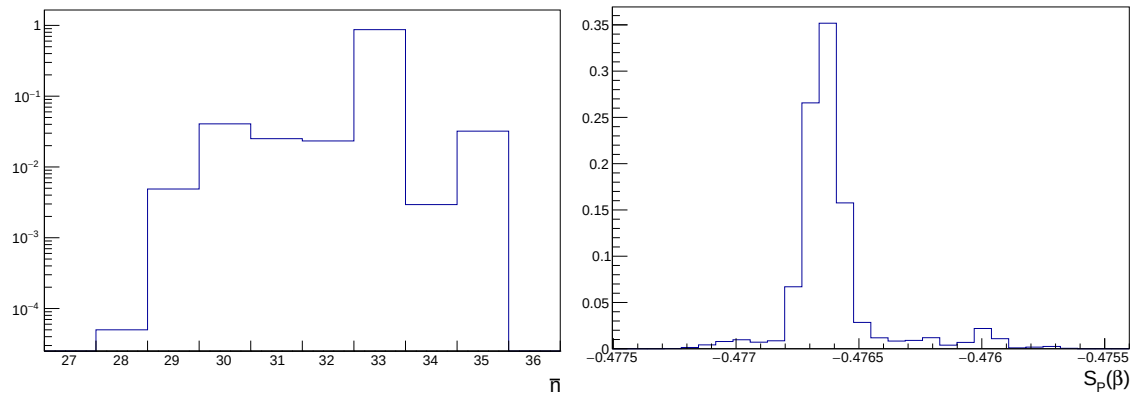

Figure 6.13 *Normalised distributions, over* 10^5 *bootstrap samples, of* $\bar{n}$ *(left panel) and* $S_P(\beta)$ *(right panel) for* $L = 48$, $\beta = 5.3$.

theory,

$$C_G^{-1}(\beta) = 1 + \frac{3}{8\pi^2}\frac{\beta_1}{\beta_0}\frac{1}{\beta} + O\left(\frac{1}{\beta^2}\right) . \tag{6.23}$$

The coefficient β_2 is not universal, and is actually unknown for the discretisation used in this work. Not knowing β_2 prevents us from going further in the expansion of C_G; since the correction due to the Wilson coefficient falls between 5% and 6% for the values of β considered, a 6% systematic uncertainty is added in quadrature after the subtraction.

The result of the subtraction is shown in the left panel of Figure 6.14, for the largest volume. Since only a few values of β are available, it is hard to assess unambiguously the presence of a plateau. We decided to discard from the analysis the two values of the coupling corresponding to the coarser lattices, and define our best estimate of the condensate as the weighted average of the values obtained at the remaining βs. Our final results are summarised in the first column of Table 6.5.

In order to put the choice of fit range on more solid ground, we studied the scaling of $a^4\langle O_G\rangle$ as a function of a^4, as shown in Figure 6.14. The slope of a linear fit of the three finest lattice spacings should give a determination of the condensate compatible with the value extracted from the weighted average. The spread between these two determinations and among the different volumes gives an idea of the magnitude of the systematic uncertainties involved. We also tried to include in the analysis all the available values of β and add a a^6 correction, in the attempt to model the deviations at large values of the lattice spacing; this procedure gives again consistent results (despite a larger χ^2).

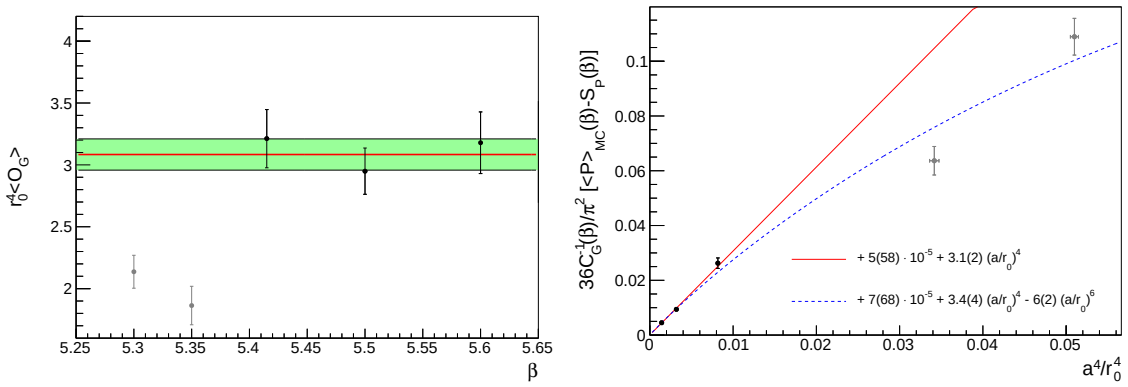

Figure 6.14 *In the left panel, determination of the gluon condensate from Eq.* (6.22)*. The line corresponds to the weighted average of the three largest values of* β*. In the right panel, scaling of the condensate with* a^4 *(solid red line, grey points are excluded), with possibly a* a^6 *correction (dashed blue line, grey points are included). Both panels refer to* $L = 48$*.*

Table 6.5 *Estimate of the gluon condensate at different volumes. The determination labelled with* 1 *is obtained from the weighted average of the values at the three largest values of* β*. The determinations labelled with* 2 *and* 3 *are obtained by studying the scaling of* $a^4\langle O_G\rangle$ *with* a^4*, as in the right panel of Figure 6.14; they correspond respectively to the fit without and with* a^6 *correction (see text for the details).*

L	$r_0^4\langle O_G\rangle_1$	$r_0^4\langle O_G\rangle_2$	$r_0^4\langle O_G\rangle_3$
24	2.6(1)	2.9(2)	3.1(4)
28	2.8(1)	3.1(2)	3.4(4)
32	2.4(1)	2.9(2)	3.2(4)
48	3.1(1)	3.1(2)	3.4(4)

Truncating the sum up to the minimal term is one of the possible prescriptions to define the sum of a divergent series. The intrinsic ambiguity associated to $\tilde{Z}_{\mathbb{1}}(\beta)$ can be defined as the imaginary part of the Borel integral, which at leading order in $1/n$ is $\sqrt{\pi\bar{n}/2}\, p_{\bar{n}}\, \beta^{-\bar{n}-1}$. In Table 6.6, the ambiguity associated to the gluon condensate

$$\delta\langle O_G\rangle = \frac{36}{\pi^2}\, C_G^{-1}(\beta)\, a^{-4} \sqrt{\frac{\pi\bar{n}}{2}}\, p_{\bar{n}} \beta^{-\bar{n}-1} \tag{6.24}$$

is summarised[4].

[4] Our definition of the ambiguity differs from the one in Ref. [98] by a factor $\sqrt{\pi/2}$.

Table 6.6 *Ambiguity of the gluon condensate determined from Eq.* (6.24) *at the three largest values of* β.

	$r_0^4 \delta\langle O_G \rangle$		
L	$\beta = 5.415$	$\beta = 5.5$	$\beta = 5.6$
24	0.4(2)	0.5(4)	0.7(5)
28	0.4(3)	0.7(4)	0.9(5)
32	0.3(2)	0.5(3)	0.3(3)
48	0.3(2)	0.5(3)	0.6(4)

Chapter 7

Conclusions

We used NSPT to perform for the first time large-order computations in lattice gauge theories coupled to massless fermions. Twisted boundary conditions for the gauge field, needed for the removal of the zero-momentum mode, required the introduction of a smell degree of freedom for fermions in the fundamental representation. Both Wilson and (for the first time in NSPT) staggered fermions have been implemented. While for the former we performed an exploratory study of the critical mass up to order $O(\beta^{-7})$, the latter are ultimately the best choice to reach very high orders, due to their residual chiral symmetry that bypasses the need of an additive mass renormalisation. We computed the perturbative expansion of the plaquette up to order $O(\beta^{-35})$ for $N_c = 3$ and $N_f = 2$: under the assumption of considering finite-volume effects as a source of systematic errors, the observed growth of the coefficients in the expansion could be compatible with the leading infrared renormalon; nevertheless, the large uncertainties and the lack of a study of finite-volume effects prevent us from drawing any definite conclusion. By choosing the prescription of summing the perturbative series up to its minimal term, we gave an estimate for the value of the gluon condensate. In this context, NSPT is crucial, being actually the only tool enabling this procedure, which asks for having the asymptotic behaviour of such series under control.

This project must be regarded as a first exploratory study. We could confirm both that the infrared renormalon can be directly inspected, and that the series can be computed up to orders where the inversion point beyond which the expansion starts to diverge (at values of the coupling which are the typical ones in lattice simulations) is clearly visible. We performed our simulations at different lattice

extents, in order to have a first estimate of finite-size effects (again, in both the study of renormalon behaviour and in the truncation of the series). This is the point which has to be better investigated in the future. At the moment, finite-size effects are still to be considered as a systematic source of errors in our procedure.

In this respect, investigating the source of the numerical instabilities would certainly help. So far, the violent fluctuations that we reported in lattice gauge theories with fermions at high orders were noticed in NSPT only in the study of simple models. It would be worth exploring different estimators for the fermion drift, like the already mentioned Hutchinson's estimator, or even considering stochastic processes governed by equations different from the Langevin one, since a higher-order integrator for the Langevin equation would probably turn out to be unpractical, as it was previously discussed. Implementing improved actions, new observables, or other fermion discretisations would represent also viable possibilities. Moreover, with a sound finite-volume extrapolation in place, it would prove to be useful having the nonperturbative plaquette at many more values of the coupling than those that were currently available for unimproved staggered fermions.

An intriguing prospect would be to perform a perturbative expansion both in the coupling and in the number of flavours. Such double expansion could be truncated consistently, as the coefficient of β^{-k} is a finite polynomial in N_f of order smaller than k. Double series have been already implemented in the past in NSPT; however, they face technical challenges, limiting the sizes of the lattices that can be simulated (to give an idea, the size of a standard NSPT configuration with $N_c = 3$, $L = 48$ and order up to α^{40} is already roughly 250 GB). Nevertheless, this study would allow analysing how the growth of the coefficients is influenced by the number of fermion flavours.

On top of the follow-ups we have already discussed, it would be interesting to extend our study to different number of colours, number of flavours and other fermionic representations. It would be of the utmost importance to assess the high-order behaviour of perturbative coefficients in gauge theories different from QCD: by looking at the asymptotic behaviour and by comparing with nonperturbative simulations, one could probe regions in the space of theories in which a (quasi-)conformal window can be present. This could be a powerful, alternative method to look for candidate theories for physics beyond the Standard Model.

Appendix A

Group theory conventions

The conventions used for group theoretical manipulations are summarised here. We consider the group $G = \mathrm{SU}(N_c)$, i.e. the group of unitary matrices with unit determinant.

The indices $a, b, c = 1, \ldots, N_c^2 - 1$ are assumed to be indices in the adjoint representation, $i, j, k, l = 1, \ldots, N_c$ in the fundamental representation, $r, s = 1, \ldots, N_c$ in the antifundamental representation.

The generators of the group are denoted by T^a; they are defined to be Hermitian, and satisfy the commutation relations

$$\left[T^a, T^b\right] = \sum_c i f^{abc} T^c \,, \tag{A.1}$$

where f^{abc} are the group structure constants. The normalisation of the generators is chosen to be such that

$$\mathrm{Tr}\left(T^a T^b\right) = \frac{1}{2}\delta^{ab} \,. \tag{A.2}$$

It is useful to introduce the operator $\Pi_{\mathfrak{g}}$ that projects on the algebra $\mathfrak{g}$ of the group,

$$\Pi_{\mathfrak{g}}(X) = \frac{1}{2}\left(X - X^\dagger - \frac{1}{N_c}\,\mathrm{Tr}\left(X - X^\dagger\right)\right) . \tag{A.3}$$

From the property of the generators

$$\sum_a T^a_{ij} T^a_{kl} = \frac{1}{2}\left(\delta_{il}\delta_{jk} - \frac{1}{N_c}\delta_{ij}\delta_{kl}\right) , \tag{A.4}$$

it is easy to see that

$$\sum_a T^a \operatorname{Tr} T^a (X - X^\dagger) = -2i \sum_a T^a \operatorname{Re}(i \operatorname{Tr} T^a X) = \Pi_{\mathfrak{g}}(X)\,. \tag{A.5}$$

Representations

The matrices T^a are the generators in the *fundamental representation*, whose dimension is N_c. Since we are dealing with matrix groups, the action of $g = e^{i\sum_a \omega^a T^a} \in G$ on a vector v is simply the matrix multiplication gv. The matrices $\bar{T}^a = -(T^a)^*$ generate the *antifundamental representation*; the action of $g^* = e^{i\sum_a \omega^a \bar{T}^a}$ is given by $g^* v = v g^\dagger$. The *adjoint representation* is generated by $(T^a_{\text{adj}})_{bc} = -if^{abc}$, and therefore has dimension $N_c^2 - 1$. For every vector in the adjoint representation w_{adj}, we can define its *matrix representation* as a $N_c \times N_c$ Hermitian traceless matrix $w = w^a_{\text{adj}} T^a$. If $g_{\text{adj}} = e^{i\sum_a \omega^a T^a_{\text{adj}}}$ acts as $w'_{\text{adj}} = g_{\text{adj}} w_{\text{adj}}$, in the matrix representation it holds $w' = g w g^\dagger$. In particular, it is very useful the relation

$$(g_{\text{adj}})_{ab} = 2 \operatorname{Tr} T^a g T^b g^\dagger\,. \tag{A.6}$$

We define the trace normalisation factor $T(R)$ and the *quadratic Casimir* $C_2(R)$ from

$$\operatorname{Tr} T^a_R T^b_R = T(R)\delta^{ab} \tag{A.7a}$$

$$\sum_a T^a_R T^a_R = C_2(R)\mathbb{1}\,. \tag{A.7b}$$

They are related by $T(R)\dim(A) = C_2(R)\dim(R)$. For the group $\mathrm{SU}(N_c)$ it is

$$T(F) = \frac{1}{2}\,, \qquad C_2(F) = \frac{N_c^2 - 1}{2N_c}\,, \qquad T(A) = C_2(A) = N_c\,. \tag{A.8}$$

Lie derivative

The component a of the (left) Lie derivative of an analytic function $f : G \to \mathbb{R}$ is given by

$$\nabla^a_g f(g) = \lim_{\alpha\to 0} \frac{1}{\alpha}\left[f\left(e^{i\alpha T^a} g\right) - f(g)\right] = \frac{d}{d\alpha} f(e^{i\alpha T^a} g)\bigg|_{\alpha=0}\,. \tag{A.9}$$

From this definition, it follows that the function f admits a Taylor series expansion

$$f(e^{i\sum_a \omega^a T^a} g) = f(g) + \sum_a \omega^a \nabla_g^a f(g) + \frac{1}{2}\sum_{a,b} \omega^a \omega^b \nabla_g^a \nabla_g^b f(g) + \ldots = \\ = f(g) + \sum_{n=1}^{\infty} \frac{1}{n!} \sum_{a_1,\ldots,a_n} \omega^{a_1} \ldots \omega^{a_n} \nabla_g^{a_1} \ldots \nabla_g^{a_n} f(g)\,, \tag{A.10}$$

and that the derivative of a product obeys Leibniz's rule,

$$\nabla_g^a \left[f(g)h(g)\right] = \frac{d}{d\alpha}\left[f(e^{i\alpha T^a} g) h(e^{i\alpha T^a} g)\right]\Big|_{\alpha=0} = \\ = \nabla_g^a f(g) h(g) + f(g) \nabla_g^a h(g)\,. \tag{A.11}$$

It is interesting to note that the Lie derivatives do not commute, but rather inherit the commutation relation from the group algebra,

$$[\nabla_g^a, \nabla_g^b] = -\sum_c f^{abc} \nabla_g^c\,. \tag{A.12}$$

For example, the relation in Eq. (A.12) can be verified when $f(g) = \operatorname{Tr} g$, using $\nabla_g^a \operatorname{Tr} g = i \operatorname{Tr} T^a g$ and $\nabla_g^a \nabla_g^b \operatorname{Tr} g = -\operatorname{Tr} T^b T^a g$. We will often use the abbreviations $\nabla_{x\mu}^a = \nabla_{U_\mu(x)}^a$ and $\nabla_{x\mu} = \sum_a T^a \nabla_{x\mu}^a$ when deriving with respect to a link variable.

If the function $f(g)$ has values in the algebra, then for $g = e^{i\sum_a \omega^a T^a}$ we can Taylor expand the component a of $f(g)$ as

$$2 \operatorname{Tr} T^a f(g) = 2 \operatorname{Tr} T^a f(\mathbb{1}) + \sum_b 2 \operatorname{Tr} T^a [\nabla_g^b f(g)|_{g=\mathbb{1}}] \omega^b + \ldots\,, \tag{A.13}$$

and build the matrix

$$[\nabla_g f(g)]_{ab} = 2 \operatorname{Tr} T^a [\nabla_g^b f(g)|_{g=\mathbb{1}}]\,. \tag{A.14}$$

For example, if $f(g) = g\rho g^\dagger$ with $\rho \in \mathfrak{g}$, then $\nabla_g (g\rho g^\dagger) = -i\rho_{\text{adj}}$.

Group integration

The Haar measure dg is used to define integration over G. In particular, such measure is invariant under the group multiplication,

$$\int dg\, f(g'g) = \int dg\, f(g)\,. \tag{A.15}$$

Putting together Eqs. (A.10), (A.11) and (A.15), we see that the integral of a derivative vanishes,

$$\int dg\, \nabla_g^a f(g) = 0\,, \tag{A.16}$$

and that it is possible to integrate by parts without any boundary term,

$$\int dg\, \nabla_g^a f(g) h(g) = -\int dg\, f(g) \nabla_g^a h(g)\,. \tag{A.17}$$

For more details, the reader is referred to any standard textbooks on group theory, e.g. Ref. [137].

Appendix B

The MS lattice coupling

The lattice bare β-function is defined as

$$\beta_L(g) = -a\frac{dg}{da}\bigg|_{\substack{\text{physical}\\\text{quantities}}}, \tag{B.1}$$

and describes how the bare coupling must be changed to keep physical quantities constant as the continuum limit ($a \to 0$) is approached. On the other hand, given some renormalised coupling g_R, the β-function

$$\beta(g_R) = \mu\frac{dg_R}{d\mu}\bigg|_{\substack{\text{bare}\\\text{quantities}}} \tag{B.2}$$

describes how the running coupling changes with the renormalisation scale. The relation between bare and renormalised coupling is

$$g = Z(g_R, a\mu)\, g_R \tag{B.3a}$$

$$g_R = W(g, a\mu)\, g\,, \tag{B.3b}$$

where

$$Z(g_R, a\mu)\, W(Z(g_R, a\mu)g_R, a\mu) = 1\,. \tag{B.4}$$

In perturbation theory, the renormalisation constant can be expressed as a power series in the coupling and $\log a\mu$,

$$Z(g_R, a\mu) = 1 + \sum_{n=1}^{\infty}\sum_{k=0}^{n} Z_{nk}\, g_R^n\, (\log a\mu)^k = \sum_{k=0}^{\infty} Z_k(g_R)\, (\log a\mu)^k\,, \tag{B.5}$$

where we defined $Z_k(g_R)$ as the polynomial in g_R (whose lowest monomial is g_R^k) collecting all the terms that multiply $(\log a\mu)^k$. Since the bare coupling does not depend on μ, we can differentiate Eq. (B.3a) to obtain

$$0 = \mu\frac{dg}{d\mu} = \left(\mu\frac{\partial}{\partial\mu} + \beta(g_R)\frac{\partial}{\partial g_R}\right) g_R Z(g_R, a\mu) = \\ = \sum_{k=0}^{\infty}\left[(k+1)g_R Z_{k+1} + \beta(g_R)\frac{\partial}{\partial g_R}\left(g_R Z_k\right)\right](\log a\mu)^k \,. \tag{B.6}$$

The quantity in square brackets must vanish for all values of k, so there are constraints among the functions Z_k. For example, the β-function can be extracted from $k = 0$,

$$\beta(g_R) = -\frac{g_R Z_1}{\frac{\partial}{\partial g_R}\left(g_R Z_0\right)} \,. \tag{B.7}$$

Analogously, using the perturbative expansion

$$W(g, a\mu) = 1 + \sum_{n=1}^{\infty}\sum_{k=0}^{n} W_{nk}\, g^n\, (\log a\mu)^k = \sum_{k=0}^{\infty} W_k(g)\, (\log a\mu)^k \tag{B.8}$$

and the fact that the renormalised coupling does not depend on the lattice spacing, one can get similar constraints on W_k from Eq. (B.3b). In particular, the lattice β-function can be expressed as

$$\beta_L(g) = \frac{gW_1}{\frac{\partial}{\partial g}\left(gW_0\right)} \,. \tag{B.9}$$

On the lattice, a perturbative definition of a renormalised coupling is in the minimal subtraction (MS) scheme: the *MS lattice coupling* is defined subtracting only powers of logarithms in the lattice cutoff. In other words, it is defined by the condition

$$Z(g_R, 1) = Z_0(g_R) = 1 \qquad \text{or} \qquad g_R(1/a) = g \,. \tag{B.10}$$

By setting $\mu = 1/a$ in Eq. (B.4), it follows that $W_0(g_R) = 1$. The β-function in this scheme can be read just by looking at the terms with one power of $\log a\mu$ in the renormalisation constant,

$$\beta(g_R) = -g_R\, Z_1(g_R) \qquad \text{and} \qquad \beta_L(g) = g\, W_1(g) \,. \tag{B.11}$$

Moreover, by applying $a\frac{d}{da}$ to Eq. (B.4) and then setting $\mu = 1/a$ it follows

that $W_1(g_R) = -Z_1(g_R)$. This result implies that the lattice β-function and the β-function for the MS lattice coupling are the same,

$$\beta(g_R) = \beta_L(g_R)\,. \tag{B.12}$$

Thus, the MS lattice coupling can be thought to represent simply the bare lattice coupling interpreted as a function of the lattice spacing.

Appendix C

Twisted lattice perturbation theory

Twisted lattice perturbation theory for a pure gauge theory was introduced in Ref. [93] (see also Ref. [138]). Recently, the computation of Wilson loops has been treated in detail in Ref. [128]. Here we focus on two vertices, introducing Wilson and staggered fermions with smell in the fundamental representation. Feynman rules are fairly similar to those of lattice perturbation theory, apart from phases in propagators and vertices; all phases cancel in the first-order computations we considered. We recall also that the sum over momenta is inherited from the Fourier transform in Sect. 4.3,

$$\sum\!\!\!\!\!\!\int_k = \frac{1}{N_c L^4} \sum_{k_\parallel, k_\perp} , \tag{C.1}$$

and each fermion loop has to be divided by N_c, i.e. by the numbers of smells running in the loop. The gluon propagator is

$$\left\langle \tilde{A}_\mu(p) \tilde{A}_\nu(-p) \right\rangle_{\text{free}} = \frac{N_c L^4}{2} (1 - \delta_{p_\perp,0}) f(p_\perp, p_\perp) \cdot \\ \cdot \frac{1}{4 \sum_\rho \sin^2\left(\frac{p_\rho}{2}\right)} \left[\delta_{\mu\nu} - (1-\xi) \frac{\sin\left(\frac{p_\mu}{2}\right) \sin\left(\frac{p_\nu}{2}\right)}{\sum_\sigma \sin^2\left(\frac{p_\sigma}{2}\right)} \right] , \tag{C.2}$$

where ξ is the gauge fixing parameter; note that the traceless property of the gauge field forces the propagator to vanish for $p_\perp = 0$. The Wilson and staggered

propagators are defined respectively in Eqs. (4.47) and (4.52). Below we write the fermion-fermion-gluon and fermion-fermion-gluon-gluon vertices in the Wilson and staggered case; p_1, p_2 are respectively the incoming and outgoing momenta of the fermions, k_1, k_2 are the outgoing momenta of the gluons.

Wilson fermions

$$V_{ffg}(p_1, p_2, k_{1\perp})_\mu = -g\, f(k_{1\perp}, p_{2\perp}) \left[i\gamma_\mu \cos\frac{1}{2}\,(p_1+p_2)_\mu + \sin\frac{1}{2}\,(p_1+p_2)_\mu \right] \tag{C.3a}$$

$$V_{ffgg}(p_1, p_2, k_{1\perp}, k_{2\perp})_{\mu\nu} = -g^2\delta_{\mu\nu} f(k_{1\perp}+k_{2\perp}, p_{2\perp})\,\frac{1}{2}[f(k_{1\perp}, k_{2\perp}) + f(k_{2\perp}, k_{1\perp})] \cdot \cdot \left[\cos\frac{1}{2}\,(p_1+p_2)_\mu - i\gamma_\mu \sin\frac{1}{2}\,(p_1+p_2)_\mu \right] \tag{C.3b}$$

Staggered fermions Here momentum conservation is made explicit, because the vertices are not diagonal in momentum space.

$$V_{ffg}(p_1, p_2, k_1)_\mu = -ig\, f(k_{1\perp}, p_{2\perp})\, \cos\left(p_2 + \frac{k_1}{2}\right)_\mu \cdot \cdot\, \bar{\delta}(-p_{1\parallel} + k_{1\parallel} + p_{2\parallel} + \pi\bar{\mu})\delta_{-p_{1\perp}+k_{1\perp}+p_{2\perp},0} \tag{C.4a}$$

$$V_{ffgg}(p_1, p_2, k_1, k_2)_{\mu\nu} = ig^2\, f(k_{1\perp}+k_{2\perp}, p_{2\perp})\frac{1}{2}\,[f(k_{1\perp}, k_{2\perp}) + f(k_{2\perp}, k_{1\perp})] \cdot \cdot\, \sin\left(p_2 + \frac{k_1}{2} + \frac{k_2}{2}\right)_\mu \cdot \cdot\, \delta_{\mu\nu}\, \bar{\delta}(-p_{1\parallel} + k_{1\parallel} + k_{2\parallel} + p_{2\parallel} + \pi\bar{\mu})\delta_{k_{1\perp}-p_{1\perp}+k_{2\perp}+p_{2\perp},0} \tag{C.4b}$$

It is also interesting to examine how the momentum conservation is implied by translation invariance in this formalism. Since $\langle A^a(x)A^b(y)\rangle = \delta^{ab}g(x-y)$ is a function of the distance $x-y$ only, then with the Fourier expansion in Eq. (4.26)

we have

$$\begin{aligned}
\left\langle \tilde{A}(p)\tilde{A}(q)\right\rangle &= \sum_{xy}\sum_{ij}\sum_{lm} e^{-ixp}\, e^{-iyq}\, (\Gamma^{\dagger}_{p_\perp})_{ij}(\Gamma^{\dagger}_{q_\perp})_{lm}\, \langle A(x)_{ji}A(y)_{ml}\rangle = \\
&= \sum_{xy}\sum_{ij}\sum_{lm}\sum_{ab} e^{-ixp}\, e^{-iyq}\, (\Gamma^{\dagger}_{p_\perp})_{ij}(\Gamma^{\dagger}_{q_\perp})_{lm}\, T^a_{ji}T^b_{ml}\, \delta^{ab} g(x-y) = \\
&= \frac{1}{2}\sum_{xy} e^{-ixp}\, e^{-iyq}\, g(x-y)\, \left(\operatorname{Tr}\Gamma^{\dagger}_{p_\perp}\Gamma^{\dagger}_{q_\perp} - \frac{1}{N_c}\operatorname{Tr}\Gamma^{\dagger}_{p_\perp}\operatorname{Tr}\Gamma^{\dagger}_{q_\perp}\right) = \\
&= \frac{N_c}{2}\, f(p_\perp,p_\perp)(1-\delta_{p_\perp,0})\sum_{xy} e^{-ixp_\parallel} e^{-iyq_\parallel} e^{-i(x-y)p_\perp}\, \delta_{p_\perp,-q_\perp}\, g(x-y) = \\
&= \frac{N_c}{2}\, f(p_\perp,p_\perp)(1-\delta_{p_\perp,0})\sum_{yz} e^{-izp_\parallel} e^{-iy(p_\parallel+q_\parallel)} e^{-izp_\perp}\, \delta_{p_\perp,-q_\perp}\, g(z) \; = \\
&= \frac{N_c L^4}{2}\, f(p_\perp,p_\perp)(1-\delta_{p_\perp,0})\delta_{p,-q}\sum_{z} e^{izp}\, g(z)\,. \qquad \text{(C.5)}
\end{aligned}$$

Momentum is conserved, $p = -q$, and modes with $p_\perp = 0$ are absent. Moreover, compared to the PBC case, there is an additional factor $1/2$ playing the role of the normalisation of the generators, and an additional (convention-dependent) phase $f(p_\perp, p_\perp)$.

Appendix D

Autocorrelations and cross-correlations

We consider a sample $\{a_i, b_i\}_{i=1}^N$ of measures of two observables A, B taken from the stochastic process at equilibrium. Let $\langle A\rangle = a$, $\langle B\rangle = b$ be the expectation values of the observables A, B. The *cross-correlation function* is defined as

$$\Gamma_{AB}(t) = \langle (a_i - a)(b_{i+t} - a)\rangle = \langle a_i b_{i+t}\rangle - ab\,, \tag{D.1}$$

where we used the fact that the expectation value is not dependent on i because the equilibrium distribution is time-independent. The cross-correlation function is not an even function, $\Gamma_{AB}(-t) = \Gamma_{BA}(t)$. In particular, $\Gamma_{AB}(0) = \mathrm{Cov(A,B)}$ is the covariance between A and B. The average $\bar{a} = \frac{1}{N}\sum_{i=1}^N a_i$ is a stochastic variable that satisfies $\langle \bar{a}\rangle = a$. The covariance between the estimators $\bar{a}$ and $\bar{b}$ is

$$\begin{aligned}\mathrm{Cov}(\bar{a},\bar{b}) = \big\langle (\bar{a}-a)(\bar{b}-b)\big\rangle = \frac{1}{N^2}\sum_{i,j=1}^{N}\Gamma_{AB}(i-j) = \\ = \frac{\mathrm{Cov(A,B)}}{N}\left[1 + \sum_{r=1}^{N-1}\left(1-\frac{r}{N}\right)\frac{\Gamma_{AB}(r)}{\Gamma_{AB}(0)} + \sum_{r=1}^{N-1}\left(1-\frac{r}{N}\right)\frac{\Gamma_{AB}(-r)}{\Gamma_{AB}(0)}\right]\end{aligned} \tag{D.2}$$

but since the cross-correlation function is expected to drop exponentially at large times, it is possible to approximate

$$\mathrm{Cov}(\bar{a},\bar{b}) \simeq \frac{\mathrm{Cov(A,B)}}{N}\left(\tau_{AB}^{\mathrm{int}} + \tau_{BA}^{\mathrm{int}}\right) \tag{D.3}$$

with the *integrated cross-correlation time*

$$\tau_{AB}^{\text{int}} = \frac{1}{2} + \sum_{r=1}^{\infty} \frac{\Gamma_{AB}(r)}{\Gamma_{AB}(0)} \,. \tag{D.4}$$

We expect $\tau_{AB}^{\text{int}} \neq \frac{1}{2}$ when the observable B has some dependence on A. If B is independent of A, we can assume $\tau_{AB}^{\text{int}} = \frac{1}{2}$. An estimator for the cross-correlation function is

$$\bar{\Gamma}_{AB}(t) = \frac{1}{N-t} \sum_{i=1}^{N-t} (a_i - \bar{a})(b_{i+t} - \bar{b}) \,. \tag{D.5}$$

and the integrated cross-correlation time can be extracted in the Madras-Sokal approximation [139, 140]. Note that when $A = B$ then $\Gamma_{AA}(t)$ is the *autocorrelation function* and Eq. (D.3) becomes $\text{Var}(\bar{a}) = 2\tau_{AA}^{\text{int}} \text{Var}(\bar{a})/N$, where τ_{AA}^{int} is the *integrated autocorrelation time*.

Appendix E

Code development

We developed two independent NSPT codes in order to cross-check and improve our implementation.

PRlgt[1] stems from the first NSPT codes developed by the Parma lattice gauge theory group, allowing for SU(3) simulations with Wilson fermions. We implemented twisted boundary conditions, smell for Wilson fermions and added support for SU(2) simulations. The code is tailored for perturbation theory. The underlying idea is to have base classes `ptSU2` and `ptSU3` that describe perturbative matrices. The operator `*` is overloaded with the Cauchy product, so that it is possible to write the product of two series in a natural way. This is one of the operations that, especially at high orders, becomes very time-consuming: thus, having perturbative matrices as base classes allows keeping the perturbative orders close in memory to speed up the multiplication of series. In particular, the perturbative expansion is hardcoded to start from 1 for an element of the group and from 0 for an element of the algebra, in order to avoid multiplying by the identity or zero matrix; this choice also improves numerical stability in keeping the series within the group or algebra. All the other structures are built from the base classes by adding Lorentz, Dirac or lattice degrees of freedom. The fermion field too is described by matrices in colour-smell space. The update of the configuration is done one link at a time: this is possible, faster and less memory consuming for the first order integrator we are using; indeed the staples around a link can be computed also if the neighbour links have already been updated, since the effect of doing so gives higher-order effects in the time step. Twisted

[1] For recent developments of the code see Ref. [141].

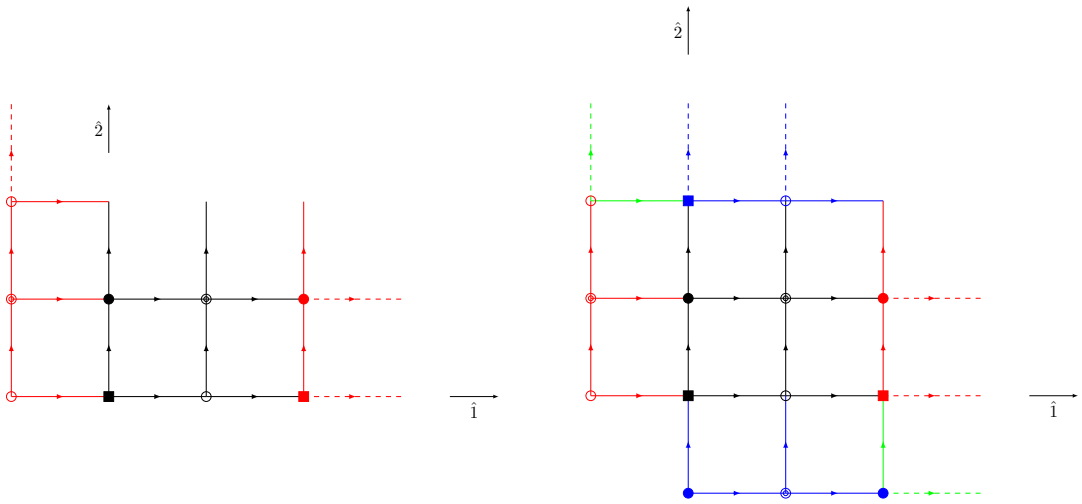

Figure E.1 *Sketch of the PRlgt auxiliary links in a plane of a 2×2 lattice. Physical links are in black and sites identified by the same symbol represent the same physical site. Dashed lines highlight links that are allocated but do not participate in the update. In the left panel direction $\hat{1}$ is twisted, $\hat{2}$ is not: in red there are the auxiliary sites (two forward, three backward) and the red links beginning there correspond to physical links twisted according to the matrix Ω_1. In the right panel both $\hat{1}$ and $\hat{2}$ are twisted directions: in blue there are auxiliary sites whose links are twisted according to the matrix Ω_2. In the latter case there are sites which pass the boundary in two twisted directions: the green links undergo both the Ω_1 and the Ω_2 twist (the two operations commute by definition).*

boundary conditions are implemented ad hoc for the Wilson action, as shown in Figure E.1: a system of twisted copies of the links on the boundary is updated at each Langevin step. The code makes heavy use of multithreading in all loops over lattice sites. Even though the performance of PRlgt is extremely good for small lattices, it is hard to scale to large volumes due to the scalar nature of the code.

We have also developed the GridNSPT code[2], based on the Grid library [142]. GridNSPT has been debugged against PRlgt, and we are able to obtain the very same outputs from these two completely different implementations (but staggered fermions have been implemented in GridNSPT only). The Grid library provides an environment where message passing, multithreading and vector parallelism are fully exploited: the lattice is geometrically decomposed into MPI domains, each one mapped to a set of processors; it is also overdecomposed over virtual nodes in order to fill a SIMD vector, assuring very high vectorisation

[2]Available at `https://github.com/gfilaci/GridNSPT`.

efficiency. For example, on KNL and Skylake machines we can exploit the AVX-512 instruction set and a SIMD vector has room for 4 complex numbers in double precision; the virtual node decomposition results in the layout 1.1.2.2, where we are referring respectively to the coordinates $x.y.z.t$. Within the MPI task, multithreading is automatic because it is included in the closure of Grid lattice object expression templates. Grid incorporates C++11 internal template classes representing scalars, vector or matrices. We introduced a new template class representing a perturbative series, that embeds the overloading of the * operator.

```
template<class vtype, int Np> class iPert
{
vtype _internal[Np];
};
```

All the structures are tensors built from these templates: for example, the gauge field is `Lattice<iVector<iScalar<iPert<iMatrix<vComplexD,Nc>,Np>>,Nd>>`, where (starting from the outer template) we have the lattice, Lorentz, spin, perturbative, colour structure and the base type is a vectorised complex number in double precision. With this in place, every operation in Grid is performed consistently with almost no modification. We rely on the Grid library for the optimal implementation of the gauge action and for the Wilson and staggered fermion kernel. Twisted boundary conditions have been implemented modifying the covariant circular shifts. Even though GridNSPT lacks of many optimisations compared to PRlgt (for example the Langevin update is not performed one link at a time, but all operations and shifts are performed on the lattice as whole), its flexible environment allows scaling easily and very efficiently to large volumes. We also point out that it might be worth investigating in the future if a significant speed-up could be achieved at high orders by performing the Cauchy product as a multiplication of Fourier modes (with the Fourier transform computed in the perturbative order), instead of the usual convolution.

Appendix F

The nearest covariance matrix

If C is a covariance matrix, the corresponding correlation matrix is defined as

$$\hat{C} = S^{-1/2}\, C\, S^{-1/2}\,, \tag{F.1}$$

where S is the matrix which is equal to C on the diagonal and vanishes everywhere else. $\hat{C}$ has 1 on the diagonal by construction; it might have some negative or zero eigenvalue if the estimator used in the determination of the covariance does not guarantee positive definiteness. Given $\hat{C}$, Higham's algorithm [143] allows finding the nearest (in a weighted Frobenius norm) positive semidefinite matrix with unit diagonal. The core of the procedure is alternating a projection P_S onto the space of positive semidefinite matrices and a projection P_U onto the matrices with unit diagonal. The projection $P_S(X) = Y$ consists in

- diagonalising $X = U^T\, \Lambda\, U$, where U is an orthogonal matrix and Λ is a diagonal matrix with the eigenvalues of X on the diagonal
- setting to zero all the negative elements in Λ, obtaining $\tilde{\Lambda}$
- returning $Y = U^T\, \tilde{\Lambda}\, U$.

The projection $P_U(X)$ consists simply in putting 1 on the diagonal of X. We refer to the original work for the presentation and proof of the complete algorithm: after some iterations, the algorithm converges and returns a matrix $\hat{C}_H$ which is positive semidefinite and has 1 on the diagonal.

However, the algorithm allows $\hat{C}_H$ to have some zero (within machine precision)

eigenvalue, preventing the inversion of the covariance matrix. If this is the case, we additionally project $\hat{C}_H$ onto the space of positive definite matrices. This projection consists in

- diagonalising $\hat{C}_H = V^T \Gamma V$, where V is an orthogonal matrix and Γ is a diagonal matrix with the eigenvalues of $\hat{C}_H$ on the diagonal
- identifying $\epsilon = \delta \lambda_{max}$, where λ_{max} is the maximum eigenvalue and δ is the tolerance of the projection
- setting to ϵ all the diagonal elements of Γ whose absolute value is smaller than ϵ, obtaining $\tilde{\Gamma}$
- returning $\hat{C}_P = V^T \tilde{\Gamma} V$.

In conclusion, the nearest covariance matrix is

$$C_P = S^{1/2} \hat{C}_P S^{1/2} . \tag{F.2}$$

Bibliography

[1] L. Del Debbio, F. Di Renzo and G. Filaci, *High-order perturbative expansions in massless gauge theories with NSPT*, *EPJ Web Conf.* **175** (2018) 11023.

[2] L. Del Debbio, F. Di Renzo and G. Filaci, *Large-order NSPT for lattice gauge theories with fermions: the plaquette in massless QCD*, *Eur. Phys. J.* **C78** (2018) 974 [1807.09518].

[3] L. Del Debbio, F. Di Renzo and G. Filaci, *Non perturbative physics from NSPT: renormalons, the gluon condensate and all that*, *PoS* **LATTICE2018** (2018) 238 [1811.05427].

[4] K. G. Wilson, *Confinement of Quarks*, *Phys. Rev.* **D10** (1974) 2445.

[5] H. B. Nielsen and M. Ninomiya, *Absence of Neutrinos on a Lattice. 1. Proof by Homotopy Theory*, *Nucl. Phys.* **B185** (1981) 20.

[6] H. B. Nielsen and M. Ninomiya, *Absence of Neutrinos on a Lattice. 2. Intuitive Topological Proof*, *Nucl. Phys.* **B193** (1981) 173.

[7] K. G. Wilson, *Quarks and strings on a lattice*, in *New Phenomena in Subnuclear Physics: Part A* (A. Zichichi, ed.), pp. 69–142, Springer US, 1977, 10.1007/978-1-4613-4208-3_6.

[8] J. B. Kogut and L. Susskind, *Hamiltonian Formulation of Wilson's Lattice Gauge Theories*, *Phys. Rev.* **D11** (1975) 395.

[9] L. Susskind, *Lattice Fermions*, *Phys. Rev.* **D16** (1977) 3031.

[10] S. R. Sharpe, *Rooted staggered fermions: Good, bad or ugly?*, *PoS* **LAT2006** (2006) 022 [hep-lat/0610094].

[11] F. J. Dyson, *Divergence of perturbation theory in quantum electrodynamics*, *Phys. Rev.* **85** (1952) 631.

[12] A. D. Sokal, *An improvement of Watson's theorem on Borel summability*, *J. Math. Phys.* **21** (1980) 261.

[13] J. Fischer, *On the role of power expansions in quantum field theory*, *Int. J. Mod. Phys.* **A12** (1997) 3625 [hep-ph/9704351].

[14] G. 't Hooft, *Can We Make Sense Out of Quantum Chromodynamics?*, *Subnucl. Ser.* **15** (1979) 943.

[15] *Methods and simple examples*, in *Large-Order Behaviour of Perturbation Theory* (J. L. Guillou and J. Zinn-Justin, eds.), vol. 7 of *Current Physics–Sources and Comments*, pp. 1 – 12, Elsevier, 1990, 10.1016/B978-0-444-88597-5.50006-5.

[16] M. Beneke, *Renormalons*, *Phys. Rept.* **317** (1999) 1 [hep-ph/9807443].

[17] L. N. Lipatov, *Divergence of the Perturbation Theory Series and the Quasiclassical Theory*, *Sov. Phys. JETP* **45** (1977) 216 [*Zh. Eksp. Teor. Fiz.* **72** (1977) 411].

[18] L. Hörmander, *The Analysis of Linear Partial Differential Operators I: Distribution Theory and Fourier Analysis*, Springer, 1990, 10.1007/978-3-642-61497-2.

[19] A. A. Belavin, A. M. Polyakov, A. S. Schwartz and Yu. S. Tyupkin, *Pseudoparticle Solutions of the Yang-Mills Equations*, *Phys. Lett.* **B59** (1975) 85.

[20] I. M. Suslov, *Divergent perturbation series*, *Zh. Eksp. Teor. Fiz.* **127** (2005) 1350 [hep-ph/0510142].

[21] V. Zakharov, *High orders perturbation theory and dual models for Yang-Mills theories*, *Nucl. Phys. Proc. Suppl.* **207-208** (2010) 306 [1010.4482].

[22] K. G. Wilson, *Nonlagrangian models of current algebra*, *Phys. Rev.* **179** (1969) 1499.

[23] W. Zimmermann, *Local operator products and renormalization in quantum field theory*, in *Proceedings, 13th Brandeis University Summer Institute in Theoretical Physics, Lectures On Elementary Particles and Quantum Field Theory*, p. 395, 1970.

[24] K. G. Wilson and W. Zimmermann, *Operator product expansions and composite field operators in the general framework of quantum field theory*, *Commun. Math. Phys.* **24** (1972) 87.

[25] W. Zimmermann, *Normal products and the short distance expansion in the perturbation theory of renormalizable interactions*, *Annals Phys.* **77** (1973) 570 [*Lect. Notes Phys.* **558** (2000) 278].

[26] M. A. Shifman, A. I. Vainshtein and V. I. Zakharov, *QCD and Resonance Physics. Theoretical Foundations*, *Nucl. Phys.* **B147** (1979) 385.

[27] M. A. Shifman, A. I. Vainshtein and V. I. Zakharov, *QCD and Resonance Physics: Applications*, *Nucl. Phys.* **B147** (1979) 448.

[28] L. Del Debbio and R. Zwicky, *Renormalisation group, trace anomaly and Feynman-Hellmann theorem*, *Phys. Lett.* **B734** (2014) 107 [1306.4274].

[29] G. Leibbrandt, *Introduction to the Technique of Dimensional Regularization*, *Rev. Mod. Phys.* **47** (1975) 849.

[30] V. A. Novikov, M. A. Shifman, A. I. Vainshtein and V. I. Zakharov, *Wilson's Operator Expansion: Can It Fail?*, *Nucl. Phys.* **B249** (1985) 445.

[31] M. A. Shifman, *Snapshots of hadrons or the story of how the vacuum medium determines the properties of the classical mesons which are produced, live and die in the QCD vacuum*, *Prog. Theor. Phys. Suppl.* **131** (1998) 1 [hep-ph/9802214].

[32] F. David, *On the Ambiguity of Composite Operators, IR Renormalons and the Status of the Operator Product Expansion*, *Nucl. Phys.* **B234** (1984) 237.

[33] B. E. Lautrup, *On High Order Estimates in QED*, *Phys. Lett.* **69B** (1977) 109.

[34] G. Parisi, *Singularities of the Borel Transform in Renormalizable Theories*, *Phys. Lett.* **76B** (1978) 65.

[35] G. Parisi, *On Infrared Divergences*, *Nucl. Phys.* **B150** (1979) 163.

[36] A. H. Mueller, *On the Structure of Infrared Renormalons in Physical Processes at High Energies*, *Nucl. Phys.* **B250** (1985) 327.

[37] F. Di Renzo, E. Onofri and G. Marchesini, *Renormalons from eight loop expansion of the gluon condensate in lattice gauge theory*, *Nucl. Phys.* **B457** (1995) 202 [hep-th/9502095].

[38] G. Burgio, F. Di Renzo, G. Marchesini and E. Onofri, Λ^2*-contribution to the condensate in lattice gauge theory*, *Phys. Lett.* **B422** (1998) 219 [hep-ph/9706209].

[39] E. Gardi and G. Grunberg, *Conformal expansions and renormalons*, *Phys. Lett.* **B517** (2001) 215 [hep-ph/0107300].

[40] F. Di Renzo and L. Scorzato, *A Consistency check for renormalons in lattice gauge theory:* β^{-10} *contributions to the SU(3) plaquette*, *JHEP* **10** (2001) 038 [hep-lat/0011067].

[41] G. S. Bali, C. Bauer, A. Pineda and C. Torrero, *Perturbative expansion of the energy of static sources at large orders in four-dimensional SU(3) gauge theory*, *Phys. Rev.* **D87** (2013) 094517 [1303.3279].

[42] M. Campostrini, G. Curci, A. Di Giacomo and G. Paffuti, *Renormalization and Continuum Limit of Composite Operators in Lattice Gauge Theories*, *Z. Phys.* **C32** (1986) 377.

[43] H. Panagopoulos and E. Vicari, *The Trilinear Gluon Condensate on the Lattice*, *Nucl. Phys.* **B332** (1990) 261.

[44] A. Di Giacomo, H. Panagopoulos and E. Vicari, *The Topological Susceptibility and Lattice Universality*, *Nucl. Phys.* **B338** (1990) 294.

[45] A. Di Giacomo, H. Panagopoulos and E. Vicari, *The Scale Dependence of Lattice Condensates*, *Phys. Lett.* **B240** (1990) 423.

[46] M. Testa, *Some observations on broken symmetries*, *JHEP* **04** (1998) 002 [hep-th/9803147].

[47] G. Martinelli, C. Pittori, C. T. Sachrajda, M. Testa and A. Vladikas, *A General method for nonperturbative renormalization of lattice operators*, *Nucl. Phys.* **B445** (1995) 81 [hep-lat/9411010].

[48] A. Di Giacomo and G. C. Rossi, *Extracting* $\left\langle (\alpha/\pi) \sum_{a,\mu\nu} G^a_{\mu\nu} G^a_{\mu\nu} \right\rangle$ *from Gauge Theories on a Lattice*, *Phys. Lett.* **B100** (1981) 481.

[49] J. Kripfganz, *Gluon Condensate From SU(2) Lattice Gauge Theory*, *Phys. Lett.* **101B** (1981) 169.

[50] A. Di Giacomo and G. Paffuti, *Precise Determination of Vacuum Expectation Value of* $\left\langle (\alpha/\pi) \sum_{\alpha,\mu\nu} G^a_{\mu\nu} G^a_{\mu\nu} \right\rangle$ *From Lattice Gauge Theories*, *Phys. Lett.* **108B** (1982) 327.

[51] E.-M. Ilgenfritz and M. Müller-Preussker, *SU(3) Gluon Condensate From Lattice MC Data*, *Phys. Lett.* **119B** (1982) 395.

[52] M. Campostrini, A. Di Giacomo and Y. Gunduc, *Gluon Condensation in SU(3) Lattice Gauge Theory*, *Phys. Lett.* **B225** (1989) 393.

[53] B. Allés and G. Di Giacomo, *A new method to determine the chiral QCD gluon condensate on the lattice*, *Phys. Lett.* **B294** (1992) 269.

[54] B. Allés, M. Campostrini, A. Feo and H. Panagopoulos, *The three-loop lattice free energy*, *Phys. Lett.* **B324** (1994) 433 [hep-lat/9306001].

[55] L. F. Abbott, *The Background Field Method Beyond One Loop*, *Nucl. Phys.* **B185** (1981) 189.

[56] D. G. Boulware, *Gauge Dependence of the Effective Action*, *Phys. Rev.* **D23** (1981) 389.

[57] B. Grinstein and L. Randall, *The Renormalization of* G^2, *Phys. Lett.* **B217** (1989) 335.

[58] M. Lüscher and P. Weisz, *Background field technique and renormalization in lattice gauge theory*, *Nucl. Phys.* **B452** (1995) 213 [hep-lat/9504006].

[59] H. Kluberg-Stern and J. B. Zuber, *Renormalization of Nonabelian Gauge Theories in a Background Field Gauge. 1. Green Functions*, *Phys. Rev.* **D12** (1975) 482.

[60] A. O. Barvinsky, D. Blas, M. Herrero-Valea, S. M. Sibiryakov and C. F. Steinwachs, *Renormalization of gauge theories in the background-field approach*, *JHEP* **07** (2018) 035 [1705.03480].

[61] R. Tarrach, *The Renormalization of FF*, *Nucl. Phys.* **B196** (1982) 45.

[62] S. L. Adler, J. C. Collins and A. Duncan, *Energy-Momentum-Tensor Trace Anomaly in Spin 1/2 Quantum Electrodynamics*, *Phys. Rev.* **D15** (1977) 1712.

[63] J. C. Collins, A. Duncan and S. D. Joglekar, *Trace and Dilatation Anomalies in Gauge Theories*, *Phys. Rev.* **D16** (1977) 438.

[64] P. H. Damgaard and H. Hüffel, *Stochastic Quantization*, *Phys. Rept.* **152** (1987) 227.

[65] F. Di Renzo and L. Scorzato, *Numerical stochastic perturbation theory for full QCD*, *JHEP* **10** (2004) 073 [hep-lat/0410010].

[66] G. Parisi and Y.-S. Wu, *Perturbation Theory Without Gauge Fixing*, *Sci. Sin.* **24** (1981) 483.

[67] E. Wong and M. Zakai, *On the convergence of ordinary integrals to stochastic integrals*, *Ann. Math. Statist.* **36** (1965) 1560.

[68] W. Grimus and H. Hüffel, *Perturbation Theory From Stochastic Quantization of Scalar Fields*, *Z. Phys.* **C18** (1983) 129.

[69] E. Floratos and J. Iliopoulos, *Equivalence of Stochastic and Canonical Quantization in Perturbation Theory*, *Nucl. Phys.* **B214** (1983) 392.

[70] F. Di Renzo, G. Marchesini, P. Marenzoni and E. Onofri, *Lattice perturbation theory on the computer*, *Nucl. Phys. Proc. Suppl.* **34** (1994) 795.

[71] M. Dalla Brida and M. Lüscher, *SMD-based numerical stochastic perturbation theory*, *Eur. Phys. J.* **C77** (2017) 308 [1703.04396].

[72] M. Dalla Brida, M. Garofalo and A. D. Kennedy, *Investigation of New Methods for Numerical Stochastic Perturbation Theory in φ^4 Theory*, *Phys. Rev.* **D96** (2017) 054502 [1703.04406].

[73] G. Parisi, *Correlation Functions and Computer Simulations*, *Nucl. Phys.* **B180** (1981) 378.

[74] A. Ukawa and M. Fukugita, *Langevin Simulation Including Dynamical Quark Loops*, *Phys. Rev. Lett.* **55** (1985) 1854.

[75] G. G. Batrouni, G. R. Katz, A. S. Kronfeld, G. P. Lepage, B. Svetitsky and K. G. Wilson, *Langevin Simulations of Lattice Field Theories*, *Phys. Rev.* **D32** (1985) 2736.

[76] I. T. Drummond, S. Duane and R. R. Horgan, *The Stochastic Method for Numerical Simulations: Higher Order Corrections*, *Nucl. Phys.* **B220** (1983) 119.

[77] A. Guha and S. C. Lee, *Stochastic Quantization of Matrix and Lattice Gauge Models*, *Phys. Rev.* **D27** (1983) 2412.

[78] M. B. Halpern, *Constrained Quenched Master Field for Continuum QCD*, *Nucl. Phys.* **B228** (1983) 173.

[79] H. A. Kramers, *Brownian motion in a field of force and the diffusion model of chemical reactions*, *Physica* **7** (1940) 284.

[80] J. E. Moyal, *Stochastic processes and statistical physics*, *Journal of the Royal Statistical Society. Series B (Methodological)* **11** (1949) 150.

[81] D. Zwanziger, *Covariant Quantization of Gauge Fields Without Gribov Ambiguity*, *Nucl. Phys.* **B192** (1981) 259.

[82] J. Groeneveld, J. Jurkiewicz and C. P. Korthals Altes, *Twist as a Probe for Phase Structure*, *Phys. Scripta* **23** (1981) 1022.

[83] A. González-Arroyo, J. Jurkiewicz and C. P. Korthals-Altes, *Ground State Metamorphosis for Yang-Mills Fields on a Finite Periodic Lattice*, in *Freiburg ASI 1981:0339*, p. 339, 1981.

[84] A. Coste, A. González-Arroyo, J. Jurkiewicz and C. P. Korthals Altes, *Zero-Momentum Contribution to Wilson Loops in Periodic Boxes*, *Nucl. Phys.* **B262** (1985) 67.

[85] P. van Baal, *Surviving Extrema for the Action on the Twisted $SU(\infty)$ One Point Lattice*, *Commun. Math. Phys.* **92** (1983) 1.

[86] A. González-Arroyo, *Yang-Mills fields on the four-dimensional torus. Part I: Classical theory*, in *Nonperturbative quantum field physics. Proceedings, Advanced School, Peniscola, Spain, June 2-6, 1997*, pp. 57–91, 1997, `hep-th/9807108`.

[87] C. Bauer and G. Bali, *Hunting the static energy renormalon*, *PoS* **LATTICE2010** (2010) 221 [`1011.1165`].

[88] C. Bauer, G. S. Bali and A. Pineda, *Compelling Evidence of Renormalons in QCD from High Order Perturbative Expansions*, *Phys. Rev. Lett.* **108** (2012) 242002 [`1111.3946`].

[89] G. 't Hooft, *A Property of Electric and Magnetic Flux in Nonabelian Gauge Theories*, *Nucl. Phys.* **B153** (1979) 141.

[90] J. Ambjørn and H. Flyvbjerg, *'t Hooft's Non-Abelian Magnetic Flux has Zero Classical Energy*, *Phys. Lett.* **97B** (1980) 241.

[91] M. Lüscher and P. Weisz, *Efficient Numerical Techniques for Perturbative Lattice Gauge Theory Computations*, *Nucl. Phys.* **B266** (1986) 309.

[92] A. González-Arroyo and M. Okawa, *A Twisted Model for Large N Lattice Gauge Theory*, *Phys. Lett.* **120B** (1983) 174.

[93] A. González-Arroyo and M. Okawa, *The Twisted Eguchi-Kawai Model: A Reduced Model for Large-N Lattice Gauge Theory*, *Phys. Rev.* **D27** (1983) 2397.

[94] E. Cohen and C. Gomez, *A Computation of* $\mathrm{Tr}(-1)^F$ *in Supersymmetric Gauge Theories With Matter*, *Nucl. Phys.* **B223** (1983) 183.

[95] G. Parisi, *Prolegomena to any future computer evaluation of the QCD mass spectrum*, in *Proceedings of a NATO Advanced Study Institute on Progress in Gauge Field Theory (Cargèse, Corsica, France)*, pp. 531–541, 1984.

[96] Z. Hao, G. M. von Hippel, R. R. Horgan, Q. J. Mason and H. D. Trottier, *Unquenching effects on the coefficients of the Lüscher-Weisz action*, *Phys. Rev.* **D76** (2007) 034507 [0705.4660].

[97] U. M. Heller and F. Karsch, *One Loop Perturbative Calculation of Wilson Loops on Finite Lattices*, *Nucl. Phys.* **B251** (1985) 254.

[98] G. S. Bali, C. Bauer and A. Pineda, *Perturbative expansion of the plaquette to* $\mathcal{O}(\alpha^{35})$ *in four-dimensional SU(3) gauge theory*, *Phys. Rev.* **D89** (2014) 054505 [1401.7999].

[99] T. Eguchi and R. Nakayama, *Simplification of Quenching Procedure for Large N Spin Models*, *Phys. Lett.* **122B** (1983) 59.

[100] F. Di Renzo and L. Scorzato, *Fermionic loops in numerical stochastic perturbation theory*, *Nucl. Phys. Proc. Suppl.* **94** (2001) 567 [hep-lat/0010064].

[101] G. G. Batrouni, *Variations on the Langevin Equation for Lattice QCD With Fermions*, *Phys. Rev.* **D33** (1986) 1815.

[102] A. S. Kronfeld, *Another Higher Order Langevin Algorithm for QCD*, *Phys. Lett.* **B172** (1986) 93.

[103] M. Fukugita, Y. Oyanagi and A. Ukawa, *Langevin Simulation of the Full QCD Hadron Mass Spectrum on a Lattice*, *Phys. Rev.* **D36** (1987) 824.

[104] M. Hutchinson, *A stochastic estimator of the trace of the influence matrix for laplacian smoothing splines*, *Communications in Statistics - Simulation and Computation* **19** (1990) 433.

[105] M. Bochicchio, L. Maiani, G. Martinelli, G. C. Rossi and M. Testa, *Chiral Symmetry on the Lattice with Wilson Fermions*, *Nucl. Phys.* **B262** (1985) 331.

[106] E. Follana and H. Panagopoulos, *The Critical mass of Wilson fermions: A Comparison of perturbative and Monte Carlo results*, *Phys. Rev.* **D63** (2001) 017501 [hep-lat/0006001].

[107] S. Caracciolo, A. Pelissetto and A. Rago, *Two loop critical mass for Wilson fermions*, *Phys. Rev.* **D64** (2001) 094506 [hep-lat/0106013].

[108] F. Di Renzo, A. Mantovi, V. Miccio, L. Scorzato and C. Torrero, *Two and three loops computations of renormalization constants for lattice QCD*, *Nucl. Phys. Proc. Suppl.* **140** (2005) 716 [hep-lat/0409149].

[109] F. Di Renzo, V. Miccio, L. Scorzato and C. Torrero, *High-loop perturbative renormalization constants for Lattice QCD. I. Finite constants for Wilson quark currents*, *Eur. Phys. J.* **C51** (2007) 645 [hep-lat/0611013].

[110] A. S. Kronfeld, *The Perturbative pole mass in QCD*, *Phys. Rev.* **D58** (1998) 051501 [hep-ph/9805215].

[111] P. Rossi, C. T. H. Davies and G. P. Lepage, *A Comparison of a Variety of Matrix Inversion Algorithms for Wilson Fermions on the Lattice*, *Nucl. Phys.* **B297** (1988) 287.

[112] F. Di Renzo, *Landau-gauge-fixed numerical-stochastic perturbation theory*, *Nucl. Phys. Proc. Suppl.* **53** (1997) 819.

[113] C. T. H. Davies, G. G. Batrouni, G. R. Katz, A. S. Kronfeld, G. P. Lepage, K. G. Wilson et al., *Fourier Acceleration in Lattice Gauge Theories. 1. Landau Gauge Fixing*, *Phys. Rev.* **D37** (1988) 1581.

[114] F. Di Renzo, M. Laine, Y. Schroder and C. Torrero, *Four-loop lattice-regularized vacuum energy density of the three-dimensional SU(3) + adjoint Higgs theory*, *JHEP* **09** (2008) 061 [0808.0557].

[115] M. Constantinou, V. Lubicz, H. Panagopoulos and F. Stylianou, *$O(a^2)$ corrections to the one-loop propagator and bilinears of clover fermions with Symanzik improved gluons*, *JHEP* **10** (2009) 064 [0907.0381].

[116] P. F. Bedaque, *Aharonov-Bohm effect and nucleon nucleon phase shifts on the lattice*, *Phys. Lett.* **B593** (2004) 82 [nucl-th/0402051].

[117] K. M. Bitar, R. G. Edwards, U. M. Heller and A. D. Kennedy, *QCD with dynamical Wilson fermions at $\beta = 5.5$*, *Nucl. Phys. Proc. Suppl.* **53** (1997) 225 [hep-lat/9607043].

[118] TXL collaboration, N. Eicker et al., *Light and strange hadron spectroscopy with dynamical Wilson fermions*, *Phys. Rev.* **D59** (1999) 014509 [hep-lat/9806027].

[119] F. Di Renzo, E. Onofri, G. Marchesini and P. Marenzoni, *Four loop result in SU(3) lattice gauge theory by a stochastic method: Lattice correction to the condensate*, *Nucl. Phys.* **B426** (1994) 675 [hep-lat/9405019].

[120] X.-D. Ji, *Gluon condensate from lattice QCD*, hep-ph/9506413.

[121] R. Horsley, P. E. L. Rakow and G. Schierholz, *Separating perturbative and nonperturbative contributions to the plaquette*, *Nucl. Phys. Proc. Suppl.* **106** (2002) 870 [hep-lat/0110210].

[122] P. E. L. Rakow, *Stochastic perturbation theory and the gluon condensate*, *PoS* **LAT2005** (2006) 284 [hep-lat/0510046].

[123] Y. Meurice, *The non-perturbative part of the plaquette in quenched QCD*, *Phys. Rev.* **D74** (2006) 096005 [hep-lat/0609005].

[124] T. Lee, *Renormalon Subtraction from the Average Plaquette and the Gluon Condensate*, *Phys. Rev.* **D82** (2010) 114021 [1003.0231].

[125] R. Horsley, G. Hotzel, E. M. Ilgenfritz, R. Millo, H. Perlt, P. E. L. Rakow et al., *Wilson loops to 20th order numerical stochastic perturbation theory*, *Phys. Rev.* **D86** (2012) 054502 [1205.1659].

[126] G. S. Bali, C. Bauer and A. Pineda, *Model-independent determination of the gluon condensate in four-dimensional SU(3) gauge theory*, *Phys. Rev. Lett.* **113** (2014) 092001 [1403.6477].

[127] A. González-Arroyo, I. Kanamori, K.-I. Ishikawa, K. Miyahana, M. Okawa and R. Ueno, *Numerical stochastic perturbation theory applied to the twisted Eguchi-Kawai model*, 1902.09847.

[128] M. García Pérez, A. González-Arroyo and M. Okawa, *Perturbative contributions to Wilson loops in twisted lattice boxes and reduced models*, *JHEP* **10** (2017) 150 [1708.00841].

[129] U. M. Heller and F. Karsch, *Finite Temperature SU(2) Lattice Gauge Theory With Dynamical Fermions*, *Nucl. Phys.* **B258** (1985) 29.

[130] R. Alfieri, F. Di Renzo, E. Onofri and L. Scorzato, *Understanding stochastic perturbation theory: Toy models and statistical analysis*, *Nucl. Phys.* **B578** (2000) 383 [hep-lat/0002018].

[131] B. Allés, A. Feo and H. Panagopoulos, *Asymptotic scaling corrections in QCD with Wilson fermions from the three loop average plaquette*, *Phys. Lett.* **B426** (1998) 361 [hep-lat/9801003].

[132] G. S. Bali and P. Boyle, *Perturbative Wilson loops with massive sea quarks on the lattice*, hep-lat/0210033.

[133] S. Tamhankar and S. A. Gottlieb, *Scale determination using the static potential with two dynamical quark flavors*, *Nucl. Phys. Proc. Suppl.* **83** (2000) 212 [hep-lat/9909118].

[134] U. M. Heller, K. M. Bitar, R. G. Edwards and A. D. Kennedy, *The Heavy quark potential in QCD with two flavors of dynamical quarks*, *Phys. Lett.* **B335** (1994) 71 [hep-lat/9401025].

[135] R. Sommer, *A New way to set the energy scale in lattice gauge theories and its applications to the static force and α_s in SU(2) Yang-Mills theory*, *Nucl. Phys.* **B411** (1994) 839 [hep-lat/9310022].

[136] ALPHA collaboration, M. Della Morte, R. Frezzotti, J. Heitger, J. Rolf, R. Sommer and U. Wolff, *Computation of the strong coupling in QCD with two dynamical flavors*, *Nucl. Phys.* **B713** (2005) 378 [hep-lat/0411025].

[137] G. S. Chirikjian, *Stochastic Models, Information Theory, and Lie Groups, Volume 2: Analytic Methods and Modern Applications*, Birkhäuser Boston, Boston, 2012, 10.1007/978-0-8176-4944-9.

[138] J. R. Snippe, *Computation of the one loop Symanzik coefficients for the square action*, *Nucl. Phys.* **B498** (1997) 347 [hep-lat/9701002].

[139] N. Madras and A. D. Sokal, *The Pivot algorithm: a highly efficient Monte Carlo method for selfavoiding walk*, *J. Statist. Phys.* **50** (1988) 109.

[140] M. Lüscher, *Schwarz-preconditioned HMC algorithm for two-flavour lattice QCD*, *Comput. Phys. Commun.* **165** (2005) 199 [hep-lat/0409106].

[141] M. Brambilla, D. Hesse and F. Di Renzo, *Code development (not only) for NSPT*, *PoS* **LATTICE2013** (2014) 418.

[142] P. A. Boyle, G. Cossu, A. Yamaguchi and A. Portelli, *Grid: A next generation data parallel C++ QCD library*, *PoS* **LATTICE2015** (2016) 023.

[143] N. J. Higham, *Computing the nearest correlation matrix—a problem from finance*, *IMA Journal of Numerical Analysis* **22** (2002) 329.